

Thermodynamic studies and applications of polymeric membranes to fuel cells and microcapsules

Luizildo Pitol Filho

Supervisor: Dr. Ricard Garcia-Valls

**Departament d'Enginyeria Química
Universitat Rovira i Virgili
Tarragona
Spain**

June 2007

Aquest treball ha estat desenvolupat en major terme als laboratoris del Grup de Recerca de Biopolímers Vegetals, del Departament d'Enginyeria Química de la Universitat Rovira i Virgili (Av. Països Catalans 26, 43007 Tarragona, Catalunya, Espanya) sota finançament de la Universitat Rovira i Virgili i del projecte IMPULSE (FP6-2003-NMP-IN-3) de la Unió Europea. El treball presentat en aquest document no s'ha fet servir per l'obtenció de qualsevol altre títol o qualificació, i ha estat fruit íntegrament del treball realitzat pel sotasignat, excepte els casos que específicament s'indiqui el contrari.

Luizildo Pitol Filho
Juny de 2007

Tribunal de la tesi

Dr. João Paulo Serejo Goulão Crespo

Universidade Nova de Lisboa, Portugal

Dr. Marta Giamberini

Universitat Rovira i Virgili, Espanya

Dr. Josep Bonet i Avalos

Universitat Rovira i Virgili, Espanya

Dr. Juana Benavente

Universidad de Málaga, Espanya

Dr. José Luis Toca Herrera

Centro de Investigación Cooperativa de Biomateriales, Espanya

Suplents

Dr. Carlos Moreno Aguilar

Universidad de Cádiz, Espanya

Dr. Laura Palacio Martinez

Universidad de Valladolid, Espanya

Ithaca^{*}

K. Kavafis

As you set out for Ithaca
hope your road is a long one,
full of adventure, full of discovery.
Laistrygonians, Cyclops,
angry Poseidon - don't be afraid of them:
you' ll never find things like that on your way
as long as you keep your thoughts raised high,
as long as a rare excitement
stirs your spirit and your body.
Laistrygonians, Cyclops,
wild Poseidon - you won't encounter them
unless you bring them along inside your soul,
unless your soul sets them up in front of you.

Hope your road is a long one.
May there be many summer mornings when,
with what pleasure, what joy,
you enter harbours you're seeing for the first time;
may you stop at Phoenician trading stations
to buy fine things,
mother of pearl and coral, amber and ebony,
sensual perfume of every kind -
as many sensual perfumes as you can;
and may you visit many Egyptian cities
to learn and go on learning from their scholars.

Keep Ithaca always in your mind.
Arriving there is what you're destined for.
But don't hurry the journey at all.
Better if it lasts for years,
so you're old by the time you reach the island,
wealthy with all you've gained on the way,
not expecting Ithaca to make you rich.

Ithaca gave you the marvellous journey.
Without her you wouldn't have set out.
She has nothing left to give you now.
And if you find her poor, Ithaca won't have fooled you.
Wise as you will have become, so full of experience,
you'll have understood by then what these Ithacas mean.

* I have previously used this text of Kavafis in my MSc. Thesis. I know people should always evolve and think different, but such piece of poetry still has a strong meaning for me. When I was 24-25, however, I thought those verses were full of irony, and very appropriate to challenge the whole world. This does not apply anymore, since one gets wiser and wiser after so many Ithacas. Surely, the present Ithaca was one of the most complete and amazing ones. One should feel like Ulysses after completing the true ordeal of getting a PhD degree. When I commented to Carles Torras I wanted to put it in the thesis, he told me that Lluís Llach had immortalized those verses in the Catalan collective soul...

Agraïments / Acknowledgments / Teşekkürler

After four years, it is quite difficult to list all the people that have contributed to the PhD work either in the technical way or in the emotional one. Many people were part of my life those years and I want to dedicate those lines to them.

As most people who are going to appear in this list know, my previous PhD supervisor left URV before we really started to work and, since my scholarship was provided by the University, I had to choose another supervisor. Those changing times were somehow turbulent, because the rules were not so clear in the beginning, but finally I chose Ricard Garcia-Valls as my supervisor and I really think I won the lottery. Working with Ricard and the team (Carles, Tània, Vanessa, Kelly, Xiao, and, for a short time, Dawit, Vero, Gautier, Nihal, Agnieszka and Santi) was amazing, we had a lot of interesting discussions and – why not? – also a great time. I think I owe to Ricard my scientific maturity and I'd like to thank him because he gave me freedom to search for information and to investigate any crazy idea I got after my weekend trips (oops!).

In four years at the university we don't make just research: we also teach, and some of us were engaged as student representatives to the department councils. I'd like to thank Jaume Giralt and Joan Herrero, whose classes I participated as a teaching assistant, for being very helpful, for their attention and time and I'm sorry if in any moment I didn't accomplish your expectations. When I was representative of PhD students, I have invested a lot of time negotiating mainly with Azael Fabregat, Ioanis Katakis, Jordi Grifoll and Josep Font. Sometimes our opinions diverged in several subjects concerning students or teaching or working spaces, but for me it was a great experience and I hope I helped my colleagues and also the department during this time. I also thank my PhD colleagues who trusted in me and in the other representatives of my generation – Alicia, Carles, Haydée, Henry, Jorgelina, Isabela, Sònia, Ilham, Irama and Laura Pramparo – to be their mediators in the department. Naturally I thank those representative colleagues, and also Maria Eugenia, a former representative who gave her advice whenever we needed.

I also would like to mention Flor Siperstein and Josep Bonet, who always showed themselves willing to cooperate in the development of this thesis, by giving precious advice, that were accompanied by nice talks, coffee and pastries in their private cafeteria (their office). More recently, the discussions with Marta Giamberini were very useful, either to save me from unexpected questions in congresses or to foresee other applications of our approaches. Of course, the talks about Italy also were very nice. Thanks a lot.

Either working or having fun, some people have been important to me: Alicia (the most constant teacher of Catalan I ever had), Debora (we shared Morella, Collbató, and the pity that our research stays were at the same time – we couldn't visit each other!), Carles & Lina (my guides in the Priorat, the coffees in the harbour, the adventure of Sicilia), Henry & Jorgelina (Christmas in Prague, U2 in San Sebastian, and even my pancreatitis in Bilbao), Pepa & family, José António & Teresa, Carmelo (the only one I could convince to come to Benicàssim), Isabela, Clara, Paco & Cristina, Dan & Simona & their plants when they were not in Tarragona, Maria Eugenia & Pedro, Ana Dias (besides her friendship, I cannot forget to mention the unexpected help she gave me when I was just having a look in her thesis), Fatima Varanda & Pedro Carvalho (el Fòrum, Olot, Aveiro, Aveiro reloaded and some more adventures), Restrepiño (who introduced me to the Flemish beer and who told me about the Pergamon Museum in Berlin), Baltazar & Chimentão & Paulo & Luciana, and, more recently, Güray & Arcan (Winterthur Barcelona x Efes Pilsen Istanbul, the hospitality of their parents in Karşıyaka, my tree in their garden in Dikili), Oana, Fredy “muy formal” and Alexandre, my colleague from the *previous life* in PETROBRAS and old friend. Thank you all for having fun with me those years. One feels much better far from home having friends like you.

I'd like to dedicate some words to my supervisor from Izmir Institut of Technology, Sacide Alsoy Altinkaya, for her attention and also for being very kind, always ready for giving me technical advice and very curious about my weekend adventures in Turkey, a really amazing country. I cannot forget my office friends there: Sevdiye, Mehmet, Yılmaz and Seyhun, you all are great. Of course, Ismail Gönen deserves some special words, he showed me Istanbul

(Ortaköy, the dervishes and the neighbourhood of Fatih!). Besides them, I had a great time with Özge Malay, Öñiz, Can, Şükrü, Onur, Figen, Murat, Serdar, Deniz, Zelal, Emrah, Ilker, Gözde & Beren, Ulaş and Güler. I had also the opportunity to remember my French in Turkey with Yasser (you are going to be my guide in Iran someday), Hedi, Alban, Grégory (the French Erasmus students in Izmir), and Professor Michel Duclot, who stayed there a short time. And, last but not least, a big hug to the owners of Café Calipso in Gühlbahçe Koyu, good friends, although they didn't speak English at all and my poor Turkish just allowed me to explain very briefly what I visited on weekends, and to order food by phone. Teşekkür ederim!

Finalmente reservo as últimas palavras dos agradecimentos a quem mais os merecem, que são meus pais. Sem o seu apoio, não poderia ter empreendido essa jornada tão longa de quatro anos e alguns meses e, apesar de não parecer, tenho de dizer que senti muito a sua falta aqui longe. Tudo seria muito mais fácil se eu não tivesse saído de Itapema, mas sem essa etapa eu não me sentiria completo e sei que vocês também não. Beijos, muitos beijos, todos esses que eu não pude dar, estando tão longe.

Abstract

As raw materials, polymers have wide applications in chemical engineering, especially in novel technologies, such as membranes. Polymeric membranes are structures formed from organic solutions once the solvent is removed either by evaporation or by the addition of a non-solvent. Flat-sheet membranes are formed when a thin layer of polymeric solution is deposited over a glass plate. To form dense membranes, just evaporation of the solvent is needed. On the other hand, if the polymeric film is immersed into a non-solvent (usually water), porous structures are formed. A similar mechanism may produce microcapsules. However, in this case, an important step is the formation of droplets of polymeric solution, either in batch mode or by using micromixers. Thermodynamics may be used as an assessing tool to improve the understanding of the processes mentioned above and to allow further optimization. Important thermodynamic properties for polymers are the cohesion parameters and the Flory-Huggins interaction parameters. For a given component, the cohesion parameter may be also expressed as the resultant of the three-dimensional vector that includes dispersion, polar and hydrogen-bonding effects. The binary Flory-Huggins interaction parameter between a polymer and a penetrant is a function of the cohesion parameters of both components, and is related to their affinity, being useful for predictions of swelling degree of membranes, phase equilibria and even transport through polymeric structures. The literature lists several methods to calculate each of those properties, and the choice of the most adequate one for a determined case is a determinant step. Theories of transport through polymers need, apart from the thermodynamic contribution, a free-volume term, which is related to the space between polymeric molecules that is available for mass transfer, where penetrant molecules diffuse. A very-well accepted macroscopic approach for such process is the Vrentas-Duda model, that uses intrinsic properties of the components, such as viscosity (for penetrants) and relaxation times (for polymers) to obtain transport parameters, allowing to derive comprehensive models for both simulation and optimization of membrane processes, among

others. In fuel cell systems, for example, the free-volume theory may be applied to choose a polymer with determined properties, allowing a better consumption of fuel, for example. Also those theories may contribute to the knowledge of the intrinsic formation of the membrane. This thesis deals with the knowledge of intrinsic properties of chemical components, such as solvents and polymers, to understand transport properties of the materials produced from those chemicals. By using free-volume theory and a thermodynamic approach we were able to predict several kinds of data, such as swelling degree of membranes and ternary equilibrium data, recommend materials for fuel cell membranes, and even give hints about the formation of polymeric membrane structures. We point out that our predictions require very few experimental or adjustable parameters.

Nomenclature

Acronyms

3D	three-dimensional Flory-Huggins approach
CPMM	Caterpillar Micromixer
SEM	Scanning Electron Microscopy
DMFC	Direct methanol fuel cell
ENSIC	Engaged species induced clustering model
NO	microcapsules of pure polysulfone
SIMM	Slit Interdigital Micromixer
VLE	Vapor-liquid equilibrium
WLF	Williams-Landel-Ferry equation

Chemicals

2,2,4-TMP	2,2,4-Trimethylpentane
CTA	Cellulose triacetate
DMF	N-N-dimethylformamide
ETBE	Ethyl tert-butyl ether
EtGlyc	ethylene glycol
EtOAc	ethyl acetate
EtOH	Ethanol
HOAc	acetic acid
IPA	2-Propanol
MeOH	Methanol
MTBE	Methyl tert-butyl ether
NBZ	nitrobenzene
PBD	Poly(butadiene)
PDMS	Poly(dimethyl siloxane)
PEMA	Poly(ethyl metacrylate)
PIPA	Poly(isopropyl acrylate)
PP	atactic poly(propylene)
PMMA	Poly(methyl metacrylate)
PMS	Poly(α -methyl styrene)
PropGlyc	propylene glycol
PSf	polysulfone
PVA	poly vinyl alcohol
Pyr	pyridine
THF	tetrahydrofuran
VNL	vanillin

Journals

AIChe J	American Institute of Chemical Engineers Journal (ISSN: 0001-1541)
CAT	Catalysis Today (ISSN: 0920-5861)
CATA	Applied Catalysis A: General (ISSN: 0926-3373)
CATB	Applied Catalysis B: Environmental (ISSN: 0926-860X)
ChEJ	Chemical Engineering Journal (ISSN: 1385-8947)

ChES	Chemical Engineering Science (ISSN: 0009-2509)
DES	Desalination (ISSN: 0011-9164)
EA	Electrochimica Acta (ISSN : 0013-4686)
EF	Energy & Fuels (ISSN: 0887-0624)
FCB	Fuel Cells Bulletin (ISSN: 1464-2859)
FPT	Fuel Processing Technology (ISSN: 0378-3820)
IEChR	Industrial & Engineering Chemistry Research (ISSN: 0888-5885)
JCIS	Journal of Colloid and Interface Science (ISSN: 0021-9797)
JMS	Journal of Membrane Science (ISSN: 0376-7388)
JPCS	Journal of Physics and Chemistry of Solids (ISSN: 0022-3697)
JPS	Journal of Power Sources (ISSN: 0378-7753)
PES	Polymer Engineering and Science (ISSN: 0032-3888)
PhysB	Physica B: Condensed Matter (ISSN: 0921-4526)
PhysC	Physica C: Superconductivity and its Applications (ISSN: 0921-4534)
POL	Polymer (ISSN: 0032-3861)
SPT	Separation and Purification Technology (ISSN: 1383-5866)
SSc	Surface Science (ISSN: 0039-6028)
SSI	Solid State Ionics (ISSN: 0167-2738)

Variables

A_{i3}	pre-exponential term based on the diffusivity at infinite dilution (cm ² .s ⁻¹)
B_i	thermodynamic factor based on Van Laar equation
c_i	coefficient of the water-MeOH Flory-Huggins expression
D	diameter (μm) of droplets / microcapsules or the characteristic dimension of slit, according to the subscript
D_i	binary diffusivity (cm ² .s ⁻¹)
D_{ij}	diffusion coefficient matrix for ternary systems (cm ² .s ⁻¹)
D_{i32}	composition factor of Flory-Huggins parameter
D_0	pre-exponential term on diffusivity expression (cm ² .s ⁻¹)
E^{coh}	molar cohesion energy (J. gmol ⁻¹)
E_i	activation energy for diffusion
F	molar attraction constant (MPa ^{1/2} .cm ³ .gmol ⁻¹)
F	flow rate (ml.h ⁻¹)
ΔG^E	Excess Gibbs free energy
ΔH^V	vaporization enthalpy (J. gmol ⁻¹)
J_i	diffusive flux of component i (cm ² .cm ⁻¹ .s ⁻¹)
K_r	fitting parameter of the Rayleigh-based equation
K	ratio of the diameter of the product core to the total diameter
K_{1i}/γ	free-volume parameter for component i (cm ³ .g ⁻¹ .K ⁻¹)
$K_{2i} - T_{gi}$	free-volume parameter for component i (K)
K_{lumped}	lumped free-volume parameter for polymer (cm ³ .g ⁻¹)
M_i	molecular weight of PEG (g.gmol ⁻¹)
m	microcapsule mass (g)
n	number of microchannels
n_i	number of moles of component i
P^V	vapor pressure
R	ideal gas constant

ΔS^V	vaporization entropy ($J \cdot gmol^{-1} \cdot K^{-1}$)
S_{MeOH}	selectivity for MeOH based on total diffusive flows
T	temperature, K
T_g	Glass transition temperature, K
v_i	molar volume of component i ($cm^3 \cdot g^{-1}$)
V_i	molar volume of component i ($cm^3 \cdot gmol^{-1}$)
w_i	mass fraction of component i
x_i	molar fraction of component i
y_i	molar fraction of component i in vapor phase

Greek letters

α	multiplying factor of Flory-Huggins parameter
β	linear factor of Flory-Huggins parameter
γ_i	Activity coefficient
δ_i	Cohesion parameter of component <i>i</i> , $MPa^{1/2}$
ε	porosity
ξ_{i3}	ratio of the molar volumes for solvent i and polymer jumping unit
Ψ	area between experimental and predicted binary diffusivity curves
ϕ_i	Volume fraction of component <i>i</i>
χ_{ij}	i-j Flory-Huggins interaction parameter
ρ_{molar}	molar density ($gmol \cdot cm^{-3}$)
ρ_i	Mass density, g/cm^3
μ_i	Chemical potential of component <i>i</i>
Γ	orientative function to select Flory-Huggins approach
μ_i	chemical potential of component i
χ_{ij}	i-j Flory-Huggins interaction coefficient
Ω_i	mobility of component i

Subscripts

d	dispersion
hb	hydrogen-bonding
p	polar

Contents

List of Figures	2
List of Tables	4
1 Introduction	5
2 Objectives.....	8
3 Theoretical background	9
3.1 Thermodynamics of polymers	9
3.2 Membranes	18
3.3 Diffusion in polymers: the Vrentas-Duda free-volume theory	21
3.4 Obtention of polymeric membranes	26
3.5 Production of polymeric microcapsules by using micromixers	29
3.6 Direct methanol fuel cells	33
3.7 General comments.....	41
4 Discussion and indicators of published articles	42
4.1 Impact information.....	42
4.2 Articles information.....	43
5 Conclusions	49
5.1 Thermodynamics.....	49
5.2 Microcapsules	50
5.3 Fuel cells.....	51
6 Scientific contributions of this thesis.....	53
7 Articles.....	55
8 References.....	57
Appendixes	

List of figures

Figure 1.1 – Formation of membranes by solvent evaporation or by immersion precipitation.....	5
Figure 1.2 – Production of microcapsules by immersion precipitation.....	6
Figure 3.1– Lattice model for polymer chains in solution. Empty symbols represent the solvent molecules as the hatched symbols represent the polymeric units.	9
Figure 3.2– Stereoregularity of poly(propylene).	16
Figure 3.3 - Sorption of fluid molecules on a polymeric matrix.	17
Figure 3.4 - Separation of a binary mixture by using a dense membrane.	19
Figure 3.5 - A three-layered neural network.	20
Figure 3.6 - Diffusion in polymers: free-volume and hopping mechanisms.	21
Figure 3.7– Calculation procedures to obtain the parameters for free-volume predictions.....	23
Figure 3.8 – Different membrane structures obtained by varying polymer concentration and non-solvent.	27
Figure 3.9– PSf-DMF-Water phase diagram.	28
Figure 3.10 - Typical micromixers: (a). external view, with silver and nickel mixing elements; (b): disassembled micromixer; (c). SEM image of microchannels; (d): operation mode.....	30
Figure 3.11 – Schematic representation of a possible mechanism for the formation of microcapsules. Steps:(a) droplet of polymeric solution surrounded by cyclohexane; (b) DMF leaves the droplet in the radial direction; (c) final capsule formed, hatched part is the final diameter and the grey part, the loss of mass during precipitation; (d) still remains cyclohexane in the surface of the droplet.....	32
Figure 3.12 - Schematic diagram of a direct methanol fuel cell (DMFC).	34

Figure 3.13 - Groups of publications.	36
Figure 3.14 – Variation of impact index of fuel-cell related publications.	37
Figure 3.15 – DMFC in www.sciencedirect.com.....	38
Figure 3.16 – Comparison between topics: <i>modeling membrane</i> and <i>DMFC</i> . .	40
Figure 4.1 - Phase separation curve of the system DMF-water-PSf.....	46
Figure 4.2- Molecular and mutual diffusivity of DMF in a binary system DMF-PSf.	47

List of Tables

Table 3.1– Coefficients of the Flory-Huggins interaction parameters.....	12
Table 3.2– Contribution rules to calculate molar volume.....	13
Table 3.3– Contribution rule according to Beerbower’s compilation.....	13
Table 3.4- Representative molar attraction constants.	15
Table 4.1- Impact information of categories.	42
Table 4.2- Free-volume parameters for the system DMF(1) – PSf(2)	46

1 Introduction

As raw materials, polymers have wide applications in chemical engineering, especially in novel technologies, such as membranes. Polymeric membranes are structures formed from organic solutions once the solvent is removed either by evaporation or by the addition of a non-solvent. Figure 1.1 illustrates the formation of those membranes.

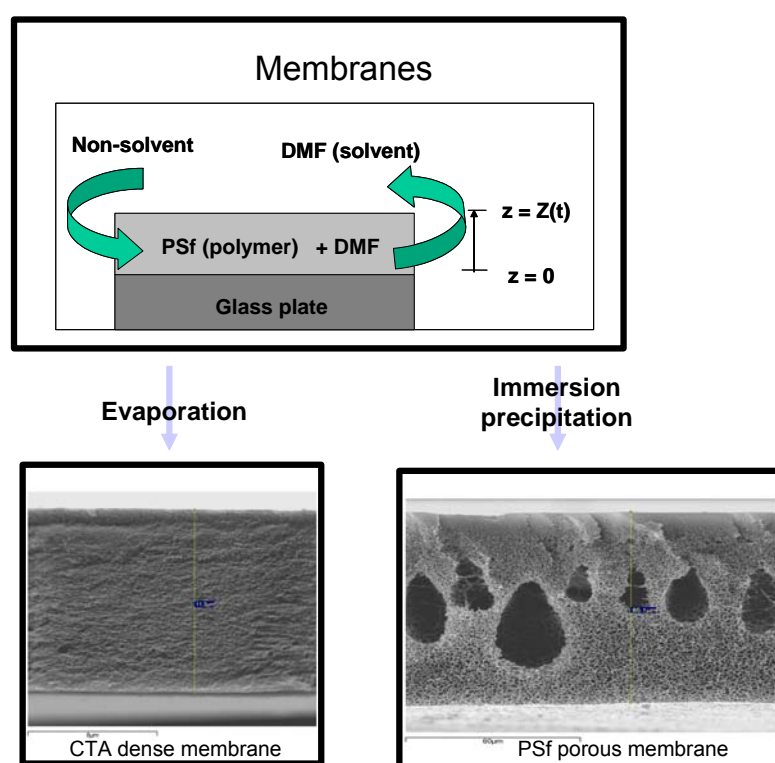


Figure 1.1 – Formation of membranes by solvent evaporation or by immersion precipitation¹.

In the obtention of the polymeric membranes is shown in Figure 1.1. A thin layer of polymeric solution is deposited over a glass plate. To form dense membranes, just evaporation of the solvent is needed. On the other hand, if the polymeric film is immersed into a non-solvent (usually water), porous structures are

¹ SEM images by Carles Torras Font (the same applies for Figure 1.2).

formed. Previous works in our group showed that the porous structures obtained can be controlled by the conditions of the coagulation bath.

A similar mechanism may produce microcapsules. However, in this case, an important step is the formation of droplets of polymeric solution, either in batch mode or by using micromixers. Figure 1.2 illustrates the formation of the microcapsules.

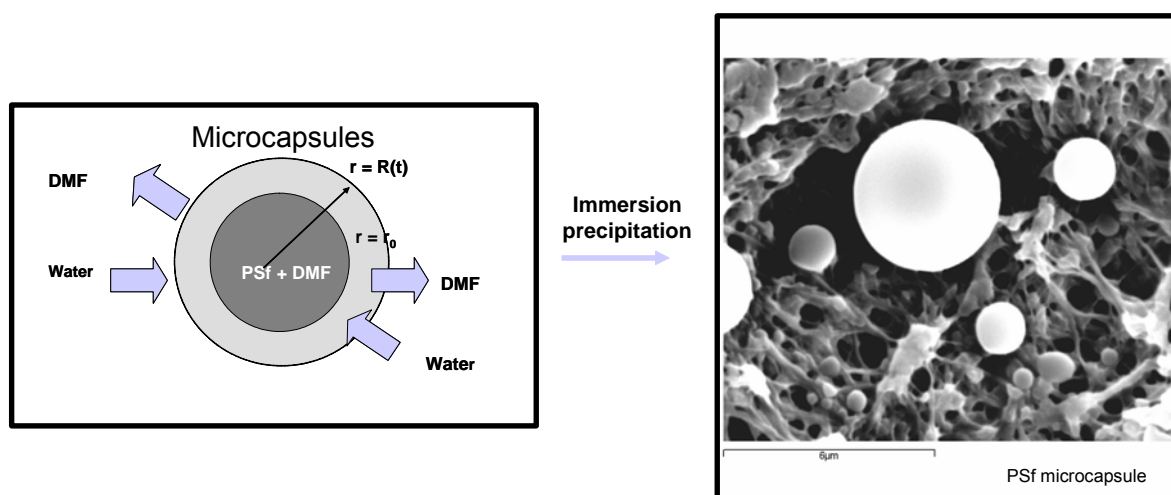


Figure 1.2 – Production of microcapsules by immersion precipitation.

In this case, however, the droplet of polymer is surrounded by a continuous phase, that does not mix either with the polymer or with the non-solvent. Therefore, the non-solvent (i.e. water, for example) should play a two-fold role: first, it should wash away the external surface of the droplet from the continuous phase, and then, precipitate the polymer by expelling the solvent (DMF). The chemistry of the system is of course affected by addition of the component to be encapsulated, leading to the formation of different structures.

In both processes described above, thermodynamics may be used as an assessing tool to improve their understanding and to allow further optimization. Important thermodynamic properties for polymers are the cohesion parameters and the Flory-Huggins interaction parameters. For a given component, the cohesion parameter may be also expressed as the resultant of the three-

dimensional vector that includes dispersion, polar and hydrogen-bonding effects. The binary Flory-Huggins interaction parameter between a polymer and a penetrant is a function of the cohesion parameters of both components, and is related to their affinity, being useful for predictions of swelling degree of membranes, phase equilibria and even transport through polymeric structures. The literature lists several methods to calculate each of those properties, and the choice of the most adequate one for a determined case is a determinant step.

Theories of transport through polymers need, apart from the thermodynamic contribution, a free-volume term, which is related to the space between polymeric molecules that is available for mass transfer, where penetrant molecules diffuse. A very-well accepted macroscopic approach for such process is the Vrentas-Duda model, that uses intrinsic properties of the components, such as viscosity (for penetrants) and relaxation times (for polymers) to obtain transport parameters, allowing to derive comprehensive models for both simulation and optimization of membrane processes, among others. In fuel cell systems, for example, the free-volume theory may be applied to choose a polymer with determined properties, allowing a better consumption of fuel, for example. Also those theories may contribute to the knowledge of the intrinsic formation of the membrane.

Therefore, the present thesis summarizes, in the form of scientific papers, some topics developed by the author and contributors, towards a better comprehension of the mechanisms of penetrant-polymer systems, as well as some results obtained while using polymers as raw materials for fuel cells or microencapsulation. However, the author is aware that all topics deserve deeper studies. The goal of this thesis, according to the author, is that it serves as a guide for future works in polymers, since it identifies specific topics in research of polymers that still lack attention.

2 Objectives

The objectives of this thesis are:

- Assess the choice of appropriate expressions to determine equilibrium-related properties, from the several methods available in the literature;
- Calculate *a priori* properties of membranes that are often determined by experimental data, such as swelling degree and ternary equilibrium data;
- Use free-volume theory to recommend polymers to manufacture fuel cells;
- Identify key parameters on the production of polymeric membrane structures, such as flat-sheet membranes and microcapsules.

3 Theoretical background

In the present thesis, polymers are studied as raw materials for membrane applications, such as fuel cells and microcapsules. In those processes, mass transfer is a key step, and its most significant contributors are the phenomena of diffusion and thermodynamic equilibrium.

3.1 Thermodynamics of polymers

In the middle of last century, Paul Flory and Maurice Huggins, working independently, derived a theory upon a simple lattice model that could be used to understand the behavior of polymeric solutions [1]. An example of a lattice, where a low-molecular-weight solvent and a high-molecular-weight polymer are mixed, is shown in Figure 3.1. This section describes the theory of Flory-Huggins, according to J.R. Fried [1].

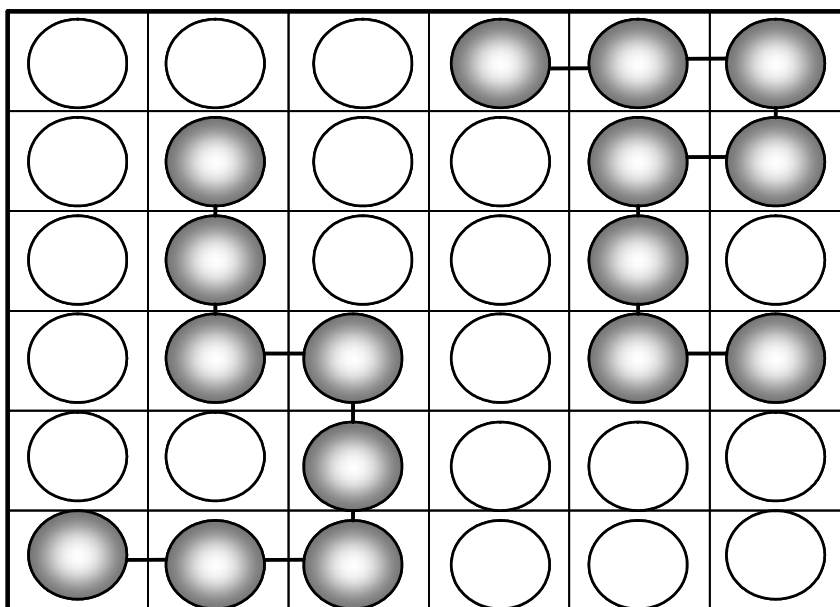


Figure 3.1– Lattice model for polymer chains in solution. Empty symbols represent the solvent molecules as the hatched symbols represent the polymeric units.

The entropy of mixing in the system represented in Figure 3.1 may be expressed by the following relationship:

$$\Delta S_m = k \ln \Omega \quad (3.1)$$

where k is the Boltzmann's constant and Ω the total number of ways to arrange n_1 solvent molecules and n_2 polymer molecules in a lattice with N positions. Therefore, the entropy of mixing may be also expressed as a function of the volume fractions:

$$\Delta S_m = -k(n_1 \ln \phi_1 + n_2 \ln \phi_2) \quad (3.2)$$

On the other hand, to compose the Gibbs free energy of mixing, we also need to determine the enthalpic term. The Flory-Huggins model defines it as:

$$\Delta H_m = zn_1 r_1 \phi_2 \Delta \omega_{12} \quad (3.3)$$

where z is the lattice coordination number of neighbor cells to a given cells, r_1 represents the number of segments in a solvent molecule, and $\Delta \omega_{12}$ is the change in internal energy generated by unlike molecular pair (solvent-polymer or 1-2) contacts. Since z and $\Delta \omega_{12}$ are empirical parameters, it is convenient to define a single energetic parameter called Flory-Huggins interaction parameter, as in Eq.(3.4):

$$\chi_{12} = \frac{zr_1 \Delta \omega_{12}}{kT} \quad (3.4)$$

The Gibbs free energy of mixing is given by:

$$\Delta G_m = \Delta H_m - T\Delta S_m \quad (3.5)$$

Or, by applying Eqs (3.2) and (3.3):

$$\Delta G_m = kT(n_1 \ln \phi_1 + n_2 \ln \phi_2 + \chi_{12} n_1 \phi_2) \quad (3.6)$$

The chemical potential for the solvent is obtained by deriving Eq (3.6) by the number of moles of solvent at constant pressure and temperature:

$$\Delta \mu_1 = \left(\frac{\partial \Delta G_m}{\partial n_1} \right)_{T,P} \quad (3.7)$$

In the case of high-molecular-weight polymers, where the number of solvent equivalent segments r is large, the activity of the solvent is finally obtained as:

$$\ln a_1 = \frac{\Delta \mu_1}{kT} = \ln \phi_1 + \phi_2 + \chi_{12} \phi_2^2 \quad (3.8)$$

Eq. (3.8) may be expanded for multicomponent systems and is often used to determine the Flory-Huggins parameter from experimental data [2,3,4,5]. The Flory-Huggins parameter may be also predicted by using the molar volume of the solvent and the cohesion parameters of both solvent and polymer.

Eq.(3.9) expresses a general form of the Flory-Huggins interaction parameter:

$$\chi_{12} = \beta + \alpha \frac{V}{RT} D_{12}^2 \quad (3.9)$$

Table 3.1 summarizes the coefficients for the χ expression for both classic and three-dimensional (3D) approaches:

Table 3.1– Coefficients of the Flory-Huggins interaction parameters.

Approach	α	β	D_{12}^2
Classic [1]	1	0.35	$(\delta_{1,total} - \delta_{2,total})^2$
3D [6]	1	0	$(\delta_{1,d} - \delta_{2,d})^2 + 0.25(\delta_{1,p} - \delta_{2,p})^2 + 0.25(\delta_{1,hb} - \delta_{2,hb})^2$

The 3D approach implies that the overall cohesion parameter is correlated to the dispersion, polar and hydrogen bonding solubility parameters, also known as Hansen parameters. Eq.(3.10) relates the overall and the Hansen parameters:

$$\delta_{total}^2 = \delta_d^2 + \delta_p^2 + \delta_{hb}^2 \quad (3.10)$$

There are several methods in the literature to calculate the cohesion parameters and also to obtain the molar volume. The liquid molar volume at 0K may be calculated either by group contribution or by computing atom by atom in the molecular structure. Table 3.2 lists the Sugden and Blitz atomic contribution rules [7].

A more extensive contribution rule was compiled by Beerbower [8], where groups are considered instead of atoms. Some examples are found in Table 3.3.

In the literature, the molar volume is found either on a molar or on a mass basis. All the rules presented here allow us to obtain the molar-based property. Therefore, to compare to the mass-based values often found in literature, we just divided the calculated values by the molar mass.

Table 3.2– Contribution rules to calculate molar volume.

Component	Sugden (cm ³ /gmol)	Blitz (cm ³ /gmol)
H	6.7	6.45
C (aliphatic)	1.1	0.77
C (aromatic)	1.1	5.1
N	3.6	-
O	5.9	-
Cl	19.3	16.3
S	14.3	-
Triple bond	13.9	16.0
Double bond	8.0	8.6
5-membered ring	1.8	-
6-membered ring	0.6	-
OH (alcoholic)	-	10.5
OOH (carboxyl)	-	23.2

Table 3.3– Contribution rule according to Beerbower's compilation.

Group	Beerbower's rule (cm ³ /gmol)
- CH ₃	31.70
-CH ₂ -	16.60
=CH-	12.40
>CH-	-1.00
-COO-	8.20
-O-	3.60
-OH	10.47
>SiO<	3.80

The use of the cohesion parameters just aims to provide a simple method for prediction of cohesive and adhesive properties of materials from the properties of the pure components [8]. Very often the cohesion, or Hildebrand, parameter is referred as solubility parameter, but such nomenclature is quite restrictive for

a quantity that may be helpful to correlate a wide range of physical and chemical properties, such as the Flory-Huggins interaction parameter. The cohesion parameter [1] is related to the molar energy of vaporization of a pure liquid, also known as the cohesive energy-density by Eq. (3.11):

$$\delta_i = \sqrt{E_i^{coh}} = \sqrt{\frac{\Delta E_i^v}{V_i(T_{ref})}} \quad (3.11)$$

Therefore, when the enthalpy of vaporization and the molar volume are known, the cohesion parameter can be easily obtained. Eq.(3.12) expresses the enthalpy of vaporization in terms of vapor pressure [9]:

$$\Delta H^v = T\Delta S^v = RT^2 \frac{d \ln P^v}{dT} \quad (3.12)$$

Finally Eq. (3.11) becomes:

$$\delta_i = \sqrt{\frac{\Delta H^v - RT}{V_i(T_{ref})}} = \sqrt{\rho_{molar}(\Delta H^v - RT)} \quad (3.13)$$

Therefore, the cohesion parameter for the transported species may be obtained either by calculating the vapor pressure or by using commercial process simulators, like Aspen® or Hysys®, that have a very complete database of chemical compounds. In the present work we used the Antoine equation of state. This approach allows us to obtain a cohesion parameter depending on temperature, what can be useful while modeling processes that do not occur at room temperature.

However, since energy of vaporization for solids or polymers has no sense, group contribution methods are required. Among them, the most widely used are the rules provided by Small and Hoy [1], where a molar attraction constant

is given for each chemical group in the polymer repeating unit. By adding all the constants, the cohesion parameter can be easily obtained:

$$\delta_i = \frac{\sum_j F_j}{V_i} \quad (3.14)$$

Table 3.4 lists the molar attraction constants used to calculate the cohesion parameters for the most common methods available in the literature. Those values were obtained by regression analysis of physical properties data for a wide range of organic compounds (640 compounds in the case of Hoy). In the method provided by Small, however, some groups that form hydrogen bonds were excluded.

Table 3.4- Representative molar attraction constants.

Group	Molar attraction constant, F (MPa ^{1/2} cm ³ gmol ⁻¹)		
	Small	Hoy	van Krevelen
-CH ₃	438	303	420
-CH ₂ -	272	269	280
>CH-	57	176	140
>C<	-190	65.5	0
-CH=CH-	454	497	444
>C=CH-	266	422	304
-O- (ether)	143	235	256
-OH	-	462	754
-CO- (ketones)	563	538	685
-COO- (esters)	634	668	512
-OCOO- (carbonate)	-	(904)	767
-NH-	-	368	-
-S- (sulfides)	460	428	460
-Cl (primary)	552	420	471
-Si	-77	-	-

Another approach considers three aspects of the cohesion parameters: dispersion, polarity and hydrogen bonds. In a recent work [10], we proved that the 3D modeling should be preferred rather than the classic model, especially when highly polar penetrants are involved. Extensive tables to calculate the dispersion, polar and hydrogen-bonding Hansen parameters are presented in the literature [8]. Such calculations, as the one expressed by Eq.(3.14), also involve the molar volume.

An important drawback of the presented group contribution methods, either for molar volumes or for cohesion parameters, is that it does not take into account the stereoregularity of the polymers. Stereoregularity, also known as tacticity, refers to the distribution of the substituting groups in a polymeric chain [11]. Figure 3.2 illustrates the stereoregularity of poly(propylene) (PP).

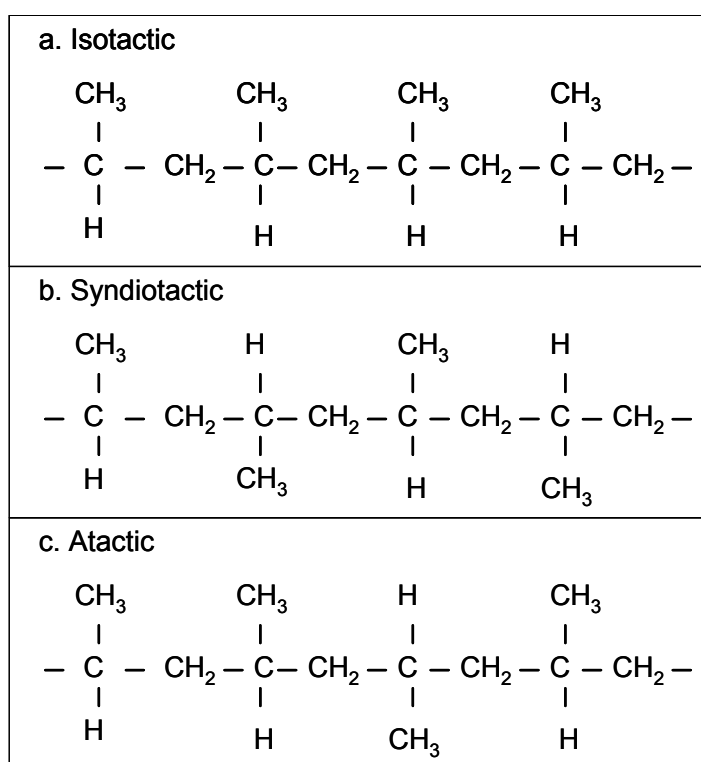


Figure 3.2– Stereoregularity of poly(propylene).

On the stereoregularity depend important properties such as the crystal conformation or the mechanical strength. As shown in Figure 3.2, isotactic PP has all the substituting methyl groups at the same relative position along the

polymeric chain, what provides a well-defined crystal structure with high stiffness, mechanical strength and chemical resistance [12]. On the other hand, the distribution of the substituting groups for atactic polymers is totally random, what prevents them to have mechanical integrity. Syndiotactic polymers, however, have a regular alternance of the substituting groups. In the case of PP, molecules of different stereoregularity may be even immiscible. Further studies should be done in order to propose calculation methods that take into account such phenomena.

In the case of the total cohesion parameter, an alternative may be the determination by Atomic Force Microscopy [13] of a polymeric membrane, if the contact angles of two liquids are measured on a membrane surface, in both advancing and receding mode. It is a very interesting application when the existing contribution rules are inappropriate or incomplete.

An alternative thermodynamic model is the so-called ENSIC (Engaged Species Inducing Clustering) [14], that considers the sorption of molecules on the polymeric matrix, as shown in Figure 3.3.

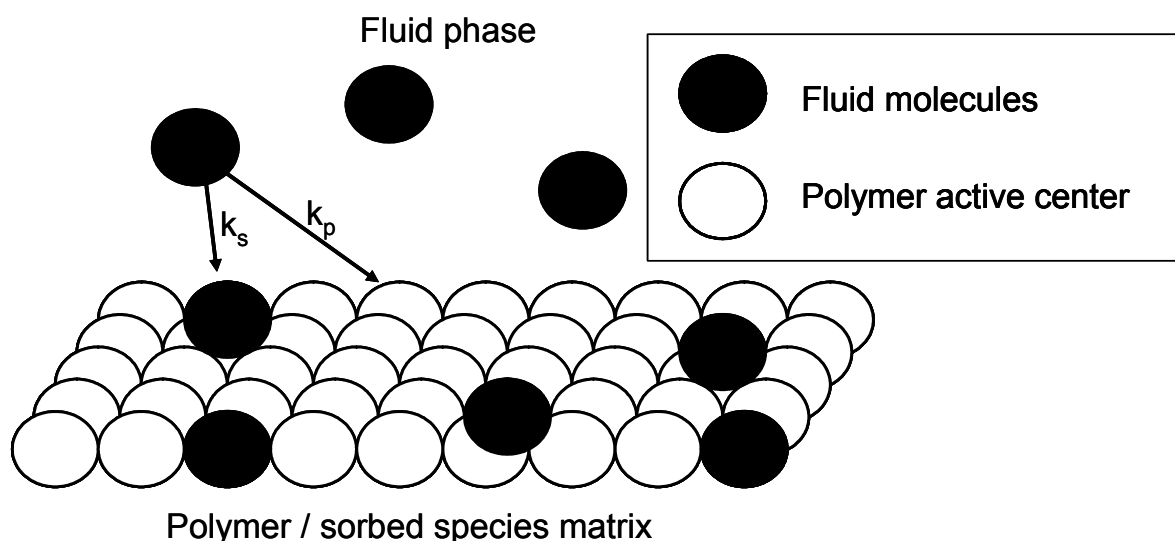


Figure 3.3 - Sorption of fluid molecules on a polymeric matrix.

According to the ENSIC model, k_p and k_s are the elementary affinity between the non-polymeric species and either a polymer segment or a previously sorbed molecule, respectively. Then, the volume fraction of the solvent on is related to its chemical activity by Eq. (3.15).

$$\phi_1 = \frac{e^{(k_s - k_p)a_1} - 1}{(k_s - k_p) / k_p} \quad (3.15)$$

Works on reverse osmosis and water permeation [14] used the ENSIC model, as well as for separation of ethanol-ETBE (ethyl tert-butyl ether) [15] and methanol-MTBE (methyl tert-butyl ether) [16] by pervaporation. However, for each ternary system, the model required 6 adjustable parameters.

In the current thesis, we are going to work with the Flory-Huggins approach, since the interaction parameters may be calculated without any adjustment from experimental data.

3.2 Membranes

A membrane is a physical barrier that allows separating a component from a mixture [17]. Each component permeates at a different rate through a membrane, and a better separation is achieved when the *permeability* coefficients of the components are different. The permeability coefficient is in fact a lumped parameter that integrates both the solubility and the diffusivity. Figure 3.4 illustrates the separation of a binary mixture by using a dense membrane.

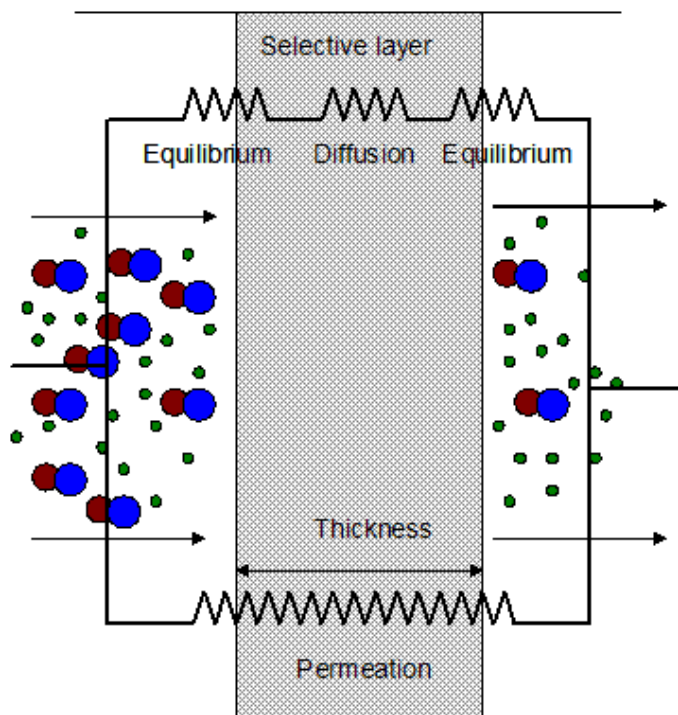


Figure 3.4 - Separation of a binary mixture by using a dense membrane.

In Figure 3.4 the permeation is shown as the product of the phenomena of equilibrium and diffusion, at the interfaces and through the membrane, respectively. If the external surface is dense, first a chemical equilibrium at the liquid-membrane interface is established. Then, the species are transported by diffusion to the opposite interface. Experimentally is easier to obtain a global transport coefficient, called permeability, than to obtain separately each contribution. The diffusion mechanisms inside the membrane are different if pores exist or not. If the membrane is porous, diffusion in liquids is dominant. On the other hand, if it is dense, the transported molecules diffuse in the free-volume among the molecules that form the membrane. The chemical equilibrium at the interfaces may be derived from thermodynamic relationships, such as the Flory-Huggins theory.

Concerning to the modeling of membrane processes, neural networks are commonly used if a large amount of experimental data is available. An example

is the dynamic modeling of milk ultrafiltration [18]. In this concrete case, such strategy was chosen instead of a phenomenological approach owing to the multiple interactions of the components of the colloidal suspension. An example of the network designed is represented in Figure 3.5.

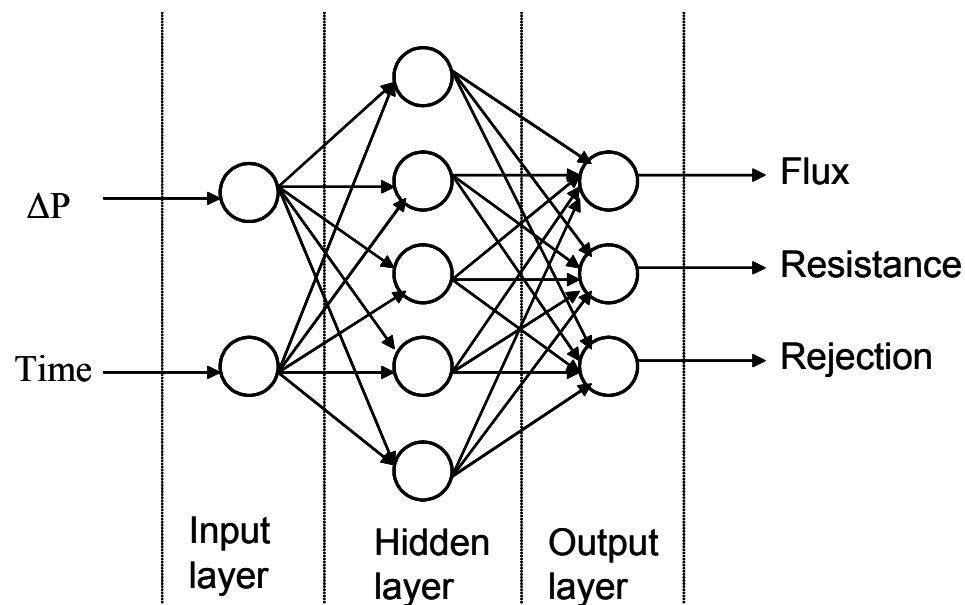


Figure 3.5 - A three-layered neural network.

In Figure 3.5, a three-layered neural network designed for the milk ultrafiltration problem is shown. This is a 2/5/3 configuration, with two inputs (transmembrane pressure and time), 5 hidden weighted functions and three calculated outputs (flux, rejection and resistance). In the paper, the authors commented that 675 experimental data were available, divided into three sets to develop the neural network: 84 data for training, 321 for validation and 270 for querying. They also concluded that a good prediction was obtained by just using a single hidden layer and a small number of training data. However, the neural network strategies do not contribute much to the knowledge of the process, since those parameters cannot be easily extrapolated to different systems. Other processes would require similar training steps.

A more phenomenological model would be more useful to both prediction and comprehension of membrane processes. Instead of working with lumped parameters, such as the permeabilities, it is possible to focus on properties that

just depend on the chemical structures of the components involved, such as diffusion and chemical equilibrium.

A scheme of free-volume diffusion, as well as the facilitated transport mechanism called *hopping* is shown in Figure 3.6, for the permeation of methanol (MeOH) and protons through a polymeric membrane.

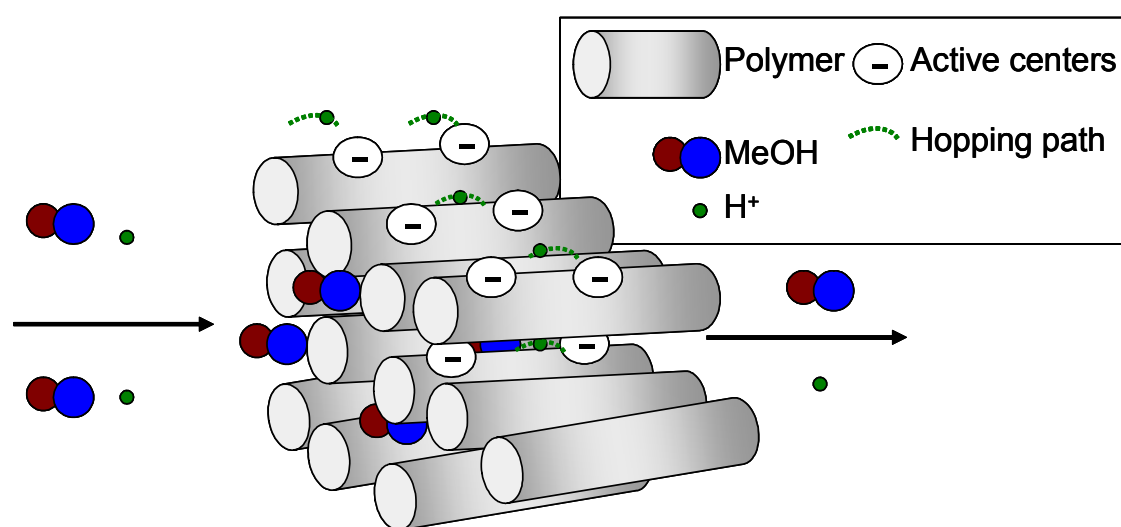


Figure 3.6 - Diffusion in polymers: free-volume and hopping mechanisms.

As seen in Figure 3.6, MeOH molecules diffuse among the in the *holes* among polymers, whereas protons jump through the negative active centers across the polymeric chains, following a hopping path [19]. The next section briefly explains the free-volume theory according to the Vrentas-Duda approach. We are not going to focus on the hopping mechanisms, because they are out of the scope of this thesis, and will be a subject for further works.

3.3 Diffusion in polymers: the Vrentas-Duda free-volume theory

Among the approaches for diffusion of components in polymers, the Vrentas-Duda free-volume theory accurately correlates polymer-solvent behavior over a wide range of concentration and temperature [7]. To describe a ternary system, for example, four diffusion coefficients are needed, whose prediction involve the

knowledge of the friction factors responsible for the self and mutual diffusion in mixtures [20]. Then, the diffusion of a pair i-j may be determined by using the following general equation:

$$D_{ik} = \frac{\rho_i}{RT} \sum_{\substack{j=1 \\ j \neq i}}^3 \phi_j \left(D_i \frac{\partial \mu_i}{\partial \rho_k} - D_j \frac{\partial \mu_j}{\partial \rho_k} \right) \quad (3.16)$$

The mutual coefficients D_k in Eq.(3.16) may be written down in terms of the free-volume parameters (solvent:1; non-solvent:2; polymer:3) :

$$D_1 = D_{01} \exp\left[-\frac{E_1}{RT}\right] \exp\left[-\frac{w_1 V_1 + w_2 \frac{\xi_{13}}{\xi_{23}} V_2 + w_3 \xi_{13} V_3}{\hat{V}/\gamma}\right] \quad (3.17)$$

$$D_2 = D_{02} \exp\left[-\frac{E_2}{RT}\right] \exp\left[-\frac{w_2 V_2 + w_1 \frac{\xi_{213}}{\xi_{13}} V_1 + w_3 \xi_{23} V_3}{\hat{V}/\gamma}\right] \quad (3.18)$$

$$\text{where } \hat{V}/\gamma = \sum_{i=1}^3 \phi_i \left(\frac{K_{1i}}{\gamma} \right) (K_{2i} - T_{gi} + T) \quad (3.19)$$

Expanding Eq.(3.16) in terms of the volume fractions of the components, we have the following diffusion coefficient matrix:

$$\begin{aligned} D_{11} &= D_1 \phi_1 (1 - \phi_1) \frac{1}{RT} \frac{\partial \mu_1}{\partial \phi_1} - D_2 \phi_1 \phi_2 \frac{1}{RT} \frac{\partial \mu_2}{\partial \phi_1} \\ D_{12} &= D_1 \phi_1 (1 - \phi_1) \frac{V_2}{V_1} \frac{1}{RT} \frac{\partial \mu_1}{\partial \phi_2} - D_2 \phi_1 \phi_2 \frac{V_2}{V_1} \frac{1}{RT} \frac{\partial \mu_2}{\partial \phi_2} \\ D_{21} &= D_2 \phi_2 (1 - \phi_2) \frac{V_1}{V_2} \frac{1}{RT} \frac{\partial \mu_2}{\partial \phi_1} - D_1 \phi_1 \phi_2 \frac{V_1}{V_2} \frac{1}{RT} \frac{\partial \mu_1}{\partial \phi_1} \\ D_{22} &= D_2 \phi_2 (1 - \phi_2) \frac{1}{RT} \frac{\partial \mu_2}{\partial \phi_2} - D_1 \phi_1 \phi_2 \frac{1}{RT} \frac{\partial \mu_1}{\partial \phi_2} \end{aligned} \quad (3.20)$$

where the chemical potentials are given by Flory-Huggins model:

$$\frac{\mu_1 - \mu_1^0}{RT} = \ln \phi_1 + \phi_3 + (\chi_{12}\phi_2 + \chi_{13}\phi_3)(1 - \phi_1) - \chi_{23}\phi_2\phi_3 \quad (3.21)$$

$$\frac{\mu_2 - \mu_2^0}{RT} = \ln \phi_2 + \phi_3 + (\chi_{12}\phi_1 + \chi_{23}\phi_3)(1 - \phi_2) - \chi_{13}\phi_1\phi_3 \quad (3.22)$$

The procedures to calculate all the parameters required may be summarized in Figure 3.7. The methods to obtain the molar volumes and the Flory-Huggins interaction parameters were already discussed in the previous sections. We can see that the properties can be divided into a free-volume group and a thermodynamic group.

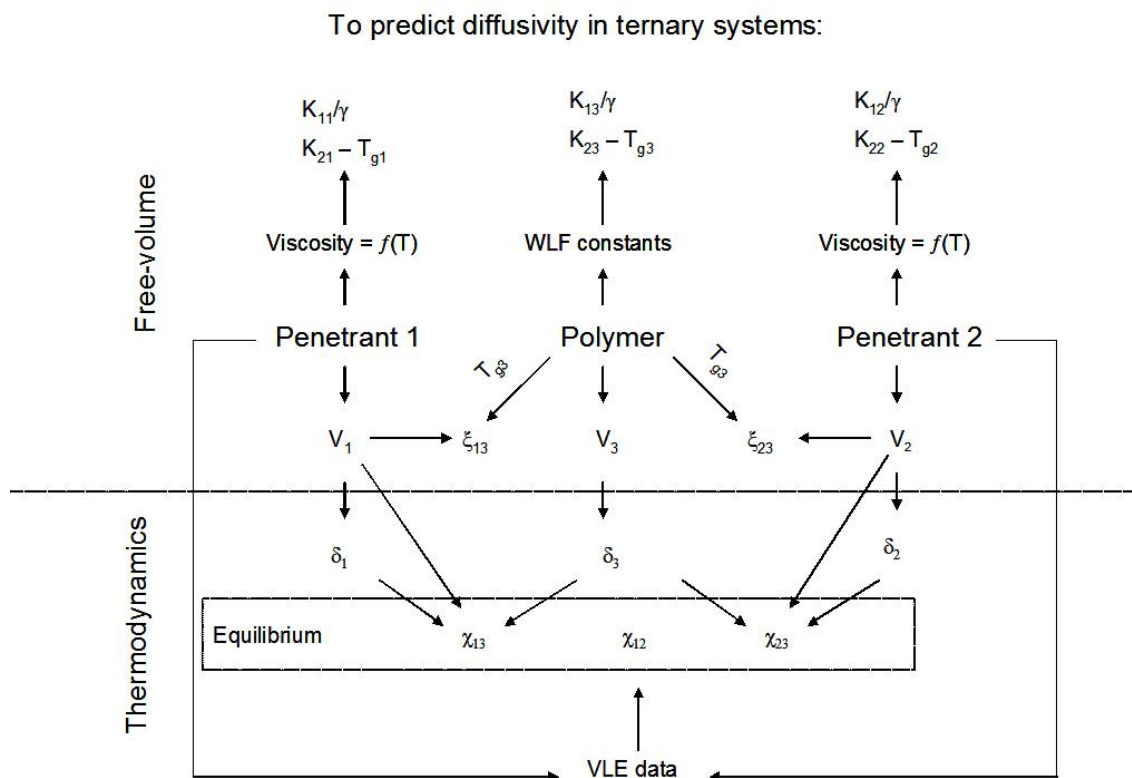


Figure 3.7– Calculation procedures to obtain the parameters for free-volume predictions

A key parameter in the free-volume theory is the ratio between the molar volume of the solvent (or non-solvent) and the molar volume of the jumping unit. If we consider that the diffusing molecules are small and move as single units, such ratio is expressed by Eq. (3.23) [7]:

$$\xi_{i3} = \frac{V_i}{V_{3j}^*} = \frac{M_i V_i^*}{M_{3j} V_3^*} \quad (3.23)$$

On the other hand, polymer molecules just exhibit segmental motion, what requires us to obtain the properties of the jumping unit, like the molar volume and the molecular mass. By dividing the molar mass of the jumping unit by that one of the monomer, Zielinski & Duda [7] demonstrated that the size of the polymer segmental motion unit is larger for stiffer molecules than for more flexible ones. Therefore, such property could be correlated to the glass transition temperature, which is an indicator of chain stiffness:

$$V_{3j}^*(\text{cm}^3 / \text{gmol}) = 0.6224T_{g3}(K) - 86.95 \quad (3.24)$$

Later such correlation has been extended [21] to take into account the difference of the glass transition temperature:

$$V_{3j}^*(\text{cm}^3 / \text{gmol}) = \begin{cases} 0.0925T_{g3}(K) + 69.47 & \text{for } T_{g3} < 295K \\ 0.6224T_{g3}(K) - 86.95 & \text{for } T_{g3} \geq 295K \end{cases} \quad (3.25)$$

Viscosity is considered as a transport property governed by the free-volume. Therefore, the remaining free-volume parameters for the penetrant species may be calculated from low-temperature viscosity data:

$$\ln \eta_1 = \ln A_1 + \frac{\left(\frac{\gamma \mathcal{W}_1}{K_{11}} \right)}{K_{21} - T_{g1} + T} \quad (3.26)$$

Once the free-volume parameters for the penetrants are calculated, it is possible to regress the pre-exponential factor D_0 and the activation energy for diffusion by using Eq.(3.27):

$$\ln\left(\frac{0.124 \times 10^{-16} V_c^{2/3} RT}{\eta_1 M_1 V_1}\right) = \ln D_0 - \frac{E}{RT} - \frac{\gamma \mathcal{W}_1 / K_{11}}{K_{21} - T_{g1} + T} \quad (3.27)$$

In many cases, however, the activation energy is neglected [20,22]. The parameters for the polymer may be calculated from the Williams-Landel-Ferry (WLF) theory, by regressing them from relaxation studies [7,21,23]. Extensive lists of WLF constants are available in literature, and their relation with the free-volume parameters are shown in Eqs (3.28) and (3.29):

$$\frac{K_{13}}{\gamma} = \frac{V_3}{2.303 c_{12}^{WLF} c_{23}^{WLF}} \quad (3.28)$$

$$K_{23} = c_{23}^{WLF} \quad (3.29)$$

Alternatively, if there is a curve of relaxation time as a function of temperature, the WLF constants may be obtained by using Eq.(3.30) once a reference temperature T_s is chosen:

$$\log \frac{\tau}{\tau_s} = - \frac{c_{13}^{WLF} (T - T_s)}{c_{23}^{WLF} + (T - T_s)} \quad (3.30)$$

Finally the only missing property is the penetrant-penetrant Flory-Huggins interaction parameter, that may be obtained from vapor-liquid equilibrium (VLE) data according to Eqs.(3.31) and (3.32) [24]:

$$\frac{\Delta G^E}{RT} = \sum x_i \ln \gamma_i \quad (3.31)$$

Once the excess Gibbs free energy is calculated, for each point of the VLE curve, a corresponding interaction parameter is obtained:

$$\chi_{12} = \frac{1}{y_1\phi_2} \left(y_1 \ln \left(\frac{y_1}{\phi_1} \right) + y_2 \ln \left(\frac{y_2}{\phi_2} \right) + \frac{\Delta G^E}{RT} \right) \quad (3.32)$$

The interaction parameter finally becomes a polynomial function varying with the volume fraction of one penetrant as in Eq.(3.33):

$$\chi_{12} = \sum_{i=1}^5 c_i \phi_2^{i-1} \quad (3.33)$$

The dependence of the model on published VLE data may be eliminated by using the UNIFAC method, since the literature cannot provide binary data for all existing systems. For the moment, however, we did not use this method in our calculations.

3.4 Obtention of polymeric membranes

The obtention of membranes from polymeric solutions depend on several factors, such as the choice of the solvent and non-solvent, as well as the initial polymer concentration [25]. Good examples of how the variation of those parameters affect the formation of the membrane are shown in Figure 3.8.

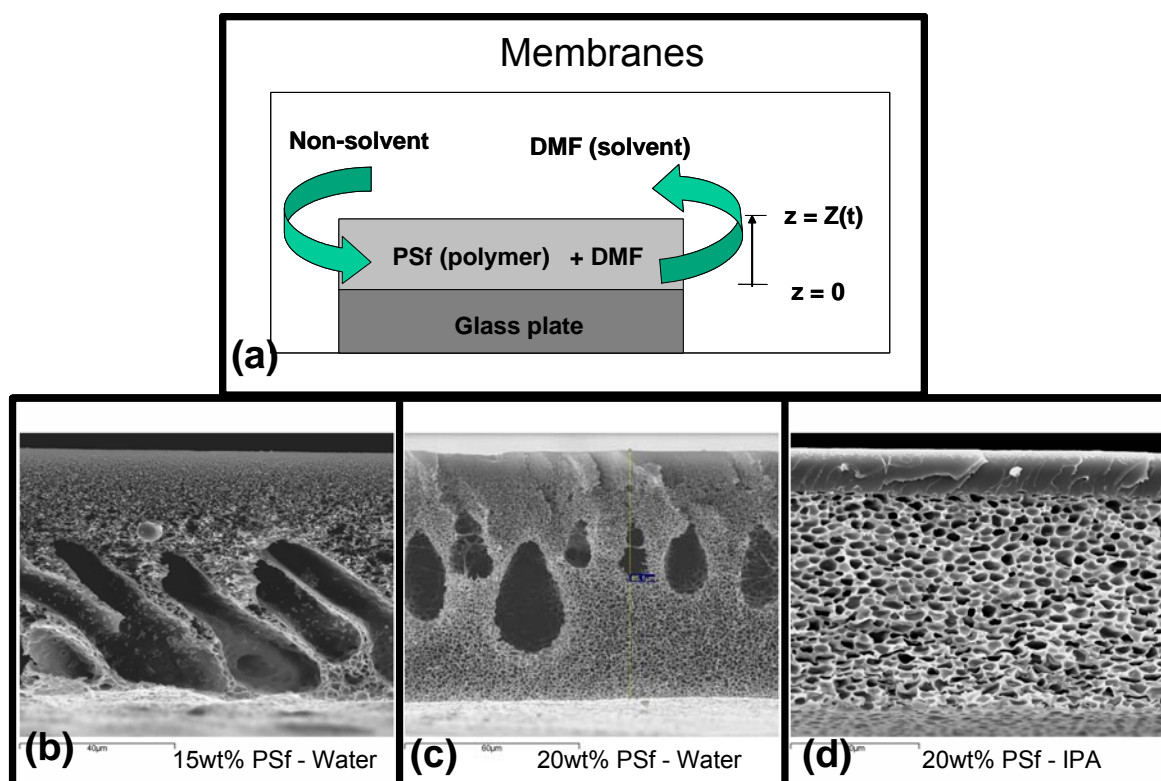


Figure 3.8 – Different membrane structures obtained by varying polymer concentration and non-solvent².

In Figure 3.8 there is the scheme of the formation of a polymeric membrane (a). From initial solutions of 15 wt% and 20 wt% of polysulfone (PSf) in N-N-dimethylformamide (DMF), the porous structures shown in (b) and (c) are obtained, by precipitation of the polymeric solution in water. On the other hand, if a solution of 20wt% of PSf in DMF is precipitated in 2-propanol (IPA), more regular structures (d) are formed. The product of the immersion precipitation is definitely dependent on the conditions of the casting bath, especially on the equilibrium between the polymeric phase and the surrounding liquid phase.

For a ternary system, the Gibbs free energy of mixing for a polymeric solution may be expressed by the following equation [24]:

$$\frac{\Delta G}{RT} = n_1 \ln \phi_1 + n_2 \ln \phi_2 + n_3 \ln \phi_3 + \chi_{12} n_1 \phi_2 + \chi_{13} n_1 \phi_3 + \chi_{23} n_2 \phi_3 \quad (3.34)$$

² The SEM images in Figure 3.8 were obtained by Carles Torras.

By using Eq. (3.34) it is possible to determine the spinodal curve, which is the line where all concentrations fluctuations lead to instability, leading to phase separation. The spinodal may be obtained by the following matrix:

$$|G| = \begin{vmatrix} G_{22} & G_{23} \\ G_{32} & G_{33} \end{vmatrix} = 0 \rightarrow G_{22}G_{33} = G_{23}G_{32} \quad (3.35)$$

where $G_{ij} = \frac{\partial^2 G_M}{\partial \phi_i \partial \phi_j}$ (3.36)

and $G_M = \frac{V_1}{\sum n_i V_i} \frac{\Delta G}{RT}$ (3.37)

The ternary diagram for the system PSf-DMF-H₂O [26] is shown in Figure 3.9, with the liquid-polymer equilibrium and spinodal lines.

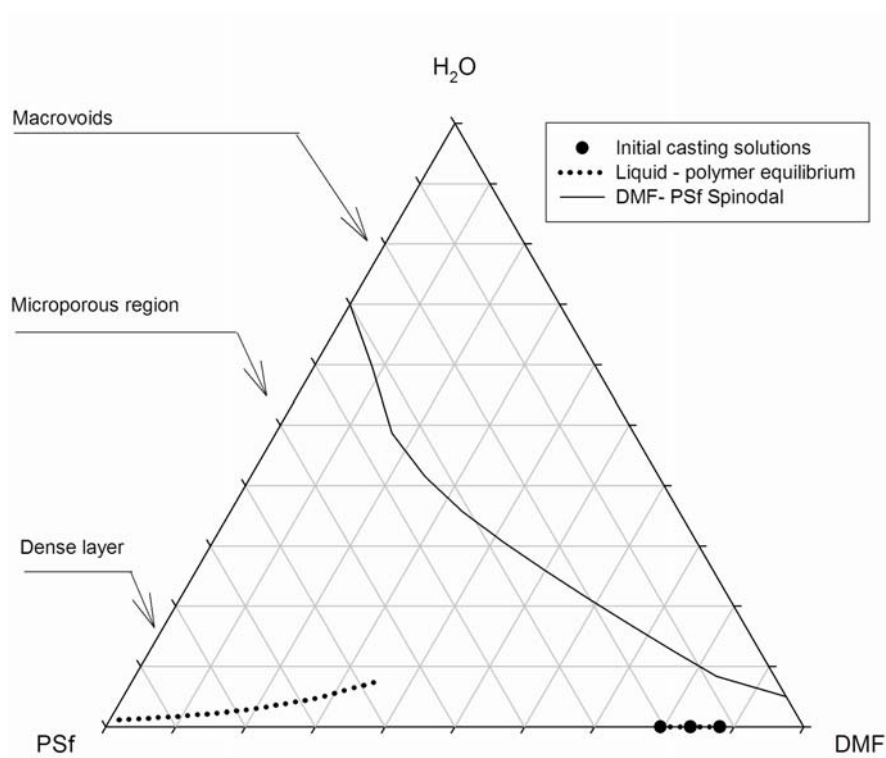


Figure 3.9– PSf-DMF-Water phase diagram.

The ternary diagram in Figure 3.9 represents the spinodal curve, the line that marks the composition where the polymer precipitates and forms the membrane. A successful modeling, by applying the concepts explained in the previous sections, would be able to draw the composition path from the initial casting solutions to the indicated regions, determining the right composition of the top dense layer, the macrovoids zone and the microporous region.

3.5 Production of polymeric microcapsules by using micromixers

Microcapsules have applications of high technological impact, such as the controlled release of drugs and perfumes, and they are composed by a polymeric dense shell covering a core full of product. The polymeric shell may have varying structure and even be porous, but its most external layer should be dense, in order to control the release rate of the product. Much attention has been done to the interfacial polymerization (a.k.a *in situ* polymerization), where droplets of a monomer solution are put in contact with a solution of a second monomer, and reaction is produced at the external surface of the droplet, reducing the kinetic reaction as long as the dense layer is formed, blocking the entrance of the external monomer and further stopping the polymerization reaction. Some good examples are the production of poly(urea-urethane) microcapsules [27] and the encapsulation of lemon oil in urea-formaldehyde [28].

Another way to produce microcapsules is dissolving both the product to be delivered and the polymer in a determined solvent. Then, microcapsules may be produced by precipitating droplets of the product-polymer solution into a non-solvent phase, in a similar way to the formation of membranes by immersion precipitation [29].

The production of microcapsules may be performed by using microchannel-based mixers, shortly called *micromixers*, that have wide applications in chemical engineering, being absorption, emulsification, foaming and reaction just some of them [30]. Microchannel-based reactors may perform at near

isothermal conditions even extremely exothermic or endothermic reactions, or controlled conversion of explosive mixtures [31]. Liquid-liquid mixing in those devices was extensively studied for several geometries [32]. The expression *micromixers* broadly designates chemical systems manufactured with techniques originally developed for electronic circuits [33]. A typical micromixer is shown in Figure 3.10, as well as its internal chip-like mixing element [34].

In Figure 3.10, the housing of the micromixer is shown externally (a) and internally (b), as well as the mixing elements (called *LIGA tool*). Typical widths of the microchannels are around $25\ \mu\text{m} - 40\ \mu\text{m}$ [35]. In (d) part, the operation of the microreactor is described. Two immiscible liquids are piped into the housing, and they mix in the LIGA tool element, flowing out of the micromixer by the outlet line in the top plate. Therefore, this conformation of micromixer allows the preparation of emulsions.

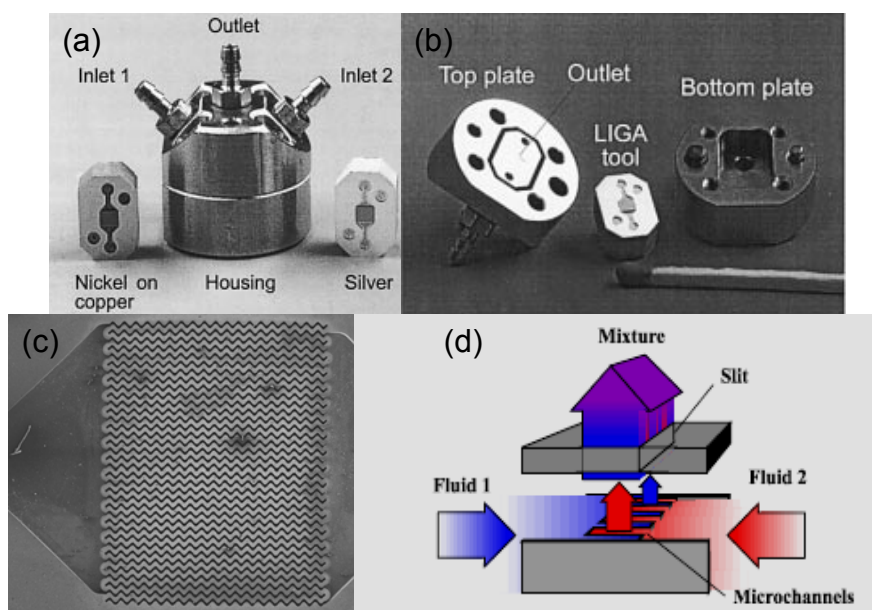


Figure 3.10 - Typical micromixers: (a). external view, with silver and nickel mixing elements; (b): disassembled micromixer; (c). SEM image of microchannels; (d): operation mode.

The emulsification of liquids involves a lot of parameters. Key factors are the viscosities of the liquids to be mixed, and the flow regime [36]. Depending on the cases, increasing the flow rates of the continuous phase would lead eventually to the formation of droplets rather than plugs, what happens in low flow rate regimes. It is not necessary, however, to have Reynolds number bigger than the unity. In fact, some studies proved, as in the case of the crystallization of barium sulfate nanoparticles [37], reduced size particles were obtained while operating the micromixer at high flow rates. So, if the objective is the production of perfectly spherical particles of a determined size, it is mandatory to find the optimal flow rate.

At low Reynolds number the dominant mechanism of formation of droplets may be the Rayleigh-Taylor instability theory [38]. At a liquid-liquid interface, when the light fluid pushes the heavy fluid with an acceleration above a critical value, droplets are ejected from the heavy fluid bulk.

Concerning polymers, an interesting application of the micromixers is the production of polymeric membrane microcapsules, possibly providing less dispersion of sizes than precipitation by batch mode [39]. However, in this case, two micromixers should be arranged in a series: the first one to promote the emulsification, and the second one to precipitate the microcapsules, in a similar way than the production of flat-sheet membranes, as explained before. We assume that the non-solvent delivered to the system should be at least enough to clean the surface of the polymeric droplets from the continuous phase. Otherwise, non-spherical structures would be formed. Figure 3.11 represents the possible steps of the formation of the microcapsules soon after the formation of the droplets.

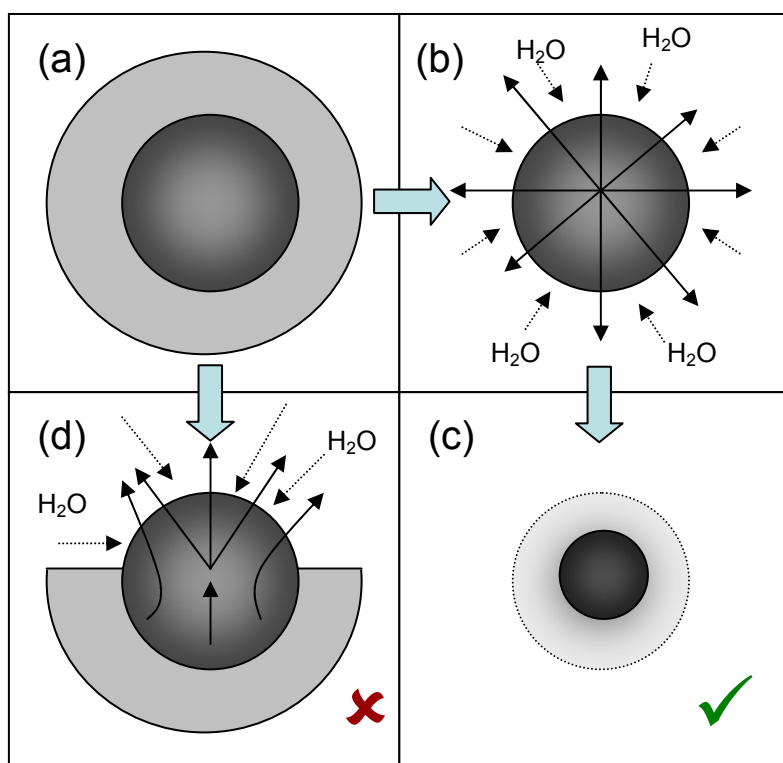


Figure 3.11 – Schematic representation of a possible mechanism for the formation of microcapsules. Steps:(a) droplet of polymeric solution surrounded by cyclohexane; (b) DMF leaves the droplet in the radial direction; (c) final capsule formed, hatched part is the final diameter and the grey part, the loss of mass during precipitation; (d) still remains cyclohexane in the surface of the droplet.

Figure 3.11 shows schematically the precipitation of the droplet. The formation path from (a) to (c) summarizes the steps required to the proper precipitation. The flow of water should be enough to complete wash away the layer of the continuous phase covering the droplet surface. Then, in (b), the extraction of solvent from the polymeric solution can occur symmetrically in the radial direction, generating a perfect microcapsule (c) by the balances of momentum. On the other hand, if the flow rate of non-solvent is not enough to clean the surface of the polymeric droplets, the fast inversion phase process generates structures that are not perfectly spherical (d). However, such assumptions should be confirmed by further modeling. The application of the free-volume theory also will be helpful to build the precipitation paths of the formation of the microcapsules membrane, as in the case of the flat-sheet membranes.

3.6 Direct methanol fuel cells

Recent applications of membranes are polymer-electrolyte membrane fuel cells (PEMFC), which obtain energy from the oxidation of hydrogen to water. In this case the membrane electrode assembly consists of gas diffusion layers, an anode, a proton exchange membrane and a cathode. Use of hydrogen to mobile applications implies in large fuel reservoirs that require a certain pressure. For safety reasons, a liquid fuel may be more appropriate and methanol is presented as an alternative, since energy can be directly obtained from its reduction to carbon dioxide and the oxidation of the produced proton to water.

Chemistry of methanol has been intensively studied, since it is an important alternative source of energy, but published papers are mainly focused on direct methanol oxidation to generate energy or methanol reforming to produce hydrogen for fuel cells [40]. In 2001, researchers commented that seeking alternative sources of energy would be stimulated if crude oil prices went beyond US\$20/barrel [41] and among liquid fuels methanol seems much more promising than ethanol. We guess that there is no need to comment the everyday rise of oil prices.

For cleaner environment, fuel cells are considered to be a promising energy alternative. The most representative kinds of fuel cells are the PEMFC and the direct methanol fuel cell (DMFC), that use proton conducting membranes [42]. Among PEMFCs, DMFC is considered to be very promising, because its theoretical potential is higher than the hydrogen-based PEMFCs [43], also allowing simple liquid handling.

Figure 3.12 shows a schematic representation of a DMFC single cell.

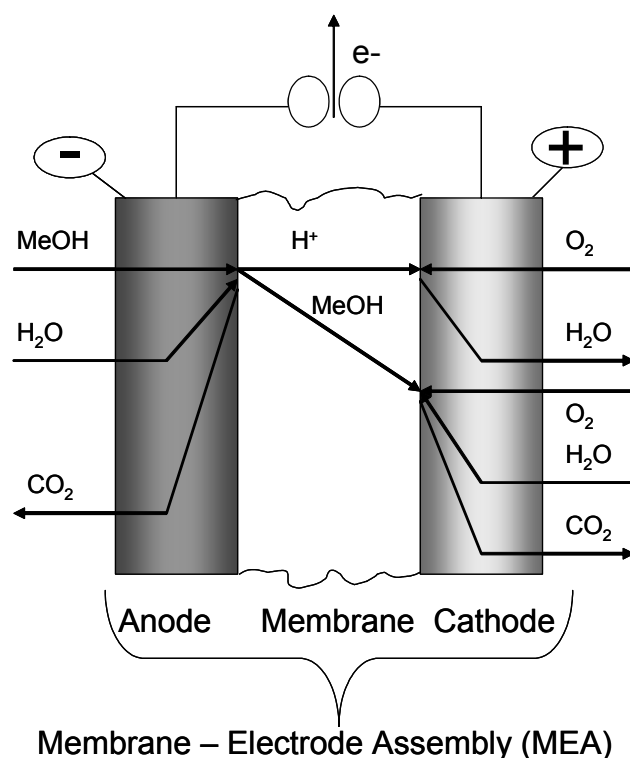
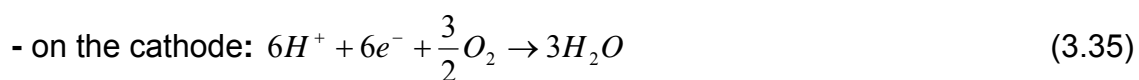
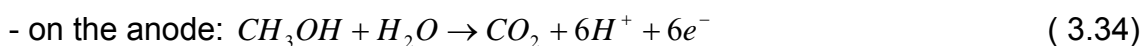


Figure 3.12 - Schematic diagram of a direct methanol fuel cell (DMFC).

On the porous anode, electrochemical oxidation of the methanol occurs, producing carbon dioxide, protons and electrons. The protons diffuse through the membrane to the cathode side, where they react with the oxygen in order to produce water. The chemical reactions are described below [44]:



The most used membranes for DMFC are the perfluorinated sulfonated NAFION® membranes of DuPont, owing to their chemical stability, high conductivity and high permeability to protons. However, such membranes also allow methanol to permeate, reducing electrochemical process efficiency, increasing consumption of fuel and also damaging the own cell. Such phenomenon is known as *methanol crossover*, and several authors have reported its influencing factors, such as cell temperature, cathode pressure,

methanol concentration and catalyst morphology [45,46]. Therefore, other membranes are being tested and results are compared to NAFION® [44,47,48], with better ratio conductivity / methanol permeability.

Fuel cells performance may be theoretically obtained by exergetic analysis [49] and compared with efficiencies of internal combustion engines. Exergy represents the maximal work obtained in any process and for fuel cells many factors contribute to exergy losses, such as:

- Activation polarization due to finite electrocatalysis;
- Ohmic resistances in membrane electrode assembly;
- Mass transport limitations;
- Incomplete reaction;
- Irreversible heat transfer and mixing processes;
- Products and heat exhausted at temperatures higher than environment temperature.

The exergetic approach would be an interesting tool to optimize thermodynamically the fuel cells.

It is clear that the range of topics involved in the design and operation of a fuel cell is so wide that, to have a complete portrait, researchers should follow the advances of several areas of knowledge: catalysis, membrane technology, polymers, transport theories, among many others. We collected information mainly by using the search tool ScienceDirect (www.sciencedirect.com) of numbers of papers containing the keywords *DMFC* and *modeling* related to fuel cell technology and we analyzed the evolution of entries from late 2003 to 2007. To complement such information, we also collected data of the impact index of those publications compared to traditional publications of Chemical Engineering. Both collection of data demonstrate the increasing interest in fuel cells and serve as a guide to search information.

The impact index of any journal may be provided by the ISI Web of Knowledge® (isiknowledge.com), from The Thomas Corporation. For a determined journal, the impact index is the ratio of the number of its cited papers in indexed publications to the total amount of published papers, calculated on a three-year basis. For scientific community it represents therefore how important is a journal, related to other journals in similar areas. We grouped the publications into five categories: catalysis, polymers, membranes, fuel technology and chemical engineering, as seen in Figure 3.13.

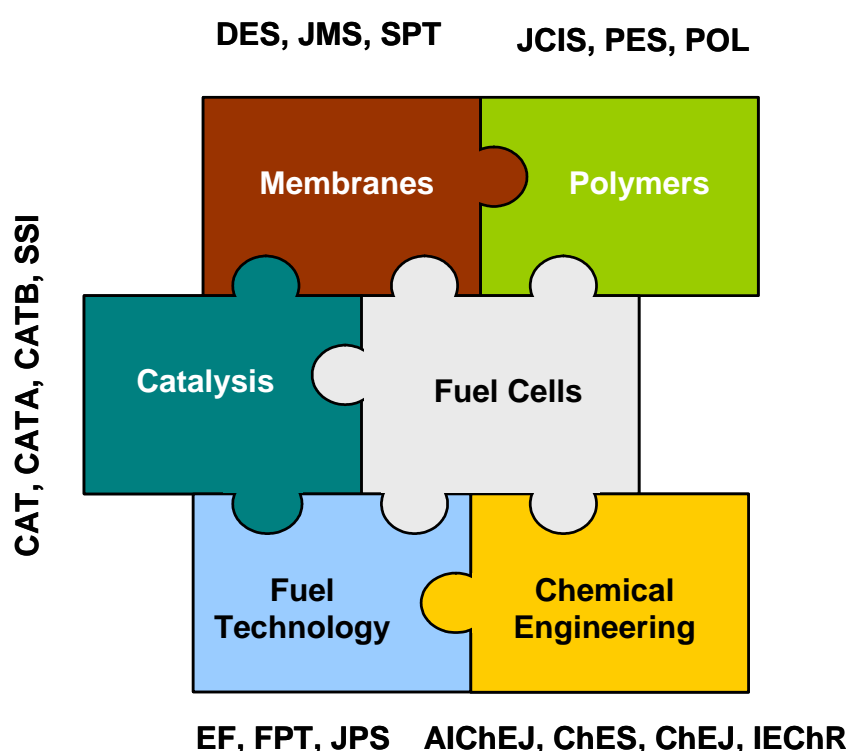


Figure 3.13 - Groups of publications.

Figure 3.13 illustrates how fuel cells are related to the groups we defined. The complete name of each journal is in the nomenclature section. The journals were chosen according to our experience in searching information; there were no other criteria. Different groups could be suggested. For those groups, Figure 3.14 shows the evolution of impact index for each journal and behavior is analyzed separately for each category.

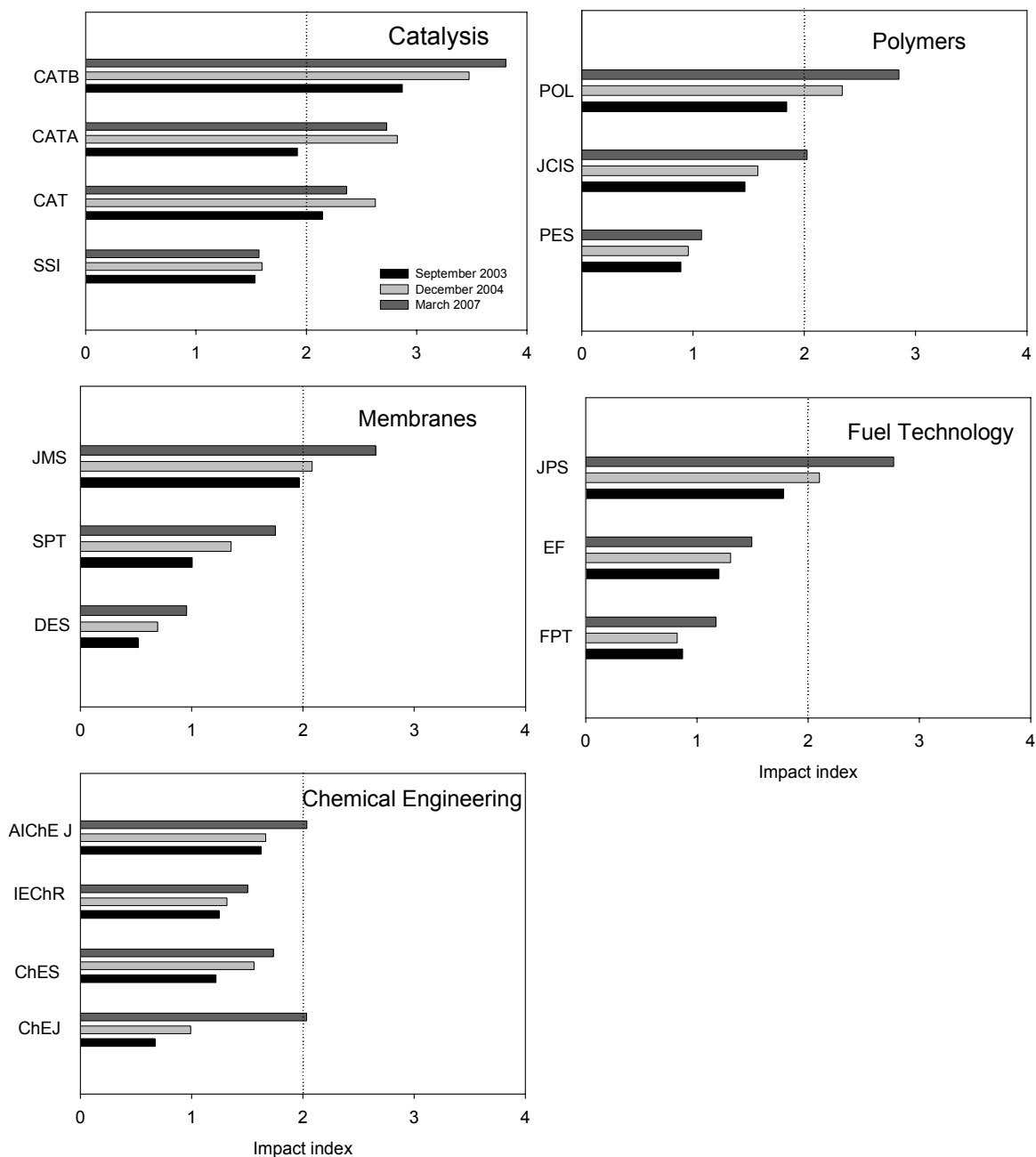


Figure 3.14 – Variation of impact index of fuel-cell related publications.

Among the groups shown in Figure 3.14, catalysis journals have the highest impact indexes. As expected, CATB has the highest number, owing to the worldwide interest in environmental issues. In the same period that the chemical engineering journals maintained a stable behavior, polymer, membranes and fuel technology journals experienced a significant increase in impact index.

Many factors should have contributed to such panorama, for the notorious advantages of the novel technologies, such as fuel cells.

Tools like ScienceDirect make much easier the time-consuming task of bibliographic review; many of us still remember how was research before the advent of internet, spending hours in the libraries to consult papers that very often were already outdated soon after publication. Any expression can be typed, but sometimes they results are quite confusing, especially if the topic has wide and different applications such as 'characterization membrane' (9516 entries in 03.27.07) or 'modeling membrane' (2618 entries in the same day). In this sense the acronym DMFC is quite positive, since it will not provide misleading results. Figure 3.15 summarizes the papers containing 'DMFC' in April 2007.

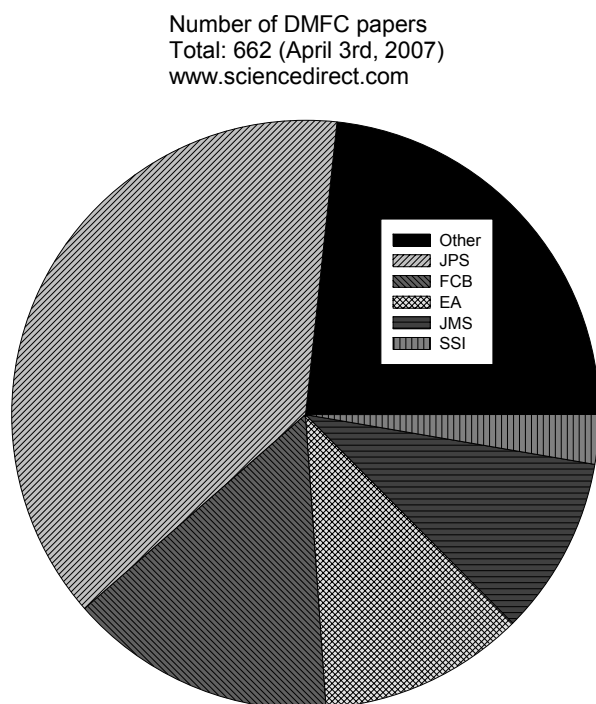


Figure 3.15 – DMFC in www.sciencedirect.com

In Figure 3.15 we observe that a significant number of articles dealing with DMFC is published in JPS and FCB, that are obvious information sources for fuel cells. However, an important number of articles is also found in EA, owing to the electrochemical reactions, followed by membrane technology (JMS) and

a catalysis journals (SSI). Therefore, any search of information in other catalysis journals (CAT, CATA, and CATB) would be useless, since researchers do not usually publish DMFC papers there (in April 3rd, 2007, just 8 papers were found in CAT and no papers in CATA and CATB).

In spite of all the interest regarding DMFCs, just a few efforts are being made in order to propose mathematical modelling comprising the mass transfer mechanism through the membrane [44,50]. Figure 3.16 compares the entries for the expression 'modeling membrane' to those for the acronym 'DMFC', in JPS and JMS for the period from late 2003 to April 2007.

In Figure 3.16 we observe that during the last years occurred a significant increase of publications dealing with modeling of membranes, especially in JMS. However, the most impacting change was in the research oriented to DMFC, mainly published in JPS. As additional information, few papers on DMFC are being currently published in JMS and interest of modeling issues is increasing among JPS authors. On the other hand, if we search the combination of 'modeling' and 'DMFC', just 34 papers were found in whole ScienceDirect, 15 of them in JPS and just 2 on JMS. Therefore, there is still room for improvement in the modeling of DMFC. Recently an interesting review of the different currently used approaches was published [51], and works were classified according to their focuses, what is very useful for researches involving specific issues of fuel cells, such as transport theories, polarization phenomena and methanol crossover, among others.

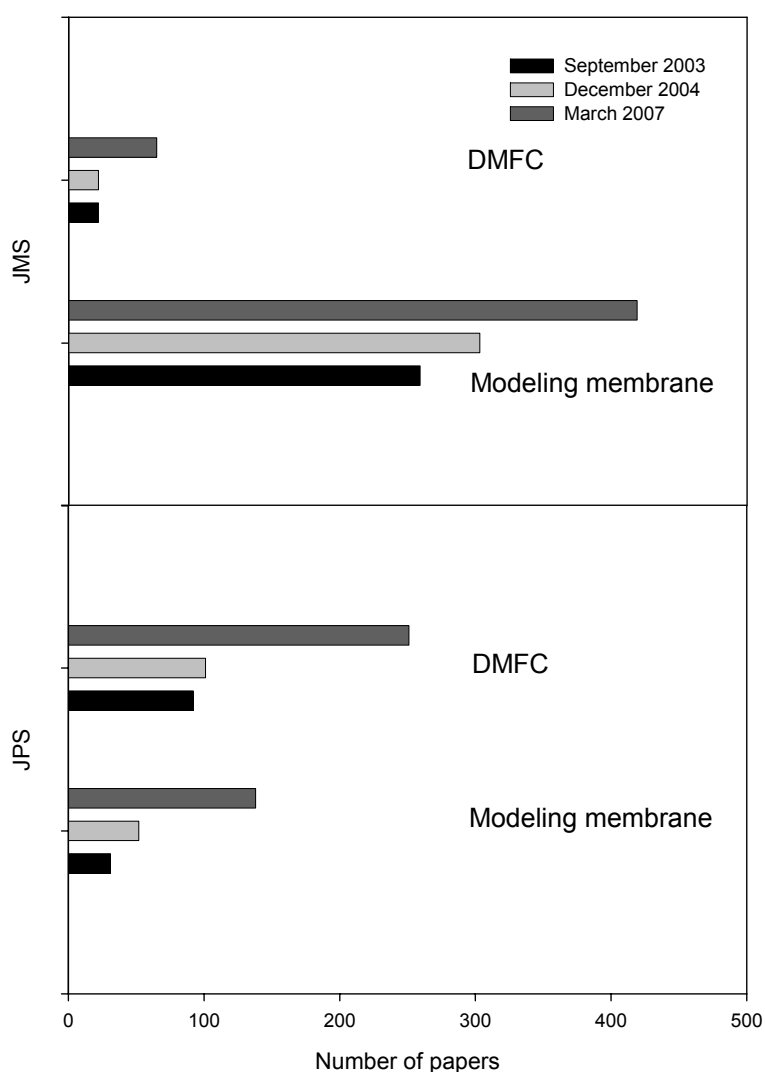


Figure 3.16 – Comparison between topics: *modeling membrane* and *DMFC*.

Experimental voltage-current curves of DMFCs were fitted to a mathematical model that included generation of protons on the anode, oxidation of methanol and its transport through the membrane, and also consumption of protons [52]. By using published data in which methanol concentration was 0.25M, fitting parameters to the model were obtained and then simulations were performed in order to build the voltage-current curves for methanol concentrations of 0.125M and 0.5M. There was a good agreement between simulated and experimental data, although the region of each curve corresponding to high current density and low cell voltage was not well predicted by the model, probably owing to the

fact that in this region also the fitted curve did not match correctly the experimental data. Also an expression for the optimal methanol concentration was derived, and the value found (0.97M) coincides with previously published experimental value. Several factors that make difficult the modeling of DMFCs were discussed, such as the controversial kinetics of methanol oxidation, poisoning of cathode surface by methanol permeation and high electroosmotic flux through the membrane owing to large amount of water on the anode side.

As exposed above, there is still room for improvement in DMFC modeling, either in the catalysis or in the membrane part. Especially, topics such as hopping and the diffusion of the chemical species in the polymeric structures deserve further attention.

3.7 General comments

As seen in the previous sections, the production of microcapsules and the operation of fuel cells depend on the properties of polymers. Therefore, the knowledge of interaction of the polymeric species either with the transported components or with solvents / non-solvents is mandatory to the optimization of those processes. In the case of fuel cells, it will be helpful to find materials suitable to maximize proton conductivity, reducing simultaneously the methanol crossover. For the encapsulation of perfume, it will be important not only to predict transport properties, but also to optimize design by choosing the most suitable materials.

4 Discussion and indicators of published articles

To the date of the publication of this thesis, three articles were already published in international journals and one was accepted and is in press now. In this section we present some impact data about the journals, and information about the papers, such as presentation in congress and number of citations, if any. The remaining articles are going to be submitted in the next weeks.

4.1 Impact information

The data collected in Table 4.1 were obtained in ISI Web of Knowledge, on May 2nd 2007.

Table 4.1- Impact information of categories.

Journal	Category	MIF	AIF	All
JPS	Electrochemistry	1.558	2.145	0.312
JPS	Energy & Fuels	0.590	1.078	0.164
PES	Polymer Science	0.926	1.784	0.299
PES, DES	Chemical Engineering	0.684	1.157	0.187
DES	Water Resources	0.875	1.220	0.174

Journals:

JPS: Journal of Power Sources – 2.77 (in 2005)

PES: Polymer Engineering and Science – 1.076 (in 2005)

DES: Desalination – 0.955 (in 2005)

Category data:

MIF: Mean Impact Factor

AIF: Aggregate Impact Factor

All: Aggregate Immediacy Index

4.2 Articles information

1. Title	Experimental and computational study of proton and methanol permeabilities through composite membranes
Authors	X. Zhang, L. Pitol-Filho, C. Torras, R. Garcia-Valls
Published in	Journal of Power Sources
Vol. (year) Initial – final page	145 (2005) 223-230
Communication in a congress	✓ Oral Poster Fuel Cells Science and Technology 2004 München (Germany)
Impact index of journal	2.77 (2005)
Cited by	Paper R. Bashyam, P. Zelenay. Nature 443 (2006) 63-66
	Presentation D.S. Cameron. Platinum Metals Rev. 49 (2005) 16-20.

In this article we presented a strategy to model the permeation of protons and methanol through a fuel cell membrane, based on mass transfer resistances. The developed model was used as a tool to interpret the experimental data for composite membranes made of polysulfone and poly(ethylene glycol) (PEG). We were able to conclude that the choice of a suitable porous support may enhance the overall selectivity. However, the model should be based on more advanced phenomenological theories of mass transfer through polymers to provide a more accurate description of the composite membrane. More experimental data than the presented would be also needed to support and validate the model.

In a following article entitled *Evaluation of poly(ethylene glycol) of different chain length as a potential selective layer for direct methanol fuel cells*, to be submitted, we used the Vrentas-Duda free volume theory to calculate the diffusive flux of water and methanol through a hypothetical PEG membrane. All

the needed data were regressed or correlated from literature. The simulations confirmed that the PEG of highest molecular weight is less selective to methanol than the others, as expected. However, those simulations should be later validated by experiments.

2. Title	A method for assessing the choice of polymeric materials for specific applications
Authors	L. Pitol-Filho, R. Garcia-Valls
Published in	Polymer Engineering and Science
Vol. (year) Initial – final page	In press
Communication in a congress	✓ Oral Poster Advanced Polymeric Materials 2006 Bratislava (Slovakia)
Impact index of journal	1.076 (in 2005)
Number of citations	-

In this article we presented a complete strategy to predict several properties of polymeric membranes, such as swelling degree and chemical equilibrium in ternary systems. We showed that the Flory-Huggins theory may predict accurately how a cellulose triacetate membrane swells in several organic components and that, in some cases, a three-dimensional approach provided better results than the classic model, as well as in the ternary system studied. We used that method as a tool to make a first guess while choosing a polymer to be a raw material for a direct methanol fuel cell.

The issue of the several methods presented in the literature to calculate all the parameters involved in the determination of the Flory-Huggins interaction parameter was explored in the article *Methods to calculate penetrant-polymer Flory-Huggins interaction parameters: comparison and validation*, to be submitted. In that article, predictions of molar volumes, total cohesion parameters and binary Flory-Huggins parameters were compared to data taken from literature for several systems. Our conclusion stressed the ones from the previous article, that the three-dimensional approach leads to lower deviations when predicted data are compared to published ones. However, still more

binary systems should be studied in order to improve the applicability criteria of this theory.

3. Title	Modelling of polysulfone membrane formation by immersion precipitation
Authors	L. Pitol-Filho, C. Torras, J. Bonet-Avalos, R. Garcia-Valls
Published in	Desalination
Vol. (year) Initial – final page	200 (2006) 427-428
Communication in a congress	Oral ✓ Poster Euromembrane 2006 Giardini-Naxos (Italy)
Impact index of journal	0.955 (in 2005)
Number of citations	-

In this article we presented a ternary diagram of the system N-N-dimethylformamide (DMF) – polysulfone (PSf) – water, with the spinodal curve, where phase separation should occur. However, this spinodal curve was built by using the water-PSf Flory-Huggins interaction parameter calculated by using the classic approach. Later we proved such binary parameter should be calculated by the three-dimensional model [53]. The spinodal curve calculated with the new parameter is shown in the Figure 4.1. The curve is more consistent with the reality, since it shows that a lower amount of water can promote the precipitation of the polymer, a fact that is easily observed experimentally.

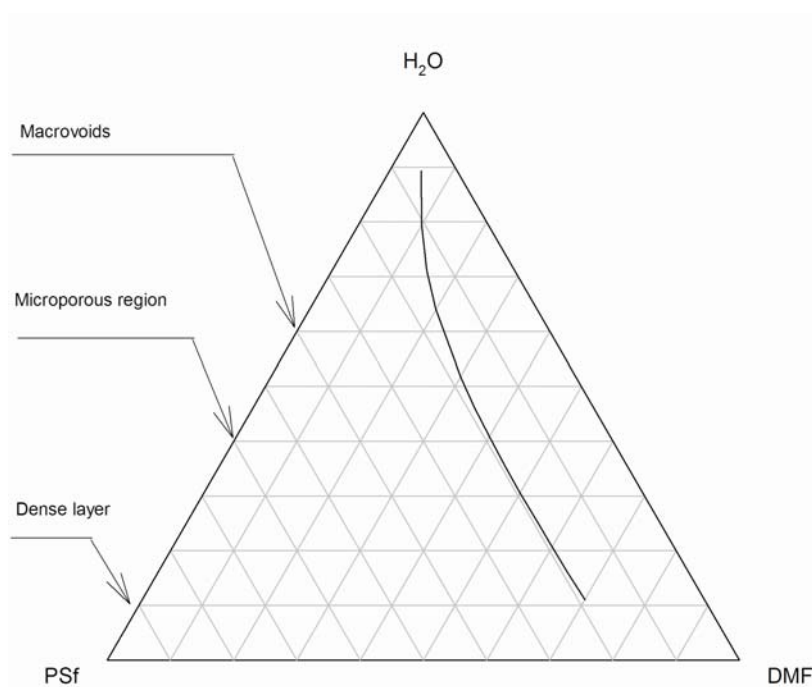


Figure 4.1 - Phase separation curve of the system DMF-water-PSf.

In Section 3.3, we discussed how to get the free-volume parameters for the polymeric systems from viscosity data and relaxation times. By using Hysys® (Hypotech), we obtained the viscosity curve of DMF with temperature at 101.33 kPa, to regress the DMF free-volume parameters. In the case of PSf, relaxation times are needed. Published data of relaxation times obtained by time-resolved light scattering for polyethersulfone [54] were used to regress the WLF constants, what allowed us to finally get approximated values for the PSf free-volume parameters. Table 4.2 relates all the data collected.

Table 4.2- Free-volume parameters for the system DMF(1) – PSf(2)

Component	DMF(1)	PSf(2)
$V, \text{cm}^3/\text{g}$	0.927	0.747
K_{1i}/γ	0.089	0.0002728
$K_{2i} - T_{gi}$	-263	-293
$E, \text{J/gmol}$	1777.13	-
$D_{01}, \text{cm}^2/\text{s}$	1.82E-05	-
$\chi_{i\text{-PSf}}$	0.9	-
$\xi_{i\text{-PSf}}$	0.3364	-

By using the data collected in Table 4.2, it is possible to calculate how the diffusivity of DMF varies with concentration in a binary system DMF-PSf. Figure 4.2 shows both the molecular diffusivity, which is calculated just by free-volume theory, and the mutual diffusivity, that includes the thermodynamic contribution.

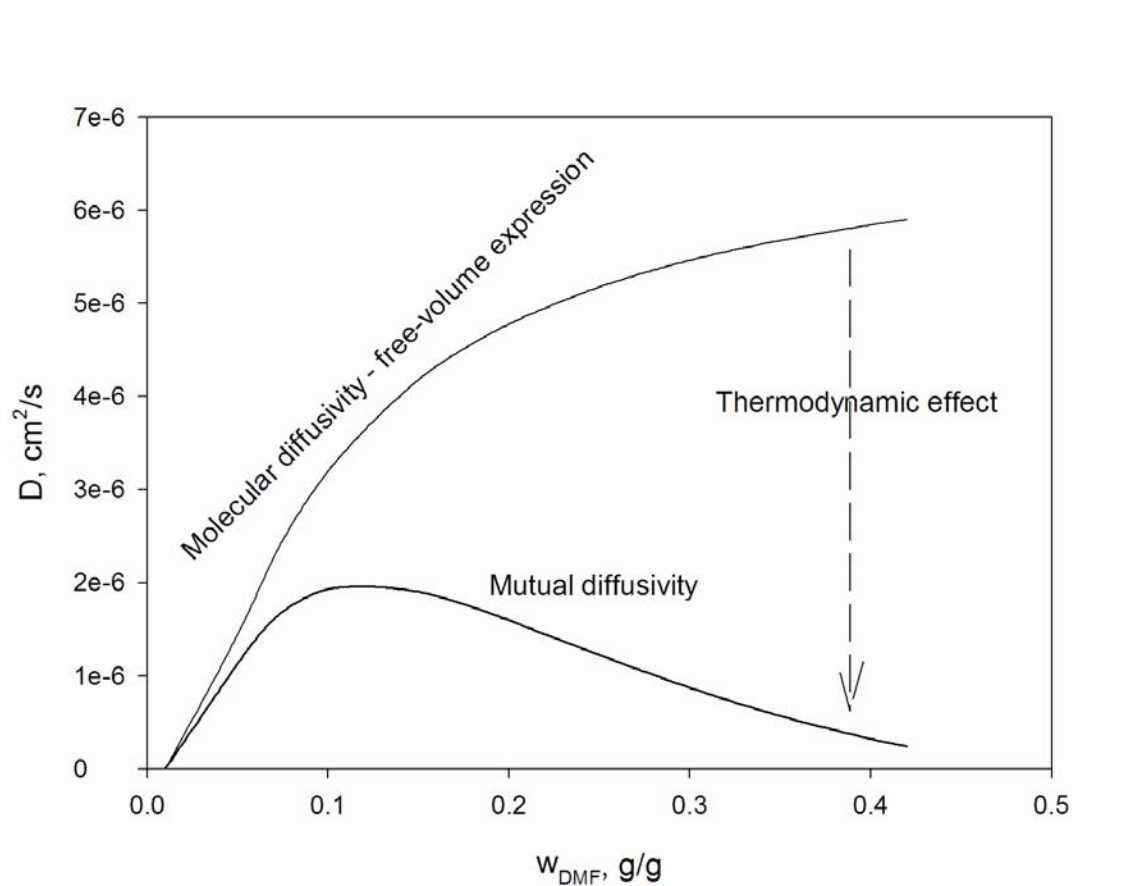


Figure 4.2- Molecular and mutual diffusivity of DMF in a binary system DMF-PSf.

Figure 4.2 allows to understand how the thermodynamics of the binary system affects the diffusivity of DMF. The molecular diffusivity tends to increase as far as the weight fraction of DMF increases, since there is more space among the polymer molecules for the diffusion of DMF. On the other hand, the thermodynamic interaction between polymer and solvent reduces the total diffusivity, and its effect is more significant as far as the solvent concentration increases, generating a maximal point in the diffusivity curve. The free-volume theory and the Flory-Huggins thermodynamic theory may be useful tools to derive a complete model able to predict the membrane formation, as in cases listed previously in Section 3.3.

4. Title	Novel polymeric membrane structures: microcapsules
Authors	C. Torras, D. Gezahegn, L. Pitol-Filho, R. Garcia-Valls
Published in	Desalination
Vol. (year) Initial – final page	200 (2006) 12-14
Communication in a congress	Oral ✓ Poster Euromembrane 2006 Giardini-Naxos (Italy)
Impact index of journal	0.955 (in 2005)
Number of citations	-

In this article we presented some preliminar results of microcapsules production by the immersion precipitation method, where a polymeric solution was dropped into water. As soon as the polymeric solution touched the water surface, the precipitation process started, forming the microcapsules. This mode of batch operation provided low efficiency of precipitation, wide distribution of diameters and formation of polymeric aggregates. An alternative to the batch mode is the continuous production of the microcapsules by using micromixers technology. In the article *Fluidic and thermodynamic insights on the formation of polymer microcapsules by using micromixers* we explored some aspects of the microcapsules production, by analyzing the flow regime and the thermodynamic equilibrium during emulsification, as well as results of encapsulation of vanillin (VNL) by varying the flow rate of the polymeric solution. We proposed a mechanism of microcapsules formation where the non-solvent plays a significant role, being necessary in a first moment to wash away the continuous phase from the external surface of the droplets of the polymeric solution and, then, to precipitate the polymer, forming spherical particles. However, such hypothesis should be confirmed by further experiments and modeling. Phase diagrams of the multicomponent systems will be useful tools to assess the formation of the structures.

5 Conclusions

The specific conclusions from the thesis may be condensed into three subjects: thermodynamics, microcapsules and fuel cells.

5.1 Thermodynamics

To explain the behavior of penetrant-polymer systems, a popular approach is the Flory-Huggins theory, since it provides good results *a priori* and it is based on the molecular structures of the components. Those calculations involve a series of parameters and very often the criteria of applicability of the group contribution methods are not so clear. We could observe the following:

- for molar volumes, the Sugden and Blitz contribution methods have, in average, equivalent results;
- the vaporization method provides lower deviation than Hoy or Small methods. Those methods also include the molar volume, and accumulated errors may exist;
- Three-dimensional (3D) approach for Flory-Huggins parameters leads to lower deviations from the experimental results collected. However, the criterion of applicability of the 3D approach should be improved.

By writing down the chemical equilibrium according to the Flory-Huggins theory, it was possible to predict the swelling degree of dense cellulose triacetate (CTA) membranes immersed in organic solvents, such as n-decane and 2,2,4-TMP (trimethylpentane) and also in some alcohols, as ethanol, isopropanol and 1-octanol. Methanol (MeOH) and water did not fit to the concentration predicted by Flory-Huggins equilibrium, due likely to the very polar character of such compounds, as shown in the literature. However, the swelling degree of CTA in cyclohexane yielded a lower value than predicted, what was not expected at all. For penetrant-penetrant-polymer systems, the simulated results agree with literature for methyl tert-butyl ether (MTBE), but not for MeOH. By comparing

with our own experiments and literature data, we observed that 3D Flory-Huggins model is more helpful than the classic one.

With the concerns about the interactions between MeOH and polymers, we used a free-volume theory coupled to the Flory-Huggins thermodynamic model to recommend atactic poly(propylene) (aPP) as a raw material for membranes that should provide less methanol crossover than NAFION®. However, it should be also considered the mechanical strength of an aPP membrane.

5.2 *Microcapsules*

In the present work, by analyzing results of microcapsules production by using micromixers, we were able to identify key parameters for a further robust modeling strategy. According to the flow rate and chemistry of system, we were able to obtain spherical particles of different diameters. By the addition of vanillin, we obtain capsules up to 2 times bigger than the ones produced by just precipitating polymer. By a mass balance based on the amount of polymer, we deduced that the volume fraction available for the storage of products inside the capsules may reach a value up to 0.88. The fluidodynamic model based on Rayleigh mechanism allowed us to predict a microcapsule diameter closer to the experimental one, for pure polysulfone capsules. At low flow rates of polymeric solution, the resultant diameter of the microcapsule containing vanillin was closer to the predicted value of the droplet, what evidences that was no significant change in volume during precipitation. However, this does not apply for the experiment with the maximal flow rate.

Further modeling, including the composition of thermodynamic equilibrium diagrams, should be taken into account to understand the complete formation of the microcapsules. Besides, it should include the study of the surface tensions, to assess the water management of the system, among other issues.

5.3 Fuel cells

We aimed to contribute to the phenomenological knowledge of the permeation transport processes occurring in a fuel cell, by identifying the dominant mechanisms and contributions to permeability of mass transfer phenomena. The permeation of protons and methanol through composite membranes provided data for modelling. The main conclusions of this study are:

- The composite membranes tested provided a lower methanol crossover than NAFION® 117. As this happens also for proton permeation, more materials should be tested in order to manufacture a fuel cell with better performance,
- Transport probabilities for protons and methanol were maximum for the membrane whose casting solution had 50 wt% of poly(ethylene glycol) (PEG). For higher PEG contents, there may be less free space for transport in the dense layer, so transport probability decreased,
- Overall selectivity is maximum for a membrane with 20 wt% of PEG in the casting solution. However, this value was higher when only the PEG layer was considered, which indicates that selectivity may be enhanced if another support layer is used,
- When evaluating the resistance of the different mass transfer phenomena, the PEG layer had the lowest resistance when the casting solution had 50 wt% of PEG. Choosing a suitable porous support may reduce total mass transfer resistance and increase overall selectivity,
- Even if we consider instantaneous membrane-reservoirs equilibrium, the interfacial mass transfer resistance may represent 12% of the total mass transfer resistance.

We evaluated several PEG chain lengths as potential materials to obtain selective layers for direct methanol fuel cells. We used literature data to regress free-volume parameters for water-PEG systems and converted them into MeOH-PEG data. We could observe the following:

- As long as the PEG chain length increases, the molar volume and the Flory-Huggins interaction parameters also increase, due to the preponderance of the aliphatic contribution to the total chain. PEGs with higher thermodynamic interaction parameters χ_{13} and χ_{23} have low affinity for water and MeOH.
- The variation of the diffusive parameter A_{13} with the molecular weight of PEG may be explained by the increasing energy of activation for diffusion when chain length increases.
- The molar volumetric ratio between the transported species and the polymer jumping unit ξ_{13} and ξ_{23} exhibit a minimum for PEG 3400 and, following this tendency, the value obtained for PEG 10000 is unexpected. Another factor not explained in the reference papers, such as crosslinking, may be the reason.
- The flux of water is significantly reduced when any PEG is used instead of PEG 200 and, naturally, the minimal one is obtained with a membrane of highest PEG.
- The flux of MeOH increases with the chain length until PEG 3400, and then it experiences a significant reduction to minimal values. The reason could be the behavior of the ξ_{13} and ξ_{23} parameters.
- Finally selectivity for MeOH increases with chain length and, for lower concentrations, just MeOH would cross the membrane. However, selectivity can be reduced when feed MeOH solutions are more concentrated, as in the case for PEG 10000.

The reasons above allowed us to conclude that PEGs with high molecular weight are promising materials to manufacture selective layers for methanol fuel cells, since it would be possible to work at higher concentrations of MeOH than 1.0M, that is typically used. However, other important aspects, such as proton conductivity and chemical resistance to the feed solution, were out of the scope of the present work and should be taken into account before final decision for a determined material.

6 Scientific contributions of this thesis

Engineering is more than just repeating a sequence of trial-and-error steps to achieve a desired result. We should be able to predict as much as possible how the chemical systems will behave, and therefore it is mandatory to establish some guidelines that allow us to optimize laboratory resources and research time.

This thesis deals with the knowledge of intrinsic properties of chemical components, such as solvents and polymers, to understand transport properties of the materials produced from those chemicals. By using free-volume theory and a thermodynamic approach we were able to predict several kinds of data, such as swelling degree of membranes and ternary equilibrium data, recommend materials for fuel cell membranes, and even give hints about the formation of polymeric membrane structures. We point out that our predictions require very few experimental or adjustable parameters.

Concerning thermodynamics, the work developed generated an article, recently accepted in *Polymer Engineering and Science*, which was also communicated at the *Advanced Polymeric Materials 2006* meeting held in Bratislava. During the congress, we realized that still today a lot of research depends on empirical methods, since very few works dealt with modeling or predictions. The same happened in *Fuel Cells Science & Technology 2004*, held in München, where the most part of the DMFCs works just considered the membrane as a black box and prediction of methanol crossover through the membrane by advanced theories was rarely considered. It is quite awkward, considering that fuel cells constitute a subject of high technological impact and high interest nowadays, when everybody is concerned about renewable power sources. At that meeting we also had an oral presentation, and the results were published in *Journal of Power Sources*.

For the formation of polymeric structures, however, a lot of work still needs to be done. Both flat-sheet membranes and microcapsules may be modelled by

the theories described in this thesis, as we indicated. Especially the knowledge of the diffusion in polymers may be a helpful tool to draw the composition path from the initial solutions to the final (porous or dense) structures. This thesis, however, provides a complete set of rules to obtain each one of the properties needed by those models, also discussing the limitations of some methods.

7 Articles

The papers are annexed in the following order:

Thermodynamics

L. Pitol-Filho, R. Garcia-Valls. A method for assessing the choice of polymeric materials for specific applications. *Polymer Engineering and Science* (2007). *In press*

L. Pitol-Filho, R. Garcia-Valls. Methods to calculate penetrant-polymer Flory-Huggins interaction parameters: comparison and validation. *To be submitted*

Microcapsules

C. Torras, D. Gezahegn, L. Pitol-Filho, R. Garcia-Valls. Novel polymeric membrane structures: microcapsules. *Desalination* 200 (2006) 12-14.

L. Pitol-Filho, C. Torras, J. Bonet-Avalos, R. Garcia-Valls. Modelling of polysulfone membrane formation by immersion precipitation. *Desalination* 200 (2006) 427-428.

L. Pitol-Filho, C. Torras, J. Bonet-Avalos, R. Garcia-Valls. Fluidic and thermodynamic insights on the formation of microcapsules by using micromixers. *To be submitted*

Fuel Cells

X. Zhang, L. Pitol-Filho, C. Torras, R. Garcia-Valls. Experimental and computational study of proton and methanol permeability through composite membranes. *J. Power Sources* 145 (2005) 223-230.

L. Pitol-Filho, S. Alsoy Altinkaya, R. Garcia-Valls. Evaluation of poly(ethylene glycol) of different chain length as a potential selective layer for direct methanol fuel cells. *To be submitted*

8 References

-
- [1] J.R. Fried. Polymer science and technology. Prentice Hall (1995).
- [2] E. Favre. European Polymer J. 32 (1996) 1183-1188.
- [3] J.S. Woo, S.J. Kim, J.S. Choi. J. Chem Eng Data 44 (1999) 16-22.
- [4] J.S. Yang, H.J. Kim, W.H. Jo, Y.S. Kang. Polymer 39 (1998) 1381-1385.
- [5] S. Mandal, V.G. Pangarkar. J. Membrane Science 201 (2002) 175-190.
- [6] T. Lindvig, M.L. Michelsen, G.M. Kontogeorgis. Fluid Phase Equilibria 203 (2002) 247-260.
- [7] J. M. Zielinski, J.L. Duda. AIChEJ 38 (1992) 405-415.
- [8] A.F.M. Barton. CRC Handbook of solubility parameters and other cohesion parameters. CRC Press, 2nd edition (1991).
- [9] A.M.A. Dias. Thermodynamic properties of blood substituting liquid mixtures. PhD Thesis (2005), Universidade de Aveiro, Portugal.
- [10] L. Pitol-Filho, R. Garcia-Valls. Polymer Engineering and Science (2007). In press.
- [11] T. Nakaoki, M. Kobayashi. J. Molecular Structure 655 (2003) 343-349.
- [12] T.M. Madkour, A. Soldera. European Polymer J 37 (2001) 1105-1113.
- [13] M. Khyaet, J.P.G Villaluenga, M.P. Godino, J.I. Mengual, B. Seoane, K.C. Khulbe, T. Matsuura. J. Colloid and Interface Science 278 (2004) 410-422.
- [14] E. Favre, Q.T. Nguyen, R. Clément, J. Néel. J. Membrane Science 117 (1996) 227-236.
- [15] A. Jonquières, R. Clément, D. Roizard, P. Lochon. J. Membrane Science 117 (1996) 227-236.
- [16] B.G. González, I.O. Uribe. Ind. Eng. Chem. Res. 40 (2001) 1720-1731.
- [17] M. Mulder. Basic principles of membrane technology. 2nd ed. Kluwer Academic Publishers: Dordrecht (1997).
- [18] M.A. Razavi, A. Mortazavi, M. Mousavi. J. Membrane Science 220 (2003) 47-58.
- [19] N. Ramesh, J.L. Duda. J. Membrane Science 191 (2001) 13-30.
- [20] S. Alsoy Altinkaya, B. Ozbas. J. Membrane Science 230 (2004) 71-89.

- [21] S.-U. Hong, A.J. Benesi, J.L. Duda, *Polymer International* 39 (1996) 243-249.
- [22] S. Alsoy, J.L. Duda. *J. Polymer Science B: Polymer Physics* 37 (1999) 1665-1675.
- [23] Y. Yu, M. Wang, Q. Tao, S. Li, *J. Phys. Chem. B* 108 (2004) 6208-6215.
- [24] J.H. Kim, B.R. Min, J. Won, H.C. Park, Y.S. Kang, *J. Membrane Science* 187 (2001) 47-55.
- [25] C. Torras. *Obtenció de membranes polimèriques selectives*. Thesis dissertation. Dep. Chemical Engineering, Universitat Rovira i Virgili (2005). ISBN:84-689-3628-6.
- [26] L. Pitol-Filho, C. Torras, J. Bonet-Avalos, R. Garcia-Valls. *Desalination* 200 (2006) 427-428.
- [27] Y. Matsunami, K. Ichikawa. *International J of Pharmaceutics* 242 (2002) 147-153.
- [28] S.-J. Park, Y.-S. Shin, J.-Rock Lee. *J. Colloid and Interface Science* 241 (2001) 502-508.
- [29] C. Torras. *Obtenció de membranes polimèriques selectives*, PhD Thesis, Chemical Engineering Department, Universitat Rovira i Virgili (2005). ISBN:84-689-3628-6.
- [30] V. Hessel, H. Löwe, F. Schönfeld. *Chemical Engineering Science* 60 (2005) 2479-2501.
- [31] St. Walter, St. Malmberg, B. Schmidt, M.A. Liaw. *Catalysis Today* 110 (2005) 15-25.
- [32] S. Hardt, F. Schönfeld. *AIChE J* 49 (2003) 578-584.
- [33] K. F. Jensen. *Chemical Engineering and Science* 56 (2001) 293-303.
- [34] W. Ehrfeld, K. Golbig, V. Hessel, H. Löwe, T. Richter. *Ind. Eng. Chem. Res.* 38 (1999) 1075-1082.
- [35] P. Löb, H. Pennemann, V. Hessel. *Chemical Engineering J* 101 (2004) 75-85.
- [36] J.D. Tice, A.D. Lyon, R.F. Ismagilov. *Analytica Chimica Acta* 507 (2004) 73-77.
- [37] Y. Ying, G. Chen, Y. Zhao, S. Li, Q. Yuan. *Chemical Engineering J* (2007), doi:10.1016/j.cej.2007.03.099

- [38] H. Kim, *Physica B* 389 (2007) 377-379.
- [39] C. Torras, D. Gezahegn, L. Pitol-Filho, R. Garcia-Valls. *Desalination* 200 (2006) 12-14.
- [40] C.B. Roberts, N.O. Elbashir, *Fuel Processing Technology* 83 (2003) 1-9.
- [41] W.J. Piel, *Fuel Processing Technology* 71 (2001) 161-179.
- [42] H.Y. Chang, C.W. Lin, *J. Membrane Science* 218 (2003) 295-306.
- [43] C.K. Dyer, *J. Power Sources* 106 (2002) 31-34.
- [44] H. Dohle, J. Divisek, R. Jung, *J. Power Sources* 86 (2000) 469-477.
- [45] A. Heinzl, V.M. Barragán, *J. Power Sources* 84 (1999) 70-74.
- [46] K. Scott, W.M. Taama, P. Argyropoulos, K. Sundmacher, *J. Power Sources* 83 (1999) 204-216.
- [47] B.S. Pivovar, Y. Wang, E.L. Cussler, *J. Membrane Science* 154 (1999) 155-162.
- [48] K.D. Kreuer, *J. Membrane Science* 185 (2000) 29-39.
- [49] S.E. Wright, *Renewable Energy* 29 (2004) 179-195.
- [50] P. Argyropoulos, K. Scott, A.K. Shukla, C. Jackson, *J. Power Sources* 123 (2003) 190-199.
- [51] V.B. Oliveira, D.S. Falcão, C.M. Rangel, A.M.F.R. Pinto. *International Journal of Hydrogen Energy* 32 (2007) 415-424.
- [52] A.A. Kulikovskiy, *Electrochemical Communications* 4 (2002) 939-946.
- [53] L. Pitol-Filho, R. Garcia-Valls. Methods to calculate penetrant-polymer Flory-Huggins interaction parameter: comparison and validation. *To be submitted*.
- [54] Y. Yu, M. Wang, Q. Tao, S. Li, *J. Phys. Chem. B* 108 (2004) 6208-6215.

L. Pitol-Filho, R. Garcia-Valls

A method for assessing the choice of the polymeric materials for specific applications

Polymer Engineering and Science (2007). In Press

A method for assessing the choice of polymeric materials for specific applications

Luizildo Pitol-Filho and Ricard Garcia-Valls

Departament d'Enginyeria Química
Escola Tècnica Superior d'Enginyeria Química
Universitat Rovira i Virgili
Av. Països Catalans 26
43007 Tarragona, Spain
Tel.: +34 977 55 96 11; fax: +34 977 55 85 44
ricard.garcia@urv.net

ABSTRACT

Polymeric membranes have several applications of high technological impact: reverse osmosis, controlled drug delivery and fuel cell stacks, among many others. However, the choice of the most appropriate polymer for a specific application implies an exhaustive experimental work, which may be reduced significantly if the chemical structures of polymer and transported molecules are taken into account. From physico-chemical data such as viscosity (for penetrants) and relaxation times (for polymers), free-volume parameters might be estimated, as well as Flory-Huggins interaction coefficients. By combining both theories, diffusivity of molecules through dense polymers may be evaluated, what allows us to predict membrane properties as water uptake, or operation data as equilibrium concentrations for pervaporation and methanol crossover in the case of fuel cell applications. Simulation results are compared to the literature and agreement between the sets of data recommends the proposed method as a helpful tool to decide which polymer is more adequate for a specific purpose.

INTRODUCTION

Polymeric membranes have a wide field of applications, ranging from the purification of products to the generation of energy, as a constituent of fuel cell stacks. Among the recent studies of the membranes we can very quickly list:

- Reverse osmosis concentration of apple juice aroma components by using composite polyamide membranes [1];
- Ultrafiltration of milk, to evaluate and predict total flux, rejection of milk components and total hydraulic resistance by applying neural network strategies [2];
- Separation of MeOH-MTBE [3] and EtOH-ETBE [4] mixtures by pervaporation and subsequent prediction of fluxes by the engaged species induced clustering (ENSIC) model;
- Controlled hydrocortisone release by using membranes composed by different formulations of N,N-dimethylaminoethyl methacrylate and co-acrylamide, where the water uptake and the swelling/shrinking represent important phenomena [5];

- The application of perfluorinated polysulfonated NAFION® (DuPont) membranes in the construction of Direct Methanol Fuel Cells, where both proton conductivity and methanol crossover are important issues [6-11].

As seen above, many applications of high technological impact depend on membranes and, therefore, the knowledge of the constituent polymeric materials is crucial, as well as the interactions between the permeant molecules and the polymer molecules. Several strategies have been used to answer those questions, as the use of neural networks, and thermodynamic models, such as the ENSIC one. However, both approaches are somehow limited, because the neural networks are just predictive for the materials that have been used to train the algorithm and do not foresee situations when different polymers or molecules are involved. On the other hand, the key parameters of the ENSIC model, namely the elementary affinity between the non-polymeric species and either a polymer segment or a previously sorbed molecule, are regressed from sorption experiments. That means that no one of these approaches is useful when the system studied is completely unknown.

A good starting point to describe polymeric solutions is the Flory-Huggins theory [12], which allows us to determine the chemical equilibrium by using a single interaction parameter. Such interaction parameter can be easily determined by group contribution techniques, without the necessity of previous experimental data. However, the Flory-Huggins equation just describes the solubility contribution of the permeation phenomena [13]. To determine the other contribution, the diffusive one, the Vrentas-Duda free-volume diffusion model [14, 15] provides good accuracy without any use of any diffusion data, by just combining the intrinsic properties of the transported species and the polymers, such as viscosity and relaxation times. Several works combine the Flory-Huggins and the Vrentas-Duda theories to study the swelling or drying of polymeric films and even the formation of membranes from casting solutions [16-21].

By combining both theories we describe and apply a method to estimate properties such as swelling degree of cellulose triacetate (CTA) homemade membranes immersed in different solvents, as well as ternary equilibrium data for two chemical species adsorbing in a given polymer. We also estimate the diffusivity of chemical components in polymers without any use of previously published diffusion data. We would like to point out that all the parameters that we used in this paper are purely predictive, without any adjustment or regression from diffusive experimental data. Therefore, it can be used not only to predict properties and operation data for membranes, but also allows recommending polymers for specific applications.

METHODS

Preparation of membranes

To prepare the CTA membranes, 1.5g of CTA (Aldrich, ref 18,100-5, MW 103,000) were dissolved in 20 ml dichloromethane (Scharlau Chemie S.A, Spain, 99.9 wt %) and vigorously mixed during 12 hours at room temperature. Then the solution was cast onto a glass plate in enough volume to provide circular-shaped membranes with thickness around 100µm after solvent evaporation.

Determination of swelling degree

To determine the swelling degree, the membranes were immersed in pure organic solvents, alcohols or water during 12 hours at room temperature. After immersion, the excess of solvent was removed from the external surface of the membranes with filter paper, and then the membranes were weighed. The swelling degree was then determined by Eq. (1):

$$SD = \frac{m_{wet} - m_{dry}}{m_{dry}} \quad (1)$$

The swelling degree of the CTA membranes was measured for distilled water, methanol (99.8 wt%), ethanol (99.5 wt%), 2-propanol (99.9 wt%), 1-octanol, n-heptane, n-decane (with purity higher than 95 wt%), cyclohexane (99.5 wt%) and 2,2,4-trimethylpentane (99.5 wt%). Methanol, ethanol and cyclohexane were provided by Panreac Química S.A. (Spain), 2,2,4-trimethylpentane and 2-propanol were provided by Scharlau Chemie S.A. (Spain), and 1-octanol, n-heptane and n-decane were provided by Merck Schuchardt (Germany). The swelling degree was used to calculate the volume fraction of solvent in the membranes by Eq.(2):

$$\phi_i = \frac{SD \cdot \frac{V_i}{M_i}}{SD \cdot \frac{V_i}{M_i} + (1 - SD) \cdot \frac{V_{polymer}}{M_{polymer}}} \quad (2)$$

All the experiments of swelling degree were repeated at least three times.

Calculation of species-polymer Flory-Huggins interaction parameter

In order to determine the species-polymer Flory-Huggins parameter, we first need to calculate the molar liquid volumes at 0K and the cohesion parameters (also known as the solubility parameter) for the chemical species and the polymers. Among the methods to calculate the molar volumes, there are the group contribution rules compiled by Sugden and Blitz [14]. We used Blitz rule for the alcohols and the Sugden one for the other components, including polymers. Then, the cohesion parameter is calculated for polymers according to group contribution rules [12] and for the chemical species by using the enthalpy of vaporization method [22]. The enthalpies of vaporization were determined by the commercial software Aspen HYSYS®, by choosing the Antoine's equation of state. We selected such method since it provided closer values to those already published. The Flory-Huggins coefficient can be then calculated according to Eq.(3) [23]:

$$\chi_{i3} = 0.35 + \frac{V_i}{RT} (\delta_i - \delta_3)^2 \quad (3)$$

In Eq.(3), the subscript *i* may represent any chemical species that interacts with the polymer. However, when the components are polar or make hydrogen

bonds, a three-dimensional (3D) Flory-Huggins parameter is preferred [24], as stated in Eq (4):

$$\chi_{i3} = \alpha \frac{V_i}{RT} D_{i3}^2 \quad (4)$$

$$D_{i3}^2 = w_d (\delta_{i,d} - \delta_{3,d})^2 + w_p (\delta_{i,p} - \delta_{3,p})^2 + w_{hb} (\delta_{i,hb} - \delta_{3,hb})^2 \quad (4.1)$$

In Eq (4.1), δ_d , δ_p and δ_{hb} represent the Hansen parameters that comprehend the dispersive, polar and hydrogen-bonding effects of a given component. There are group contribution methods to calculate each one [22]. For polymers, the calculation procedures involve the repetition unit, what means that that the cohesion parameter does not depend on the molecular weight. A commonly used weight distribution for those effects is a (4:1:1) distribution, where $(w_d:w_p:w_{hb}) = (1:0.25:0.25)$ while α is equal to the unity [24].

However, in some cases either δ_p or δ_{hb} is missing for one component of the pair solvent-polymer, what requires another strategy. Since the existence of a zero in Eq (4.1) would lead to very large numbers owing to the square potency, we decided to calculate a lumped Hansen parameter, comprehending both the polar and the hydrogen bonding effects. So, if the solvent has δ_{hb} equal to zero, for example, and the polymer has all the Hansen parameters different than zero, we calculate a lumped Hansen parameter (δ_{p-hb}) for the polymer:

$$\delta_{3,p-hb}^2 = \delta_{3,p}^2 + \delta_{3,hb}^2 \quad (4.2)$$

Then Eq (4.1) becomes:

$$D_{i3}^2 = w_d (\delta_{i,d} - \delta_{3,d})^2 + w_{p-hb} (\delta_{i,p} - \delta_{3,p-hb})^2 \quad (4.3)$$

In Eq (4.3) the lumped polar-hydrogen bonding weight (w_{p-hb}) remains 0.25. Such strategy also was used when there was missing the hydrogen-bonding effect for the polymer, by calculating the lumped parameter for the solvent.

Calculation of permeant-permeant interaction parameter

In this paper when we talk about *permeant-permeant interaction parameter*, we refer to the interaction between two chemical species in contact with the polymer. In the literature, especially in the formation of membranes by phase inversion, those chemical species are usually called solvent and non-solvent. However, we think that in our present studies, this denomination is inappropriate, since no species is dissolving the polymer, but permeating into it. The permeant-permeant interaction parameters should be calculated from vapor-liquid equilibrium data, according to Eqs.(5) and (6) [25]:

$$\frac{\Delta G^E}{RT} = \sum \phi_i \ln \gamma_i \quad (5)$$

$$\chi_{12} = \frac{1}{y_1 \phi_2} \left(y_1 \ln \left(\frac{y_1}{\phi_1} \right) + y_2 \ln \left(\frac{y_2}{\phi_2} \right) + \frac{\Delta G^E}{RT} \right) \quad (6)$$

For the moment, we need vapor-liquid equilibrium data from the literature to regress the permeant-permeant interaction parameter but we are working on the determination of such data by using the UNIFAC method, since the literature cannot provide data for all the possible binary systems.

Determination of chemical equilibrium

When two phases are in equilibrium, their chemical potentials are equal. We can therefore write equilibrium expressions based on Flory-Huggins theory [19]. For a polymeric membrane (component 3) immersed in a solution with a given species molar fraction x_1 , we have:

$$\frac{\mu_1 - \mu_1^o}{RT} = \ln(x_1) = \ln(\phi_1) + (1 - \phi_1) + \chi_{13}(1 - \phi_1)^2 \quad (7)$$

For a membrane immersed in a pure solvent ($x_1 = 1$), Eq.(7) becomes:

$$\ln(\phi_1) + (1 - \phi_1) + \chi_{13}(1 - \phi_1)^2 = 0 \quad (8)$$

On the other hand, if a membrane is immersed in a mixture of two solvents, the permeant(1)-permeant(2)-membrane(3) chemical equilibrium is written similarly, but including the permeant-permeant interaction parameter χ_{12} , according to Eqs. (9) and (10):

$$\ln(x_1) = \ln(\phi_1) + \phi_3 + (\chi_{12}\phi_2 + \chi_{13}\phi_3)(1 - \phi_1) - \chi_{23}\phi_2\phi_3 \quad (9)$$

$$\ln(x_2) = \ln(\phi_2) + \phi_3 + (\chi_{12}\phi_1 + \chi_{23}\phi_3)(1 - \phi_2) - \chi_{13}\phi_1\phi_3 \quad (10)$$

Calculation of permeants free-volume parameters

The free-volume parameters of several permeants were published by Hong [26], in a paper where the author also describes a method to regress these parameters from viscosity data. Some of the studied compounds were not in the list, so we obtained the viscosity-temperature fits by using the commercial software Aspen HYSYS®, what allowed us to regress the missing data. Once more, Antoine's equation of state was chosen.

Determination of diffusivities

The free-volume theory describes the diffusivity of components in polymeric systems. For multicomponent cases, recently a friction-based diffusion model was proposed by Alsoy and Duda [21]:

$$D_{ik} = \frac{\rho_i}{RT} \sum_{\substack{j=1 \\ j \neq i}}^3 \phi_j \left(D_i \frac{\partial \mu_i}{\partial \rho_k} - D_j \frac{\partial \mu_j}{\partial \rho_k} \right) \quad (11)$$

For a binary system where MeOH diffuses through a polymer, Eq (11) becomes:

$$D_{MeOH} = D_1(1 - \phi_1)^2(1 - 2\chi_{13}\phi_1) \quad (12)$$

Where

$$D_1 = D_0 \exp\left[\frac{-E}{RT}\right] \exp\left[-\frac{\phi_1 V_1 + (1-\phi_1)\varepsilon_{13} V_3}{V/\gamma}\right] \quad (12.1)$$

$$V/\gamma = \sum \phi_i \left(\frac{K_{li}}{\gamma}\right) (K_{2i} - T_{gi} + T) \quad (12.2)$$

Literature lists values for the polymer free-volume parameters [26], as well as the calculation procedures for each one of them.

Summary of the method

The method that we propose to assess the choice of polymeric materials is based on the Vrentas-Duda free-volume theory. A scheme of the calculation steps for each property is shown in Figure 1. First, we need to know the molecular structures of the components. Then, we can arrange the properties in two different groups: a thermodynamic group and a free-volume one.

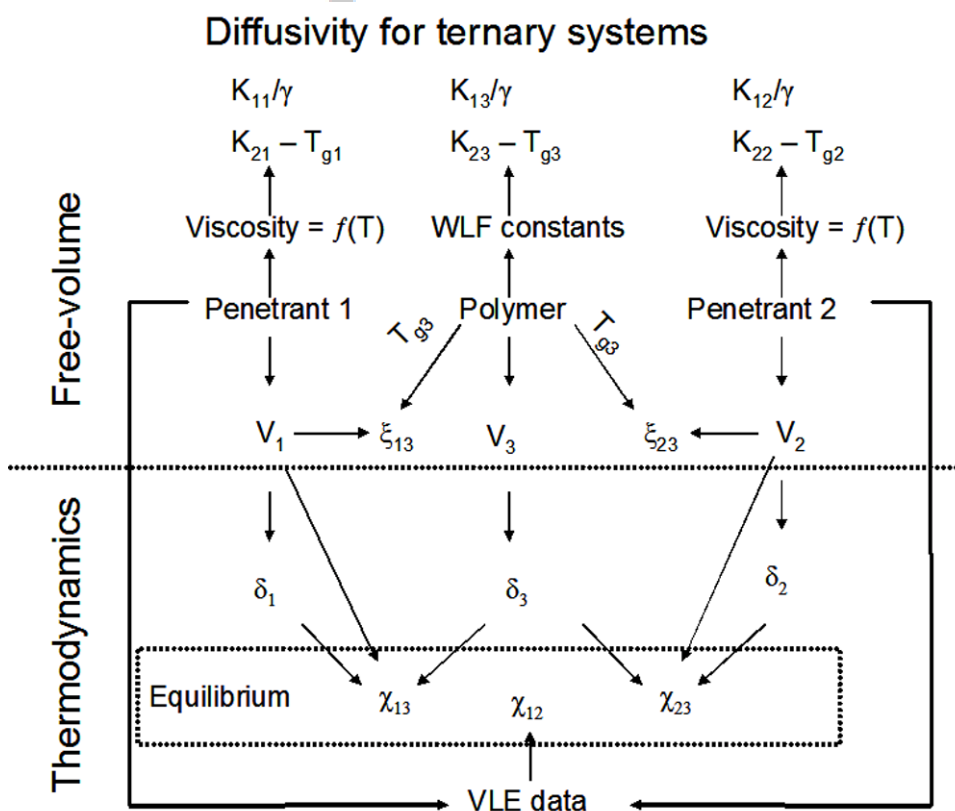


Figure 1 – Summary of the method to calculate properties for ternary systems.

In the thermodynamic group, from the chemical structures it is possible to determine the molar volume and the cohesion parameters for the polymer and both penetrants. Then, by Eqs (3) and (4), according to the case, Flory-Huggins interaction parameters between the penetrants and the polymer are calculated. Eq(4) is used when it is possible to calculate for both the penetrant and the polymer at least two of the Hansen parameters (dispersive, polar, and hydrogen bonding). Moreover, the system has to satisfy the following condition:

$$\frac{(\delta_{1,j} - \delta_{3,j})^2}{(\delta_{1,d} - \delta_{3,d})^2 + (\delta_{1,p} - \delta_{3,p})^2 + (\delta_{1,hb} - \delta_{3,hb})^2} > 0.5 \quad (13)$$

where j represents either polar or hydrogen-bonding effects. Such restriction assures us to obtain more accurate predictions.

Ternary systems also require a penetrant-penetrant interaction parameter, which can be obtained through vapour-liquid equilibrium (VLE) data. However, the data available in the literature are often incomplete, since the activity coefficients are missing in the reported VLE data for some systems [27-28]. We are going to overcome this problem in future works by including the prediction of VLE by the modified UNIFAC (Dortmund) method [29]. With this achievement, the predictive character of our method is going to be stressed and expanded.

On the other hand, the free-volume group of parameters require the calculation of the ratio of permeant to polymer jump size units (ξ), which can be obtained through the glass transition temperature of the polymer [26]. It is necessary to determine also the penetrants free-volume parameters, through analysis of viscosity-temperature data. In the case of polymer, the free-volume parameters are related to the Williams-Landel-Ferry (WLF) equation [26], whose constants can be found through the relationship between the glass transition temperature and relaxation times [30]. For the prediction of methanol crossover, however, we used the polymer free-volume parameters reported by Hong [26].

RESULTS

Swelling degree: prediction and experimental determination

The swelling degree obtained experimentally was converted to the volume fraction by using Eq (2), which is shown in Figure 2 as a function of the Flory-Huggins interaction parameter. The upper part (a) contains Flory-Huggins parameters that were correlated by the classical equation (Eq(3)) and, in the lower part (b), Flory-Huggins interaction parameters were calculated by using both Eq (3) and (4), according to the criteria previously described. Table 1 lists the sets of parameters. In Figure 2a, we observe that, although the major part of the components are very close to the curve predicted by Eq (7), cyclohexane and the short-chain alcohols are not well described by the classic model. Water was not shown in that graph, since its coordinates using the classic model were out of range. For the alcohols, the difference of polarity between the penetrant and CTA may be the reason for the divergence with the Flory-Huggins fit, because the experimental volume fraction approaches to the predicted one as far as the number of the hydrocarbons in the alcoholic chain increases. Such hypothesis is confirmed by Figure 2b, where the Flory-Huggins interaction parameter of some components was calculated by using the 3D model, considering dispersive, polar and hydrogen bonding effects. Results are much better, especially for MeOH and EtOH. For water, however, the volume fraction is still very far from the calculated value. To explain the thermodynamic aspects of diffusion of water in chains of poly(ethylene glycol) of different molecular weight, Vergara et al. [31] used the van Laar activity model instead of the Flory-Huggins approach, what confirms that other theories are needed to predict systems involving polar and hydrogen-bonding effects.

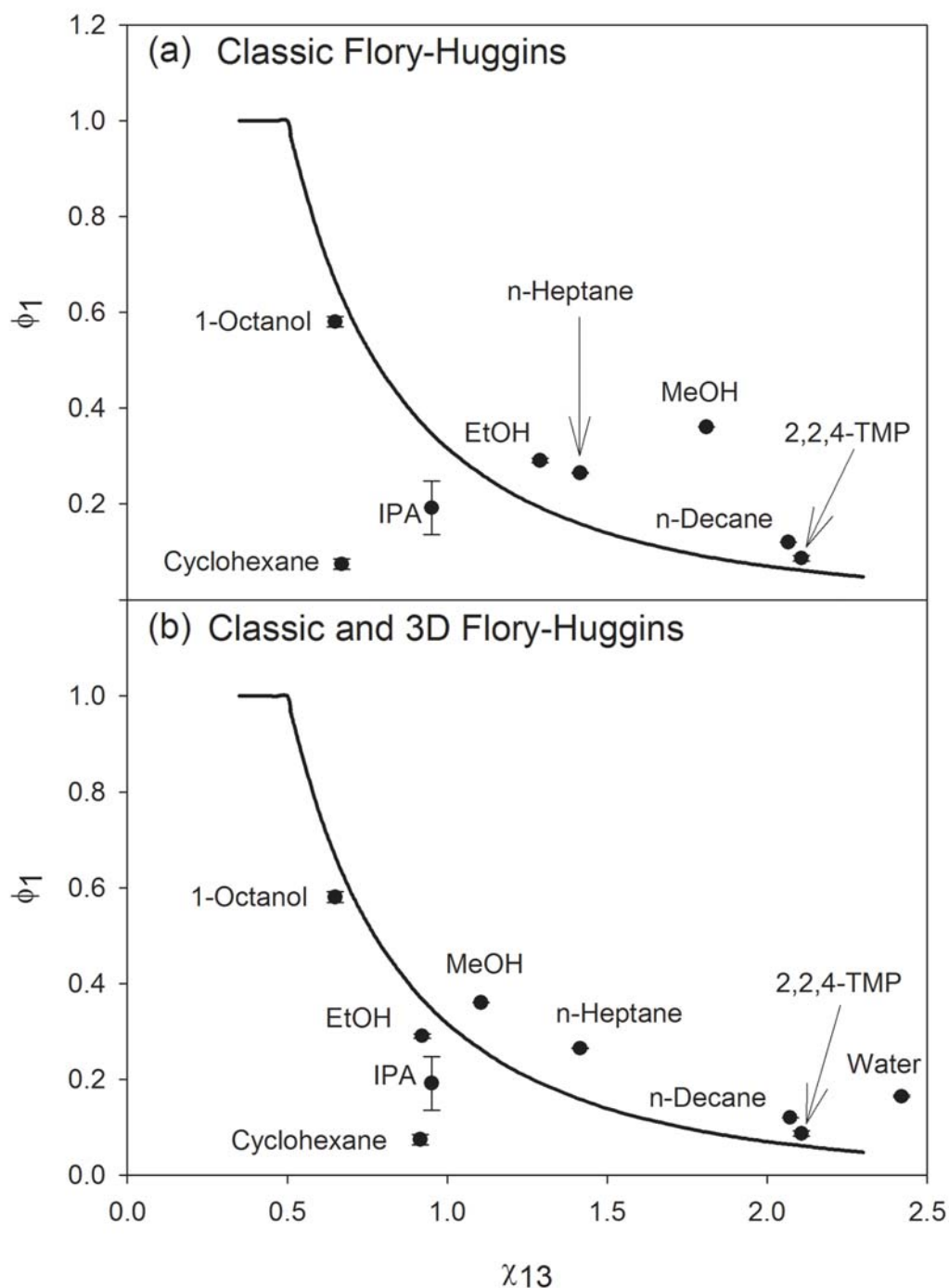


Figure 2 – Volume fraction of penetrants in CTA as a function of Flory-Huggins interaction parameter.

The interaction between the polymer and non-polar components such as n-decane and 2,2,4-TMP is appropriately correlated by the theory. However, cyclohexane exhibits a very unexpected behavior, since the experimental volume fraction is much lower than the predict one. However, for the system cyclohexane-polyisobutylene [32], it was reported that exists a good agreement between the Flory-Huggins theory and the experimental data. The interaction of cyclohexane with other polymers should be studied.

Table 1 – Cohesion and Hansen parameters for the swelling experiments and for the ternary equilibrium predictions (3: CTA).

Component i	V, cm ³ /gmol	δ_i , MPa ^{1/2}	δ_d , MPa ^{1/2}	δ_p , MPa ^{1/2}	δ_{hb} , MPa ^{1/2}	$\chi_{i3}^{\text{Classic}}$	Correction used	$\chi_{i3}^{\text{Corrected}}$	$\chi_{i3}^{\text{swelling}}$
Cyclohexane	87.6	15.8	16.5	3.1	0.0	0.67	Eq (4.3)	0.92	1.95
n-Decane	158.4	13.7	15.8	0.0	0.0	2.07	-	-	1.60
EtOH	44.3	24.9	12.6	11.2	20.0	1.29	Eq (4.1)	0.92	1.05
n-Heptane	114.9	14.0	15.3	0.0	0.0	1.42	-	-	1.10
IPA	71.6	23.4	14.0	9.8	16.0	0.95	-	-	1.29
MeOH	30.6	29.2	11.6	13.0	24.0	1.81	Eq (4.1)	1.10	0.93
MTBE	91.8	23.5	21.5	8.4	4.7	1.16	Eq (4.1)	1.07	-
1-Octanol	119.9	16.4	21.0	5.9	12.9	0.65	-	-	0.71
2,2,4-TMP	129.4	13.0	15.1	0.0	0.0	2.10	-	-	1.84
Water	19.3	46.0	12.2	22.8	40.4	6.18	Eq (4.1)	2.40	1.39
CTA	192.2	18.8	17.7	5.3	11.9				

Table 2 – Data for MeOH-MTBE-CTA equilibrium.

$\chi_{\text{MeOH-MTBE}} = a + b\phi_{\text{MeOH}} + c\phi_{\text{MeOH}}^2 + d\phi_{\text{MeOH}}^3 + e\phi_{\text{MeOH}}^4$				
a	b	c	d	e
1.15	-2.88	16.98	-26.55	13.51

Some authors use Eq.(8) to obtain the Flory-Huggins parameter from swelling experiments [25]. Table 1 also compares the interaction parameter obtained from Eqs. (3) and (4) (predicted one) to the value that could be obtained from the swelling experiments. For 1-octanol the difference between the predicted and the swelling value is minimal. Bhat and Pangarkar [33], through swelling experiments, obtained 1.0184 as the MeOH-CTA interaction parameter, what confirms the accuracy of our experiments. We point out, however, that the choice of a thermodynamic model to describe a MeOH-polymer mixture should be taken carefully.

Finally, the differences found between predicted and experimental data may be due to the change on polymer elasticity when it swells. However, for the present work we decided just to consider the thermodynamic equilibrium and neglect the effect of other phenomena.

Ternary systems: prediction and comparison to literature

To increase the number of octanes in gasoline, MTBE represents a good alternative to the lead additives that also reduces the carbon monoxide emissions [34]. MTBE is produced by reacting isobutylene with an excess of MeOH, because the reaction is equilibrium-limited. Then, MTBE should be separated from the unreacted MeOH. Some authors [34, 35] study the purification of MTBE from this mixture by pervaporation using a CTA membrane.

By using the ternary equilibrium equations (Eqs.(9) and (10)) and the Flory-Huggins interaction parameters reported in Tables 1 and 2, we obtained the volume fractions of MeOH and MTBE as a function of the MeOH molar fraction in the mixture, shown in Figure 3.

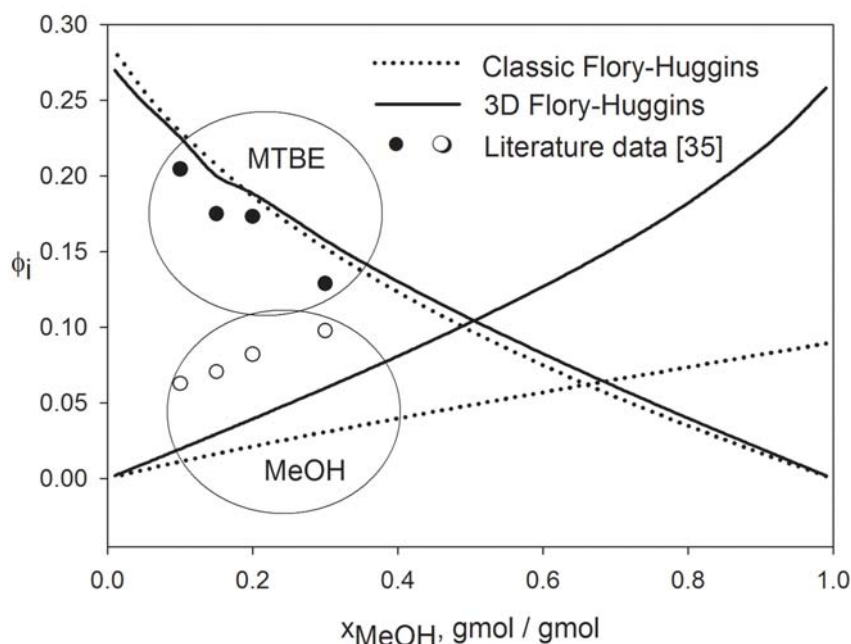


Figure 3 – Volume fraction of MeOH and MTBE in CTA varying with MeOH content in the liquid mixture.

Both classic and 3D Flory-Huggins models were used, and the 3D model provided better results, since it takes into account the polar and hydrogen-bonding effects. The data were compared to sorption experiments [35] with an excellent agreement for MTBE. As happened in the swelling experiments in the previous section, the prediction of MeOH volume fraction is lower than the experimental values. However, the 3D model curve for MeOH allowed us to observe a derivative similar to the experimental one, what made us suspect that the divergence from the predictions is caused by the MeOH-MTBE parameter. The VLE equilibrium data used to calculate the MeOH-MTBE parameter were obtained by Loras et al. [36] at 94 kPa, what may be another reason for the deviations between predicted and experimental fits. With the further calculation of the VLE data by UNIFAC method, we will reduce the dependence of our model on external data.

Prediction of methanol crossover

Lately, direct methanol fuel cells (DMFC) are being studied for as energy sources for transport and portable applications. However, a serious limitation of the fuel cell is the methanol crossover through the membrane, what represents a significant loss of fuel and also may damage the cathode, where the oxygen reacts with the protons to produce water [37]. The most used membrane for DMFC is NAFION®, which has good proton conductivity but also considerable methanol permeability.

By using the Vrentas-Duda theory, we evaluated the methanol crossover in some polymers and compared to the performance of NAFION® 117, from the literature. The thermodynamic parameters used are listed in Table 3.

Table 3 – Cohesion and Hansen parameters for polymers.

Polymer i	V, cm ³ /gmol	δ_i , MPa ^{1/2}	δ_d , MPa ^{1/2}	δ_p , MPa ^{1/2}	δ_{hb} , MPa ^{1/2}	Correction used
PMS	106	25.1	19.3	3.1	0	Eq (4.3)
PBD	58	17.8	-	-	-	-
PP	94.6	15.8	-	-	-	-
PMMA	150.6	14.7	7.6	4.2	5.8	Eq (4.1)
PEMA	167.2	14.8	8.4	3.8	5.5	Eq (4.1)
PIPA	118.9	17.0	13.8	5.3	6.5	Eq (4.1)
PDMS	67.2	14.0	groups missing	groups missing	groups missing	Eq (4.1)
NAFION®	192.1	16.1	groups missing	groups missing	groups missing	

For PDMS and NAFION it was not possible to calculate the Hansen parameters, because some of the chemical groups were lacking in the reference used [22]. To obtain the values shown in Table 4, we first predicted the Flory-Huggins interaction parameter between methanol and each polymer, and then, by using the relationship between the chemical potentials of the liquid and the polymeric phase, we calculated the equilibrium concentration when solutions of 12 gmol/l and 18.5 gmol/l of methanol are put in contact with a membrane.

Table 4 – Data for prediction of methanol crossover.

Polymer (<i>j</i>)	$\xi_{\text{MeOH},j}$	$\chi_{\text{MeOH},j}$	$\phi_{\text{MeOH}}^{(I)}$	$\phi_{\text{MeOH}}^{(II)}$	$D_{\text{MeOH}}^{(I)}, \text{cm}^2 / \text{s}$	$D_{\text{MeOH}}^{(II)}, \text{cm}^2 / \text{s}$
PMS ^(*)	0.1473	2.541	0.0054	0.0076	-	-
PBD	0.3586	2.117	0.0082	0.0118	$3.76 \cdot 10^{-5}$	$3.66 \cdot 10^{-5}$
PP	0.3297	2.774	0.0042	0.0060	$5.06 \cdot 10^{-7}$	$5.23 \cdot 10^{-7}$
PMMA ^(*)	0.3223	1.464	0.0162	0.0234	$2.46 \cdot 10^{-34}$	$5.02 \cdot 10^{-24}$
PEMA ^(*)	0.2269	1.445	0.0164	0.0237	$1.64 \cdot 10^{-10}$	$7.51 \cdot 10^{-10}$
PIPA	0.3268	1.189	0.0214	0.0310	$4.21 \cdot 10^{-6}$	$4.43 \cdot 10^{-6}$
PDMS	0.1585	3.057	0.0032	0.0045	$3.97 \cdot 10^{-4}$	$3.91 \cdot 10^{-4}$
NAFION® ^(**)	0.1942	2.668	0.0047	0.0067	$2.12 \cdot 10^{-6}$	$2.38 \cdot 10^{-6}$

^(I) Refer to 12 gmo/l of MeOH in water, and ^(II) refer to 18.5 gmo/l.

(*) Unreasonable results or infeasible solution.

(**) Experimental data [36], for NAFION®117.

Polymer and MeOH free-volume parameters were taken from the literature [25]. Polymers that likely provide lower methanol crossover than NAFION® should have bigger values of both $\xi_{\text{MeOH-polymer}}$ and $\chi_{\text{MeOH-polymer}}$, by meaning that there is less free space for the MeOH molecules diffuse within the polymeric chains, and also lower thermodynamic affinity. Therefore, good candidates could be atactic poly(propylene) (PP), poly(methyl metacrylate) (PMMA) and poly(ethyl metacrylate) (PEMA). However, we realized that the determination of diffusivity gives infeasible results when the $K_{2i-T_{gi}}$ parameter is lower than -269K , as in the case of PEMA, PMMA and PMS. For PMMA and PEMA, calculated diffusivities ranged from $10^{-34} \text{ cm}^2/\text{s}$ to $10^{-10} \text{ cm}^2/\text{s}$, that do not represent reasonable values. Poly(isopropyl acrylate) (PIPA) provided a methanol crossover around the reported for NAFION®117, while the diffusivity for poly(butadiene) and poly(dimethyl siloxane) (PDMS) are higher, even approaching the diffusivity of methanol in water. By these data and just considering the prediction of methanol crossover, atactic PP most probably will provide better results. However, before operating a fuel cell based on PP, there are two important issues to be studied: if the polymer has the desired mechanical strength and if is proton-conductive. Our results, however, can indicate the way to be pursued at the laboratory, therefore reducing the number of experiments and associated costs.

CONCLUSIONS

We present here a method to predict results of membrane operations before performing the experiments. By group contribution methods, without any adjustment from experimental data, it was possible to predict the swelling degree of CTA membranes immersed in organic solvents, such as n-decane and 2,2,4-TMP and also in some alcohols, as EtOH, IPA and 1-octanol. Methanol and water did not fit to the concentration predicted by Flory-Huggins equilibrium, due likely to the very polar character of such compounds, as shown in the literature. However, the swelling degree of CTA in cyclohexane gave a lower value than predicted, what was not expected at all. For penetrant-penetrant-polymer systems, the simulated results agree with literature for MTBE, but not for MeOH. By comparing with our own experiments and literature data, we observed that 3D Flory-Huggins model is more helpful than the classic one.

For the cases where there was no agreement between the experimental and predicted data, in the future we will substitute the Flory-Huggins-based chemical potential by the UNIFAC equilibrium model, to verify if such cases can be better predicted. Also the UNIFAC equations will help us to reinforce the predictive character of our method, since it will be possible to calculate also the VLE data, without the need of literature that presents very often incomplete data. Finally, with the concerns about the interactions between MeOH and polymers, we used the methodology to recommend atactic poly(propylene) as a raw material for membranes that, according to the theory, should provide less methanol crossover than NAFION®.

ACKNOWLEDGEMENTS

L. Pitol-Filho thanks Dr. S. Alsoy Altinkaya for the opportunity of a short research stay in her group at the Izmir Institute of Technology in 2005 and also the scientific discussions with Dr. A. M. A. Dias (Universidade de Braga, Portugal) Dr. M. Giamberini, Dr. J. Bonet-Avalos and Dr. F. Siperstein from the Chemical Engineering Department of Universitat Rovira i Virgili.

NOMENCLATURE

Chemicals and model abbreviations

3D	Three-dimensional Flory-Huggins model
2,2,4-TMP	2,2,4-Trimethylpentane
CTA	Cellulose triacetate
ENSIC	Engaged species induced clustering model
EtOH	Ethanol
ETBE	Ethyl tert-butyl ether
IPA	2-Propanol
MeOH	Methanol
MTBE	Methyl tert-butyl ether
PBD	Poly(butadiene)
PDMS	Poly(dimethyl siloxane)
PEMA	Poly(ethyl metacrylate)
PIPA	Poly(isopropyl acrylate)
PP	atactic poly(propylene)
PMMA	Poly(methyl metacrylate)
PMS	Poly(α -methyl styrene)
VLE	Vapor-liquid equilibrium
WLF	Williams-Landel-Ferry equation

Variables

D_{0i}	Pre-exponential diffusion coefficient, cm^2/s
D_{ij}	Mutual binary diffusion coefficient, cm^2/s
E_i	Activation energy for diffusion
ΔG^E	Excess Gibbs free energy
K_{1i}/γ	Free-volume parameter of component i
$K_{2i}-T_{gi}$	Free-volume parameter of component i
M_i	Molecular mass of component i , g/gmol
R	Ideal gas constant

T	Temperature, K
T_g	Glass transition temperature, K
V_i	Liquid molar volume at 0K of component i , cm^3/gmol
y_i	Molar fraction of the vapor phase

Greek letters

γ_i	Activity coefficient
δ_i	Cohesion parameter of component i , $\text{MPa}^{1/2}$
ξ_{i3}	Ratio of penetrant i to polymer (3) jump size units
ϕ_i	Volume fraction of component i
χ_{ij}	i - j Flory-Huggins interaction parameter
ρ_i	Mass density, g/cm^3
μ_i	Chemical potential of component i

Subscripts

1	Penetrant 1
2	Penetrant 2
3	Polymer
d	dispersion
hb	hydrogen-bonding
p	polar

REFERENCES

1. A. Pozderović, T. Moslavac, A. Pichler, *J. Food Engineering*, **76**, 387 (2006).
2. M.A. Razavi, A. Mortazavi, M. Mousavi, *J. Membrane Science*, **220**, 47 (2003).
3. B.G. González, I.O. Uribe, *Ind. Eng. Chem. Res.*, **40**, 1720 (2001).
4. A. Jonquière, R. Clément, D. Roizard, P. Lochon, *J. Membrane Sci.*, **109**, 65 (1996).
5. M. Grassi, S.H. Yuk, S.H. Cho, *J. Membrane Sci.*, **152**, 241 (1999).
6. A. Heinzl, V.M. Barragán, *J. Power Sources*, **84**, 70 (1999).
7. K. Scott, W.M. Taama, P. Argyropoulos, K. Sundmacher, *J. Power Sources*, **83**, 204 (1999).
8. B.S. Pivovar, Y. Wang, E.L. Cussler, *J. Membrane Sci.*, **154**, 155 (1999).
9. K. D. Kreuer, *J. Membrane Sci.*, **185**, 29 (2000).
10. H. Dohle, J. Divisek, R. Jung, *J. Power Sources*, **86**, 469 (2000).
11. X. Ye, D. Le Van, *J. Membrane Sci.*, **147**, 221 (2003).
12. J.R. Fried, *Polymer Science and Technology*, Prentice Hall (1995).
13. M. Mulder, *Basic Principles of Membrane Technology*, Kluwer Academic Publishers, 2nd edition.
14. J.M. Zielinski, J.L. Duda, *AIChE J.*, **38**, 405 (1992).
15. P.E. Price Jr, I.H. Romdhane, *AIChE J.*, **49**, 309 (2003).
16. S. Alsoy, J.L. Duda, *AIChE J.*, **45**, 896 (1999).
17. S. Alsoy, *Ind. Eng. Chem. Res.*, **40**, 2995 (2001).
18. S. Alsoy, J.L. Duda, *AIChE J.*, **48**, 1849 (2002).
19. S.-S. Wong, S. Alsoy Altinkaya, S.K. Mallapragada, *Polymer*, **45**, 5151 (2004).

20. S. Alsoy Altinkaya, Bulent Ozbas, *J. Membrane Sci.*, **230**, 71 (2004).
21. Y. Yip, A.J. McHugh, *J. Membrane Sci.*, **271**, 163 (2006).
22. A.F.M. Barton, *CRC Handbook of Solubility Parameters and Other Cohesion Parameters*, CRC Press, 2nd edition (1991).
23. F. Rodríguez, *Principles of polymer systems*, Hemisphere Publishing Co., 3rd edition (1989).
24. T. Lindvig, M.L. Michelsen, G.M. Kontogeorgis, *Fluid Phase Equilibria*, **203**, 247 (2002).
25. J.H. Kim, B.R. Min, J. Won, H.C. Park, Y.S. Kang, *J. Membrane Sci.*, **187**, 47 (2001).
26. S.-U Hong, *Ind. Eng. Chem. Res.*, **34**, 2536 (1995).
27. R.K. Toghiani, H. Toghiani, G. Venkateswarlu, *Fluid Phase Equilibria*, **122**, 157 (1996).
28. S.-J. Park, K.-J. Han, J. Gmehling, *Fluid Phase Equilibria*, **200**, 399 (2002).
29. J. Gmehling, J. Li, M. Schiller, *Ind. Eng. Chem. Res.*, **32**, 178 (1993).
30. E. Leroy, A. Alegría, J. Colmenero, *Macromolecules*, **36**, 7280 (2003).
31. A. Vergara, L. Paduano, V. Vitagliano, R. Sartorio, *Phys. Chem. Chem. Phys.*, **1**, 5377 (1999).
32. E. Keshmirizadeh, H. Modarress, A. Eliassi, G.A. Mansoori, *European Polymer J.*, **39**, 1141 (2003).
33. A.A. Bhat, V.G. Pangarkar, *J. Membrane Sci.*, **167**, 187 (2000).
34. M. Niang, G. Luo, *Separation and Purification Technology*, **24**, 427 (2001).
35. J.S. Yang, H. J. Kim, W.H. Jo, Y.S. Kang, *Polymer*, **39**, 1381 (1998).
36. S. Loras, A. Aucejo, R. Muñoz, J. Wisniak, *J. Chem. Eng. Data*, **44**, 203 (1999).
37. P. Mukoma, B.R. Jooste, H.C.M. Vosloo, *J. Membrane Sci.*, **243**, 293 (2004).

L. Pitol-Filho, R. Garcia-Valls

Methods to calculate penetrant-polymer Flory-Huggins interaction parameters

Methods to calculate penetrant-polymer Flory-Huggins interaction parameters: comparison and validation

Luizildo Pitol-Filho and Ricard Garcia-Valls

Departament d'Enginyeria Química
Escola Tècnica Superior d'Enginyeria Química
Universitat Rovira i Virgili
Av. Països Catalans 26
43007 Tarragona, Spain
Tel.: +34 977 55 96 11; fax: +34 977 55 85 44
ricard.garcia@urv.net

Abstract

The Flory-Huggins interaction parameter describes the affinity between a penetrant and a polymer. There are some contribution rules to predict its value from the molecular structures of the components, that require the calculation of the molar volume and the cohesion parameters of all the components involved. Those contribution rules do not require any experimental data. However, sometimes it is not clear which rules should be more adequate for a determined system. For several components, we compared the data of molar volume and cohesion parameters available in the literature to values calculated by some contribution rules. Besides, for some binary systems found in the literature, we calculated the Flory-Huggins interaction parameter by a classic method and by a three-dimensional approach.

Keywords: polymer, Flory-Huggins, thermodynamics, group contribution

Introduction

As polymers have a wide field of application, it is mandatory to know how they interact with chemicals such as solvents. Thus, thermodynamics of polymers may be a useful tool not only to understand how polymers behave, but also to select which materials are more suitable for a determined application, such as separation by pervaporation [1,2], coating technology [3], or membrane formation [4,5]. The well-known Flory-Huggins model describes satisfactorily the thermodynamics of polymers [6,7] with a single interaction parameter, that may be determined either by experiments [8] or by group contribution rules [6]. Eq.(1) expresses a general form of the Flory-Huggins interaction parameter (χ) for a penetrant(1)-polymer(2) system:

$$\chi_{12} = \beta + \alpha \frac{V}{RT} D_{12}^2 \quad (1)$$

Table 1 summarizes the coefficients for the χ expression for both classic and three-dimensional (3D) approaches:

Table 1 – Coefficients of the Flory-Huggins interaction parameters.

Approach	α	β	D_{12}^2
Classic [6]	1	0.35	$(\delta_{1,total} - \delta_{2,total})^2$
3D [7]	1	0	$(\delta_{1,d} - \delta_{2,d})^2 + 0.25(\delta_{1,p} - \delta_{2,p})^2 + 0.25(\delta_{1,hb} - \delta_{2,hb})^2$

The 3D approach implies that the overall cohesion parameter is correlated to the dispersion, polar and hydrogen bonding solubility parameters, also known as Hansen parameters. Eq.(2) relates the overall and the Hansen parameters:

$$\delta_{total}^2 = \delta_d^2 + \delta_p^2 + \delta_{hb}^2 \quad (2)$$

There are several methods in the literature to calculate the cohesion parameters and also to obtain the molar volume. However, very often the criteria of applicability of such methods is not presented. In the present work we compared published data of binary systems, such as molar volume, cohesion parameters and Flory-Huggins interaction parameters, to calculated values for the same parameters by using the available methods, in order to recommend a method when no information is found about a determined chemical species.

Methods

To obtain the Flory-Huggins interaction parameter for a solvent-polymer pair, first we need to determine the molar volume at 0K and the cohesion parameters for those species.

Molar volume at 0K

The liquid molar volume at 0K may be calculated either by group contribution or by computing atom by atom in the molecular structure. Table 2 lists the Sugden and Blitz atomic contribution rules [9].

Table 2 – Contribution rules to calculate molar volume.

Component	Sugden (cm ³ /gmol)	Blitz (cm ³ /gmol)
H	6.7	6.45
C (aliphatic)	1.1	0.77
C (aromatic)	1.1	5.1
N	3.6	-
O	5.9	-
Cl	19.3	16.3
S	14.3	-
Triple bond	13.9	16.0
Double bond	8.0	8.6
5-membered ring	1.8	-
6-membered ring	0.6	-
OH (alcoholic)	-	10.5
OOH (carboxyl)	-	23.2

A more extensive contribution rule was compiled by Beerbower [10], where groups are considered instead of atoms. Some examples are found in Table 3.

Table 3 – Contribution rule according to Beerbower's compilation.

Group	Beerbower's rule (cm ³ /gmol)
- CH ₃	31.70
-CH ₂ -	16.60
=CH-	12.40
>CH-	-1.00
-COO-	8.20
-O-	3.60
-OH	10.47
>SiO<	3.80

In the literature, the molar volume is found either on a molar or on a mass basis. All the rules presented here allow us to obtain the molar-based property. Therefore, to compare to the mass-based values often found in literature, we just divided the calculated values by the molar mass.

Cohesion parameters

The use of the cohesion parameters just aims to provide a simple method for prediction of cohesive and adhesive properties of materials from the properties of the pure components [10]. Very often the cohesion, or Hildebrand, parameter is referred as solubility parameter, but such nomenclature is quite restrictive for a quantity that may be helpful to correlate a wide range of physical and chemical properties, such as the Flory-Huggins interaction parameter. The cohesion parameter [6] is related to the molar energy of vaporization of a pure liquid, also known as the cohesive energy-density by Eq. (3):

$$\delta_i = \sqrt{E_i^{coh}} = \sqrt{\frac{\Delta E_i^v}{V_i(T_{ref})}} \quad (3)$$

Therefore, when the enthalpy of vaporization and the molar volume are known, the cohesion parameter can be easily obtained. Eq.(4) expresses the enthalpy of vaporization in terms of vapor pressure [11]:

$$\Delta H^v = T\Delta S^v = RT^2 \frac{d \ln P^v}{dT} \quad (4)$$

Finally Eq. (3) becomes:

$$\delta_i = \sqrt{\frac{\Delta H^v - RT}{V_i(T_{ref})}} = \sqrt{\rho_{molar}(\Delta H^v - RT)} \quad (5)$$

Therefore, the cohesion parameter for the transported species may be obtained either by calculating the vapor pressure or by using commercial process simulators, like Aspen Hysys®, that have a very complete database of chemical compounds. In the present work we used the Antoine equation of state. This approach allows us to obtain a cohesion parameter depending on temperature, what can be useful while modeling processes that do not occur at room temperature.

However, since energy of vaporization for solids or polymers has no sense, group contribution methods are required. Among them, the most widely used are the rules provided by Small and Hoy [6], where a molar attraction constant is given for each chemical group in the polymer repeating unit. By adding all the constants, the cohesion parameter can be easily obtained:

$$\delta_i = \frac{\sum_j F_j}{V_i} \quad (6)$$

Table 4 lists the molar attraction constants used to calculate the cohesion parameters for the most common methods available in the literature. Those values were obtained by regression analysis of physical properties data for a wide range of organic compounds (640 compounds in the case of Hoy). In the method provided by Small, however, some groups that form hydrogen bonds were excluded.

Table 4 - Representative molar attraction constants.

Group	Molar attraction constant, F (MPa ^{1/2} cm ³ gmol ⁻¹)		
	Small	Hoy	van Krevelen
-CH ₃	438	303	420
-CH ₂ -	272	269	280
>CH-	57	176	140
>C<	-190	65.5	0
-CH=CH-	454	497	444
>C=CH-	266	422	304
-O- (ether)	143	235	256
-OH	-	462	754
-CO- (ketones)	563	538	685
-COO- (esters)	634	668	512
-OCOO- (carbonate)	-	(904)	767
-NH-	-	368	-
-S- (sulfides)	460	428	460
-Cl (primary)	552	420	471
-Si	-77	-	-

Another approach considers three aspects of the cohesion parameters: dispersion, polarity and hydrogen bonds. In a recent work [12], we proved that the 3D modeling should be preferred rather than the classic model, especially when highly polar penetrants are involved. Extensive tables to calculate the dispersion, polar and hydrogen-bonding Hansen parameters are presented in the literature [10]. Such calculations, as the one expressed by Eq.(6), also involve the molar volume.

Flory-Huggins interaction parameters

Eq.(1) was used to calculate the Flory-Huggins parameter at 298K, once the molar volumes and cohesion parameters were calculated, for both classic and 3D models.

Results

Figure 1 shows the results for the molar volume of polymers, plotted against the values found in the literature.

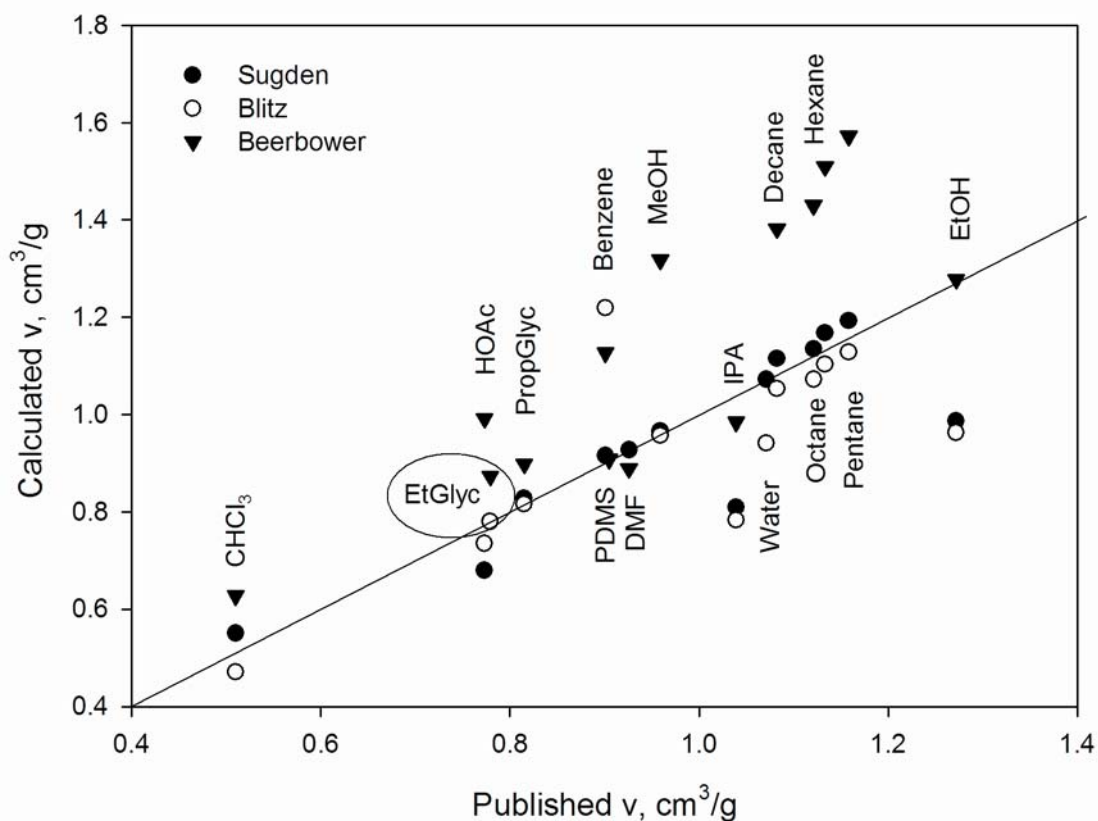


Figure 1 – Comparison between published and calculated molar volumes.

Figure 1 shows good agreement between the published data and the values predicted by both Sugden and Blitz rules for DMF [13], chloroform, HOAc, EtGlyc, PropGlyc, n-pentane, n-hexane, n-octane, n-decane, benzene, PDMS [9], water [9,13], MeOH [14,15], EtOH and IPA [16]. It is quite clear that Sugden

and Blitz rules are preferred among authors, being just EtOH and IPA the most significant exception, where the authors clearly used Beerbower rule.

Figure 2 compares the total cohesion parameters obtained to the published values [6]. It is clear that the vaporization method provides lower deviation than the other ones. We should keep in mind that, since the calculation of the cohesion parameter by either Small or Hoy method involves the molar volume, accumulated errors may exist. Therefore, by Figure 1, we can conclude that an unfortunate choice of the molar volume can lead to high deviations in the cohesion parameter. For each component we chose the method which provided more agreement with the published values.

Besides, the method of enthalpy of vaporization also allows calculating the cohesion parameter at different temperatures, what is useful for processes that do not occur at room temperature. However, it is out of the scope of the present work.

The knowledge of the cohesion parameters also may be useful for the organic synthesis and the processing of new materials. When a new polymer is synthesized, there is no other form to find an appropriate solvent for it than trial and error. However, this search can be reduced by using the cohesion parameters. A polymer is likely dissolved by a determined solvent if both have similar cohesion parameters. Polymers of substituted benzylglycidylether derivatives [17] were obtained and successfully dissolved by tetrahydrofuran (THF), chloroform and benzene. However, the polymers were not dissolved by acetone or MeOH. By using the Hoy and Small contribution rules, we calculated the cohesion parameters for a series of those co-polymers, obtaining values between 18 and 20 MPa^{1/2}. Those values are very close for the solvents reported (benzene: 18.6 MPa^{1/2}; chloroform: 19.0 MPa^{1/2}; THF: 19.4 MPa^{1/2} [6]), and quite distant for MeOH (29.7 MPa^{1/2}). However, the cohesion parameter for acetone is around 20 MPa^{1/2}. In this case we may assume that the effect of precipitation is due to other effects, what maybe can be explained by using the three-dimensional approach of Flory-Huggins theory. We will explore the correlation of cohesion parameters for co-polymers in a further work.

Literature lists the Flory-Huggins parameters for several binary systems. We collected data for the following systems:

- PDMS with benzene and MeOH [18], EtOH [19] and chloroform [19,20];
- PVA with benzene [18], water [15] and MeOH [15,18];
- CTA with benzene [18], MTBE [21] and MeOH [18,21];
- PSf with DMF, chloroform and IPA [22], HOAc [23], and water [13,23,24].

Figure 3 compares the data found in literature to the predicted ones, by using both classic and 3D models. We observe that for most of cases, quality of prediction was enhanced by considering the dispersion, polar and hydrogen-bonding effects. It was necessary to include horizontal error bars for some cases, when there was much difference between the values published for a determined binary system.

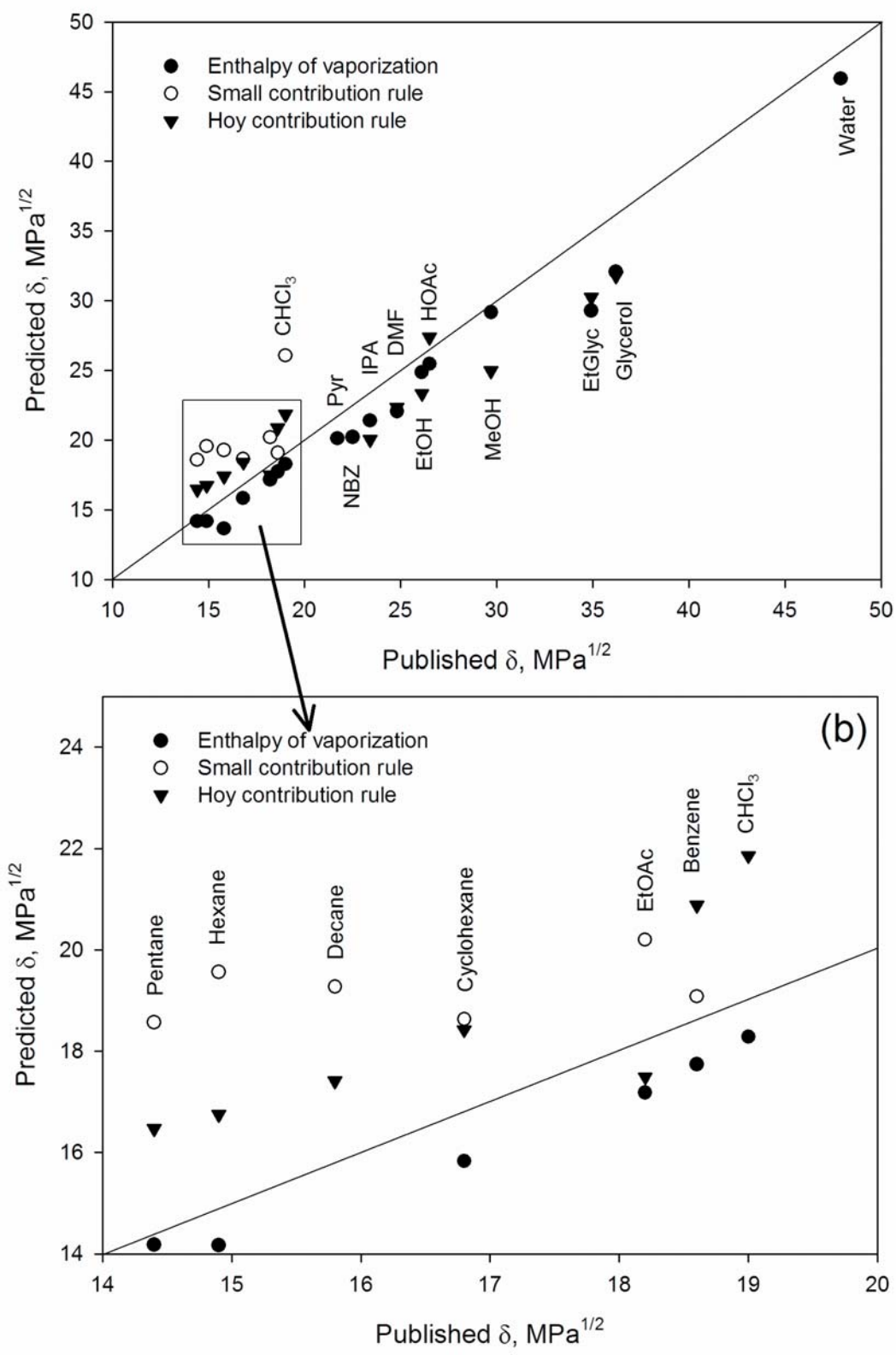


Figure 2 – Comparison between published and calculated cohesion parameters (b: reduced scale).

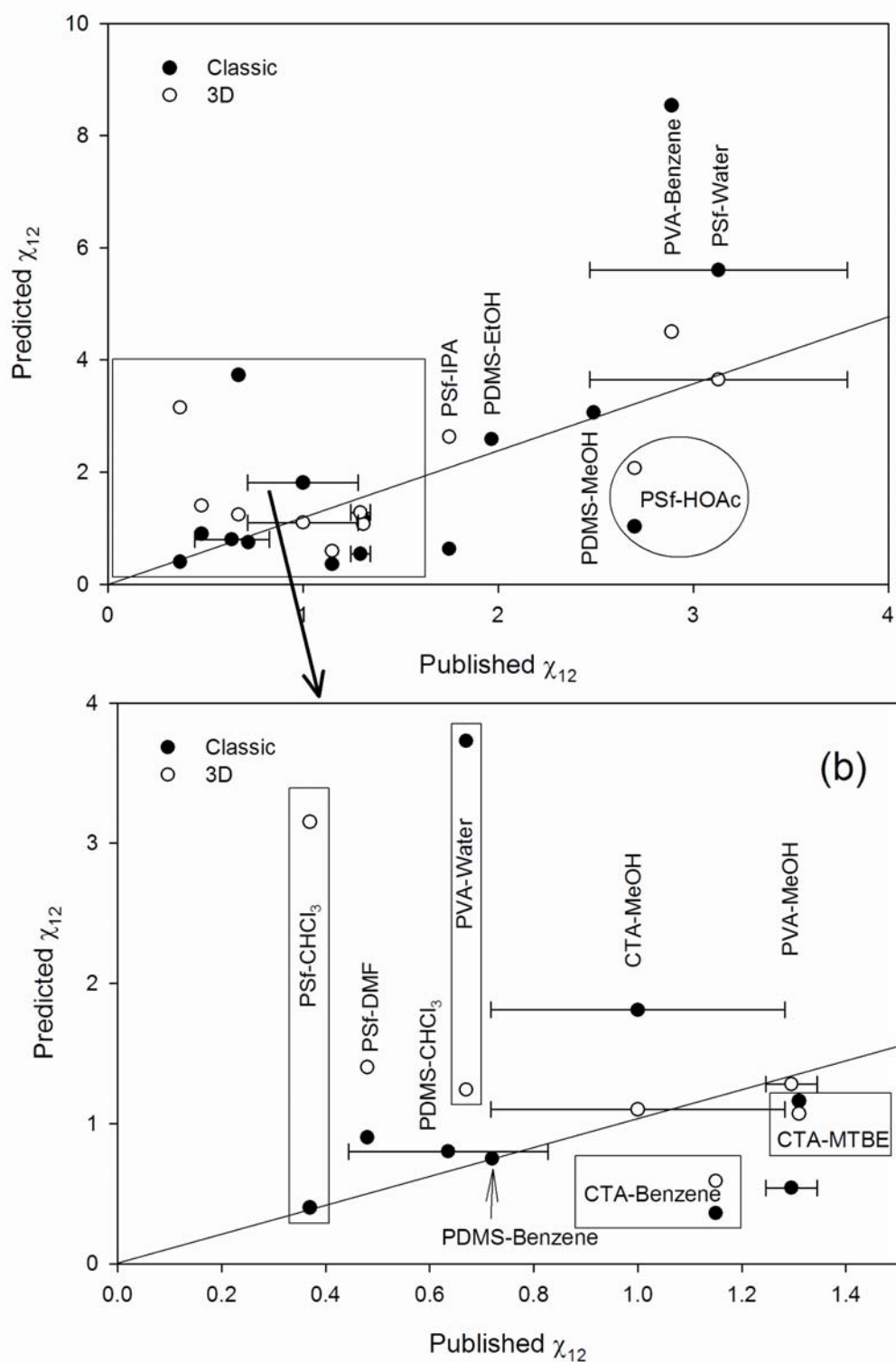


Figure 3 – Comparison between published and calculated Flory-Huggins interaction parameters for classic and 3D models (b: reduced scale).

For PDMS it was not possible to calculate the three-dimensional parameters because the group contribution tables did not contemplate the (-SiO-) group. However, PDMS-component interaction values calculated by the classic approach fit well to the data published. We would like to emphasize that most of those Flory-Huggins parameters were determined experimentally by sorption. So, the three-dimensional approach reveals to be very useful, except for the pairs PSf-CHCl₃ and PSf-DMF.

Table 5 lists the three-dimensional Hansen parameters calculated by the contribution rules for the components whose data were not found in literature.

Table 5 – Hansen parameters for polymers and penetrants.

Component	$\delta_d, \text{MPa}^{1/2}$	$\delta_p, \text{MPa}^{1/2}$	$\delta_{hb}, \text{MPa}^{1/2}$
MTBE	21.5	8.4	4.7
CTA	17.7	5.3	11.9
PVA	21.7	15.9	25.2
PSf	21.5	2.8	6.7

Recently [12] we proposed a criterion to apply the 3D approach, expressed by Eq.(7), as follows:

$$\Gamma_j = \frac{(\delta_{1,j} - \delta_{3,j})^2}{(\delta_{1,d} - \delta_{3,d})^2 + (\delta_{1,p} - \delta_{3,p})^2 + (\delta_{1,hb} - \delta_{3,hb})^2} > 0.5 \quad (7)$$

where j represents either polar or hydrogen-bonding effects. Table 6 lists the values of Γ function for the studied systems, also evaluating if applicability of Eq.(7) helped to improve predictions.

Table 6 – Applicability of criterion to choose a Flory-Huggins approach (✓: yes; ✗:no)

Polymer	Penetrant	Γ_p	Γ_{hb}	Applicability of Γ criterion is correct?
PVA	Water	0.13	0.63	✓
	MeOH	0.08	0.01	✗
	Benzene	0.10	0.84	✓
CTA	MeOH	0.24	0.60	✓
	MTBE	0.13	0.68	✓
	Benzene	0.15	0.82	✓
PSf	Chloroform	0.52	<0.01	✗
	DMF	0.76	0.13	✗
	IPA	0.26	0.45	✓
	HOAc	0.30	0.50	✓
	Water	0.25	0.70	✓

Although Figure 3 shows that the 3D approach provided less accurate predictions for the system CTA-MTBE, we consider negligible the differences. Therefore, by using the Γ function, there are just three disagreements: PVA-MeOH, PSf-Chloroform and PSf-DMF. It is remarkable that, for PSf-Chloroform

and PSf-DMF the Γ_{hb} values are much lower than the limit suggested (0.50). Then, the criterion could be updated to a one based just on the hydrogen-bonding effects. In other words, the j index in Eq. (7) should refer to hydrogen-bonding Hansen parameters. However, we still cannot explain the disagreement between our criterion and the behavior of the PVA-MeOH system. On further works, however, we will test the applicability of our method to more systems.

Conclusions

To explain the behavior of penetrant-polymer systems, a popular approach is the Flory-Huggins theory, since it provides good results without using any experimental data and it is based on the molecular structures of the components. Those calculations involve a series of parameters and very often the criteria of applicability of the group contribution methods are not so clear. In this work, we aimed to compare published data to predictions using those methods. Our conclusions may be summarized in the following points:

- for molar volumes, the Sugden and Blitz contribution methods have, in average, equivalent results;
- the vaporization method provides lower deviation than Hoy or Small methods. Those methods also include the molar volume, and accumulated errors may exist;
- 3D approach for Flory-Huggins parameters leads to lower deviations from the experimental results collected. However, the criterion of applicability of the 3D approach should be improved.

Nomenclature

Acronyms

3D	three-dimensional Flory-Huggins approach
DMF	N-N-dimethylformamide
CTA	cellulose triacetate
EtGlyc	ethylene glycol
EtOAc	ethyl acetate
EtOH	ethanol
HOAc	acetic acid
IPA	2-propanol
MeOH	methanol
MTBE	methyl tert-butyl ether
NBZ	nitrobenzene
PDMS	polydimethylsiloxane
PropGlyc	propylene glycol
PSf	polysulfone
PVA	poly vinyl alcohol
Pyr	pyridine
THF	tetrahydrofuran

Variables and parameters

D_{i2}^2	composition factor of Flory-Huggins parameter
E^{coh}	molar cohesion energy (J. gmol^{-1})
F	molar attraction constant ($\text{MPa}^{1/2} \cdot \text{cm}^3 \cdot \text{gmol}^{-1}$)
ΔH^{v}	vaporization enthalpy (J. gmol^{-1})
M_i	molecular weight (g. gmol^{-1})
P^{v}	vapor pressure
R	ideal gas constant
ΔS^{v}	vaporization entropy ($\text{J. gmol}^{-1} \cdot \text{K}^{-1}$)
T	temperature, K
V_i	molar volume of component i ($\text{cm}^3 \cdot \text{gmol}^{-1}$)
v_i	molar volume of component i ($\text{cm}^3 \cdot \text{g}^{-1}$)

Greek symbols

α	multiplier factor of Flory-Huggins parameter
β	linear factor of Flory-Huggins parameter
δ_i	Hansen parameter of component i ($\text{MPa}^{1/2}$)
Γ	orientative function to select Flory-Huggins approach
ρ^{molar}	molar density (gmol. cm^{-3})
μ_i	chemical potential of component i
χ_{ij}	i-j Flory-Huggins interaction coefficient

Subscripts

d	dispersive
hb	hydrogen-bonding
p	polar
1	penetrant
2	polymer

References

- [1] A. Hasanoğlu, Y. Salt, S. Keleşer, S. Özkan, S. Dinçer. Chemical Engineering and Processing 44 (2005) 375-381.
- [2] P. Shao, R.Y.M. Huang. J. Membrane Science 287 (2007) 162-179.
- [3] S. Alsoy, J.L. Duda. AIChE J 45 (1999) 896-905.
- [4] R.M. Boom, Th. van den Boomgaard, C.A. Smolders. Macromolecules 27 (1994) 2034-2040.
- [5] D. Wang, K. Li, W.K. Teo. J. Applied Polymer Science 71 (1999) 1789-1796.
- [6] J. R. Fried. Polymer science and technology (1995), Prentice Hall.
- [7] T. Lindvig, M.L. Michelsen, G.M. Kontogeorgis. Fluid Phase Equilibria 203 (2002) 247-260.
- [8] M. Karimi, W. Albrecht, M. Heuchel, M.H. Kish, J. Frahn, Th. Weigel, D. Hofmann, H. Modarress, A. Lendlein. J. Membrane Science 265 (2005) 1-12.
- [9] J. M. Zielinski, J.L. Duda. AIChEJ 38 (1992) 405-415.
- [10] A.F.M. Barton. CRC Handbook of solubility parameters and other cohesion parameters. CRC Press, 2nd edition (1991).

- [11] A.M.A. Dias. Thermodynamic properties of blood substituting liquid mixtures. PhD Thesis (2005), Universidade de Aveiro, Portugal.
- [12] L. Pitol-Filho, R. Garcia-Valls. Polymer Engineering and Science (2007). In press.
- [13] Y. Yip, A.J.McHugh. J. Membrane Science 271 (2006) 163-176.
- [14] S.-U. Hong, A.J. Benesi, J.L. Duda, Polymer International 39 (1996) 243-249.
- [15] S.-S. Wong, S. Alsoy Altinkaya, S.K. Mallapragada. Polymer 45 (2004) 5151-5161.
- [16] D. Bhanushali, S. Kloos, C. Kurth, D. Bhattacharyya. J. Membrane Science 189 (2001) 1-21.
- [17] M. Giamberini, J.A. Reina, J.C. Ronda. J. Polymer Science A: Polymer Chemistry 44(2006) 1722-1733.
- [18] S. Mandal, V.G. Pangarkar. J. Membrane Science 201 (2002) 175-190.
- [19] E. Favre. European Polymer J. 1996 (32) 1183-1188.
- [20] J.S. Yoo, S.J. Kim, J.S. Choi. J. Chem. Eng. Data 44 (1999) 16-22.
- [21] J.S. Yang, H.J. Kim, W.H. Jo, Y.S. Kang. Polymer 39 (1998) 1381-1385.
- [22] W.F.C. Kools. Membrane formation by phase inversion in multicomponent polymer systems. PhD Thesis (1998). Universiteit Twente, Netherlands.
- [23] I.M. Balashova, R.P. Danner, P.S. Puri, J.L. Duda. Ind. Eng. Chem. Res. 40 (2001) 3058-3064.
- [24] Y.-M. Wei, Z.-L. Xu, X.-T. Yang, H.-L. Liu. Desalination 192 (2006) 91-104.

C. Torras, D. Gezahegn, L. Pitol-Filho, R. Garcia-Valls

Novel polymeric membrane structures: microcapsules

Desalination 200 (2006) 12-14



Novel polymeric membrane structures: microcapsules

Carles Torras, Dawit Gezahegn, Luizildo Pitol-Filho, Ricard Garcia-Valls*

*Departament d'Enginyeria Química, Universitat Rovira i Virgili,
Av. Països Catalans, 26, 43007 Tarragona, Spain
Tel. +34 97755-9611; email: ricard.garcia@urv.net*

Received 21 October 2005; accepted 2 March 2006

1. Introduction

In this work, microcapsules, which are novel polymeric membrane structures, were prepared by using the immersion precipitation technique, and were morphologically characterized by using several microscopy techniques [1].

The performance potential of this structure is the possibility to encapsulate substances [2], which can be delivered with a desired velocity, by just controlling the morphology of porous structured wall and its chemical composition. Microcapsules with sizes of about 50 μm are expected to be obtained by using micro-devices [3].

2. Experimental

Microcapsules were synthesized from poly-sulfone as polymer and di-methyl formamide (DMF) as solvent. Several coagulation baths were tested by using water and iso-propanol (IPA) as non-solvents, and also their mixture with the solvent. Two types of synthesis techniques were used. The first one consisted in adding the polymer solution to the coagulation bath, which contained a dispersing agent (gelatin) and the

second one consisted in adding droplets of polymeric solution to the coagulation bath.

The morphological characterization of the external surfaces, and of the internal porous structures of microcapsules, was carried out by using several microscopy techniques: scanning electron microscopy (SEM), transmission electron microscopy (TEM) and Confocal microscopy (Confocal). SEM and TEM were used to characterize external surfaces. However, in order to characterize the internal porous structure, serious difficulties arise, since this is usually done by SEM after cryogenically cutting the membrane manually to obtain a cross-section without modifying the structure [1]. In this case, due to the size of the microcapsules (typically from 1 to 500 μm), it cannot be performed in the same manner. Therefore, two techniques were used instead: (1) a microcapsules-pellet was prepared and then included in gelatin and resin in order to obtain a full solid block that was feasible to be cut and examined by both TEM and Confocal; (2) the microcapsules were filled with a fluorescent agent and examine them with the Confocal. The main advantage of this microscopy technique is that there is no need to cut the sample in order to examine the internal structure, and a reconstruction of the entire volume can be achieved.

*Corresponding author.

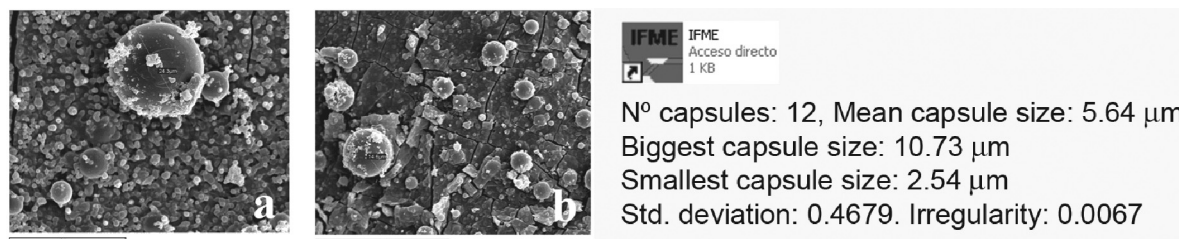


Fig. 1. SEM micrographs of microcapsules obtained with 3% PSf in DMF with a composition of the coagulation bath of 50% IPA and 50% DMF. IFME numerical results of micrograph (b).

Some of the qualitative results obtained with the SEM and TEM were interpreted by using the IFME[®] software [4], in order to obtain numerical results of the main morphological properties of the membrane. For the Confocal results, ImageJ[®] and MetaMorph[®] software were used in order to reconstruct and also interpret the 3D structure of the microcapsules.

3. Results

The microcapsule synthesis using the first technique (adding the polymer solution to the coagulation bath containing the dispersing agent) allowed us to obtain small microcapsules with sizes varying from 1 to 50 μm (Fig. 1). The use of the dispersing agent did not avoid the polymer aggregation which is caused by the fast polymer precipitation. Therefore, the efficiency (polymer transformed in microcapsule/total polymer) of the process is low.

For this reason, the use of IPA provided better results, since it has a low interaction with the solvent and the polymer, and the precipitation

requires more time than when water is used as non-solvent, where precipitation is instantaneous.

The microcapsule synthesis by using the second technique (addition of droplets to the coagulation bath) produced all the capsules with the same size that is directly related to the diameter of the needle used. Furthermore, the efficiency was 100%. Capsules between 1 and 2 mm were synthesized (Fig. 2) and characterization results obtained from novel techniques were compared to those obtained with traditional ones, while preparing the device to produce 50 μm microcapsules (to be carried out in micro-devices [3]). Results showed the free volume inside the capsule and a porous structure similar than the flat membranes obtained with the same synthesis conditions. Similar characterization results were obtained with all techniques.

4. Conclusions and present work

An optimal technique to produce microcapsules consists of two-step process, which is the synthesis of polymeric droplets and the posterior

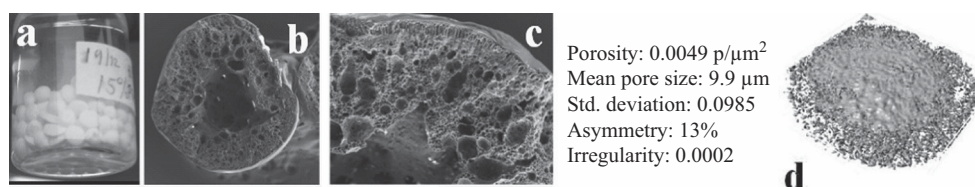


Fig. 2. (a) Capsules obtained with 15% PSf in DMF with a coagulation bath containing 50%IPA–50%DMF. (b) and (c) SEM cross-section micrographs and IFME[®] numerical results of (c). (d) 3D reconstruction of the 90 μm thickness central part of the capsule from Confocal results (without cutting the sample).

precipitation. The efficiency is 100%, the homogeneity in size is total and no further substances are needed. The confocal microscopy is a valid technique to characterize morphologically the internal structures of microcapsules.

Acknowledgement

This work is supported by the IMPULSE European Project FP6-2003-NMP-IN-3.

References

- [1] C. Torras, Obtenció de membranes polimèriques selectives, Thesis dissertation, Dep. Chemical Engineering, Universitat Rovira i Virgili, (13/10/2005.) ISBN: 84-689-3628-6.
- [2] X.C. Gong et al., Separation of organic acids by newly developed polysulfone microcapsules containing triethylamine, Separation Purification Technol., in press, Corrected Proof, Available online 30 August 2005.
- [3] T.M. Floyd, A novel microchemical system for rapid liquid–liquid chemistry, PhD. Thesis, MIT, Cambridge, MA, 2001.
- [4] C. Torras and R. Garcia-Valls, Quantification of membrane morphology by interpretation of Scanning Electron Microscopy Images, J. Membr. Sci., 233 (2004) 119–127.

L. Pitol-Filho, C. Torras, J. Bonet-Avalos, R. Garcia-Valls

Modeling of polysulfone membrane formation by immersion precipitation

Desalination 200 (2006) 427-428



Modelling of polysulfone membrane formation by immersion precipitation

Luizildo Pitol-Filho, Carles Torras, Josep Bonet-Avalos, Ricard Garcia-Valls*

*Departament d'Enginyeria Química, Universitat Rovira i Virgili,
Av. Països Catalans, 26, 43007, Tarragona, Spain
Tel. +34 977559610; Fax +34 977559621; email: ricard.garcia@urv.net*

Received 28 October 2005; accepted 3 March 2006

1. Introduction

Asymmetric membranes have a wide field of application because of its unique morphology. Its high selectivity is assured when a dense layer alternates with a porous one. Immersion precipitation is one of the processes generally used for the membrane production. In this process, a polymeric solution placed on the top of a glass plate is immersed in a bath of a non-solvent. The membranes are formed as long as the solvent leaves the polymeric layer and the non-solvent takes its place. The driving force for the membrane formation is the difference of chemical potential between the bath and the polymeric layer.

2. Experimental

A large number of membranes were obtained by immersion precipitation technique using several proportions of polysulfone (PSf) in dimethyl formamide (DMF) as solvent and several compositions in the coagulation bath from pure water to 2-propanol (IPA), as non-solvent. The cross section of membranes was characterized

by scanning electron microscopy (SEM) and the micrographs obtained were interpreted using IFME® software in order to quantify the main morphology parameters. IFME® software was developed by our group, and has been described in a previous work [1].

3. Modelling

The formation of membranes may be described by equations derived from the Free-Volume theory coupled to the Flory–Huggins thermodynamics. The equations used are very similar to those derived for the obtention of membrane by solvent evaporation [2]. Just the boundary condition at the interface changes, because here the liquid–polymer equilibrium is taken into account. The continuity equations in the polymeric phase are directly written in terms of volume fraction, as well as the boundary conditions and the equation for the thickness of the membrane.

4. Results and discussion

Fig. 1 shows the cross section of a membrane obtained with 20 wt.% PSf and its interpretation

*Corresponding author.

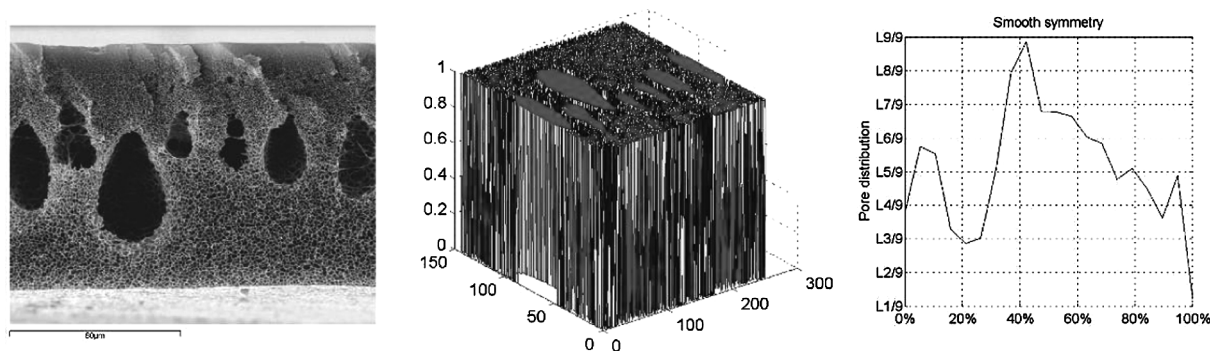


Fig. 1. SEM micrograph of a membrane synthesized with 20 w% polysulfone (PSf) in dimethyl formamide (DMF) and with pure water into the coagulation bath; IFME® micrograph interpretation and symmetry analysis [1].

by using the IFME® software. After repeating this method with a large number of different membranes, a correlation was found between the polymer concentration and the membrane mean pore size [2]: $P_s = 10.069 - 0.3961 [\text{PSf}]$. In Fig. 1, both SEM image and IFME® interpretation show a distribution of porosity through the membrane: a very dense layer on top and regions of high porosity in the middle, and intermediate porosity near the bottom. Such asymmetric configuration may be useful for several

applications that require high selectivity, for example in fuel cells based on methanol. The initial concentrations of the polymeric solutions are shown in Fig. 2, as well as the equilibrium curve that may exist when the precipitation bath has a DMF molar fraction varying from 0.04 to 0.65.

Fig. 2 also shows the spinodal curve for the system and the approximate location of the different polymer volume fractions once the membranes are formed: a dense layer on top, a region with macrovoids in the middle, and the microporous regions. The mathematical modelling of the membrane formation, by using Free-Volume theory and Flory–Huggins equilibrium approach, will provide the concentration paths that lead to the obtention of each different region within the membrane.

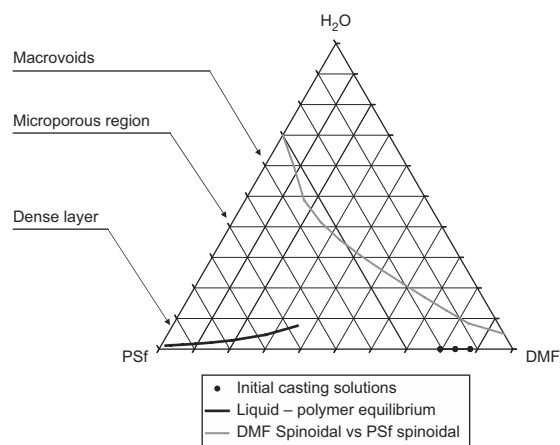


Fig. 2. Ternary diagram for the system DMF–water–PSf.

References

- [1] C. Torras and R. Garcia-Valls, Quantification of membrane morphology by interpretation of scanning electron microscopy images, *J. Membr. Sci.*, 233 (2004) 119–127.
- [2] S.A. Altinkaya and B. Ozbas, Modeling of asymmetric membrane formation by dry-casting method, *J. Membr. Sci.*, 230 (2004) 71–89.

L. Pitol-Filho, C. Torras, J. Bonet-Avalos, R. Garcia-Valls

Fluidic and thermodynamic insights on the formation of microcapsules by using
micromixers

Fluidic and thermodynamic insights on the formation of polymer microcapsules by using micromixers

Luizildo Pitol-Filho, Carles Torras, Josep Bonet-Avalos, Ricard Garcia-Valls

Departament d'Enginyeria Química
Escola Tècnica Superior d'Enginyeria Química
Universitat Rovira i Virgili
Av. Països Catalans 26
43007 Tarragona, Spain
Tel.: +34 977 55 96 11; fax: +34 977 55 85 44
ricard.garcia@urv.cat

Abstract

Microcapsules have wide applications in the field of controlled release, either for drug or fragrances delivery. One possibility to obtain microcapsules is by emulsifying a polymeric solution in a continuous phase and, then, by precipitating the droplets in a non-solvent. Micromixing technology may be used, where the solutions flow through microchannels, allowing a better control of the synthesized structures. We present some results of diameters of microcapsules obtained by varying the ratio of the polymeric solution to the continuous phase. Pure polysulfone microcapsules were smaller than the ones containing vanillin. A simple fluidodynamic model based on the Rayleigh assumption was derived to predict the diameter of the microcapsules, as well as the diameter of the vanillin core, and the species-polymer Flory-Huggins interaction parameters were calculated, for further thermodynamic studies.

Keywords: microencapsulation, modeling, fluidodynamics, Rayleigh mechanism

Introduction

Microcapsules have applications of high technological impact, such as the controlled release of drugs and perfumes, and they are composed by a polymeric dense shell covering a core full of product. The polymeric shell may have varying structure and even be porous, but its most external layer should be dense, in order to control the release rate of the product. Much attention has been done to the interfacial polymerization (a.k.a *in situ* polymerization), where droplets of a monomer solution are put in contact with a solution of a second monomer, and reaction is produced at the external surface of the droplet, reducing the kinetic reaction as long as the dense layer is formed, blocking the entrance of the external monomer and further stopping the polymerization reaction. Some good examples are the production of poly(urea-urethane) microcapsules [1] and the encapsulation of lemon oil in urea-formaldehyde [2].

Another way to produce microcapsules is dissolving both the product to be delivered and the polymer in a determined solvent. Then, microcapsules may be produced by precipitating droplets of the product-polymer solution into a non-solvent phase, in a similar way to the formation of membranes by immersion

precipitation [3]. In a previous work we produced polysulfone microcapsules by batch mode [4], without any product inside the microcapsules. It was not necessary to add any emulsifier to stabilize the droplets, since they precipitated instantaneously. However, there was a wide distribution of diameters, as well as formation of aggregates. The efficiency of the precipitation was very low.

Microchannels-based mixers, shortly called *micromixers*, have wide applications in chemical engineering, being absorption, emulsification, foaming and reaction just some of them [5]. Liquid-liquid mixing in those devices was extensively studied for several geometries [6]. We built a set-up based on two micromixers to produce microcapsules in two steps: (1) making an emulsion of a polymeric solution in cyclohexane; and (2) precipitating the droplets in water. By keeping constant the flow rate of the continuous phase (cyclohexane), we studied how the flow rate of polymeric solution affected the diameters of the produced microcapsules. Also we present some results of encapsulation of vanillin in polysulfone by using this method. We were able to adjust a fluidodynamic model based on Rayleigh mechanism to the diameters of microcapsules of pure polymer, and, by comparison with the vanillin capsules, we were able to estimate the diameter of the vanillin core.

Experimental

Description of experimental set-up

To obtain the polymeric microcapsules we designed a set-up based on micromixers that was able, in a first step, to form droplets of a polymeric solution in a continuous phase and, then, precipitate the droplets in water. We needed to choose an appropriate continuous phase (cyclohexane) that would neither mix with the solvent (N-N-dimethylformamide) nor precipitate the polymer (PSf), to assure the formation of droplets. Figure 1 shows an image of the complete set-up.

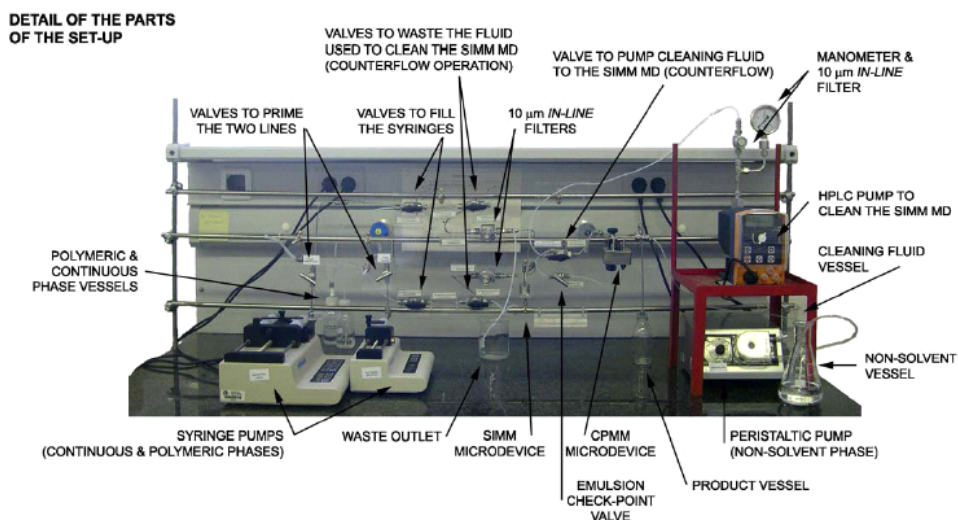


Figure 1 – Experimental set-up for the production of microcapsules.

Two syringe pumps deliver the continuous phase and the polymeric solution to the Slit Interdigital Micromixer [7] (SIMM) (IMM - Institut für Mikrotechnik Mainz, Germany), where the droplets are formed. Then, the emulsion flows to the Caterpillar Micromixer (CPMM) (also from IMM), where contact with water (pumped by a peristaltic pump), and microcapsules are formed. Details of the micromixers are seen in Figure 2.

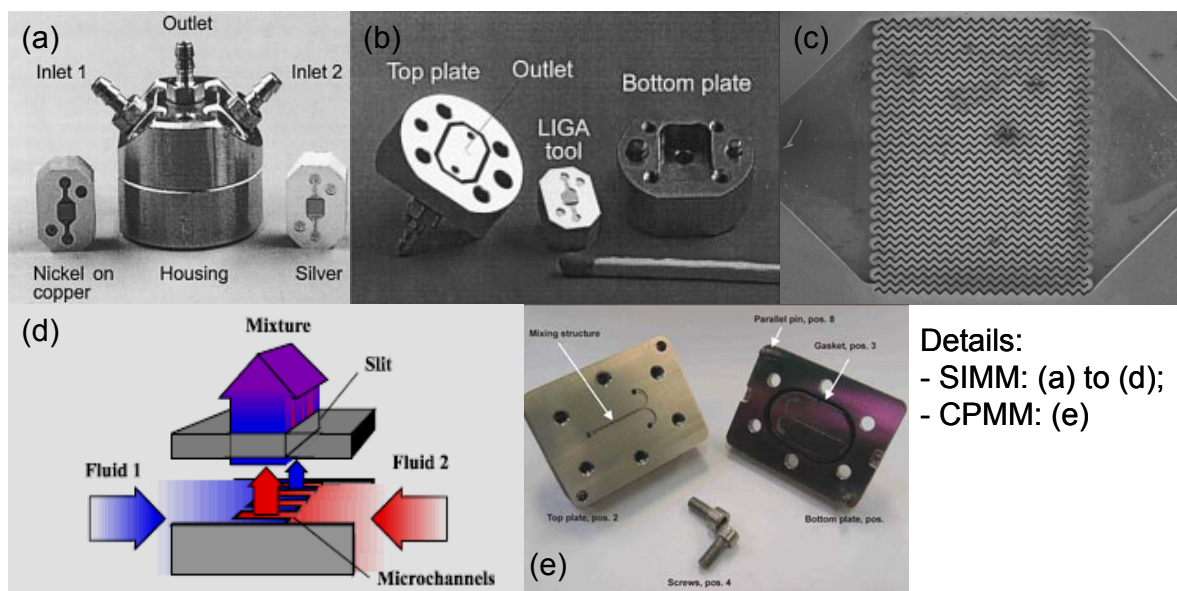


Figure 2 – Details of the micromixers used [8], except on (e) [9].

Figure 2a and 2b show the SIMM micromixer assembled and disassembled, respectively. It is composed by a chip-like interdigitated mixing element, whose SEM image is shown in Figure 2c, and a metallic housing. The micromixer has two inlets, and a diagram of flows is shown in Figure 2d. The emulsion is formed in the outlet slit, where the different liquids finally mix. Figure 2e shows the interior of the CPMM micromixer. The geometry of the SIMM micromixer used for emulsion was already described [10], and it consisted of a mixing element of 18 pairs of channels of width equal to 25 μm each, and a elliptical slit of characteristic dimension equal to 60 μm . Computational Fluid Dynamics (CFD) was used to verify if the behavior of the fluid streamlines, to check if there is mixing in the direction perpendicular to the flow, or if Rayleigh mechanism could be used to describe the formation of the droplets.

Chemicals

The chemicals used were DMF (99.8%, Scharlau, Spain), cyclohexane (99.9%, Scharlau, Spain) and PSf (Sigma-Aldrich, Germany, MW 16,000). Solid vanillin (VNL) was kindly offered by Procter&Gamble. In the experiments with pure polysulfone, solutions of 3 wt% PSf in DMF were prepared. On the other hand, for the encapsulation of vanillin, the polymeric solutions contained 3 wt% PSf and 4 wt% VNL in DMF. The liquid samples obtained were filtered and then analysed by Scanning Electron Microscopy (SEM).

Formation of droplets based on Rayleigh mechanism

For the emulsification of the polymeric solution there are three different contributions competing to determine the size of the droplets formed. This size will eventually be related to the size of the microcapsules. These contributions are:

- the kinetic energy;
- the gravitational energy;
- the surface tension.

According to this, let us assume that the fluids, being immiscible, form fluid layers that move parallel to each other when leaving the microchannels. The actual situation is very similar to that of spray formation except for the fact that we have thin layers of liquid surrounding a thin layer of solution instead of air. Following studies about this matter, there are three situations regarding the mechanism that drives drop formation at increasing Reynolds number. These are

- Rayleigh mechanism: drops of uniform size are produced,
- Inertial liquid oscillations: important size dispersion ;
- Complete atomization at short distance from the nozzle.

We expect that Rayleigh mechanism [11] is the one driving the break-up of the continuous fluid layer. This is supported by the characterization of the flow that we performed by computational fluid dynamics (CFD) taking into account the flow rates and the geometry of the discharge slit (Fluent 6.2).

Figure 3 shows the geometry of the discharge slit, where the droplets are formed (half part, since a symmetry edge can be assumed at the centre). The section area of each microchannel is $1500 \mu\text{m}^2$ and the diameter of the outlet pipe is $500 \mu\text{m}$. If we consider a total flow rate of 45 ml/h (typical operation value), it can be found that the fluid velocity in the microchannels corresponds to 0.23 m/s and thus, the Reynolds number is 10.21 (laminar flow). These conditions were used as boundary ones for the CFD simulation.

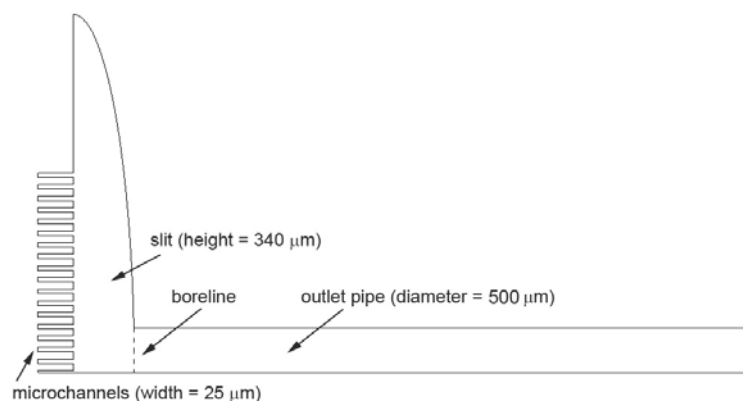


Figure 3 – Geometry of the discharge slit

Results indicate that the mean velocity in the cavity is 0.24 m/s, the mean velocity in the boreline is 0.45 m/s (which corresponds to a Reynolds number of 281), the mean 'x' velocity component in the boreline is 0.40 m/s and the mean 'y' velocity component in the boreline is -0.19 m/s. Figure 4 shows the velocity contours in the cavity and it can be seen that in the boreline (where the fluid changes the direction) there is no mixing in the vertical direction due to the relatively low velocity (and thus, Reynolds number) and that the fluid is quickly developed (both in the microchannels and in the outlet pipe).

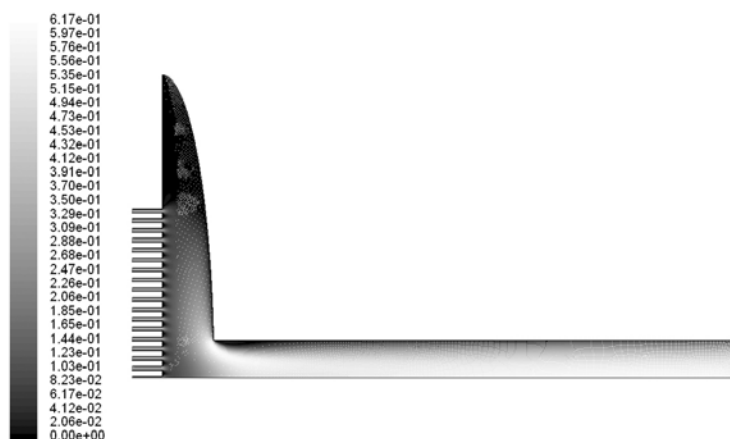


Figure 4 – Velocity contours on the cavity

Figure 5 shows the velocity vectors in the boreline (5a) and near the boreline (5b) respectively, and it can be seen that no vortices occur and also, it can be deduced that the streamlines are parallel, which supports that the dominant mechanism for the droplets formation is the Rayleigh one.

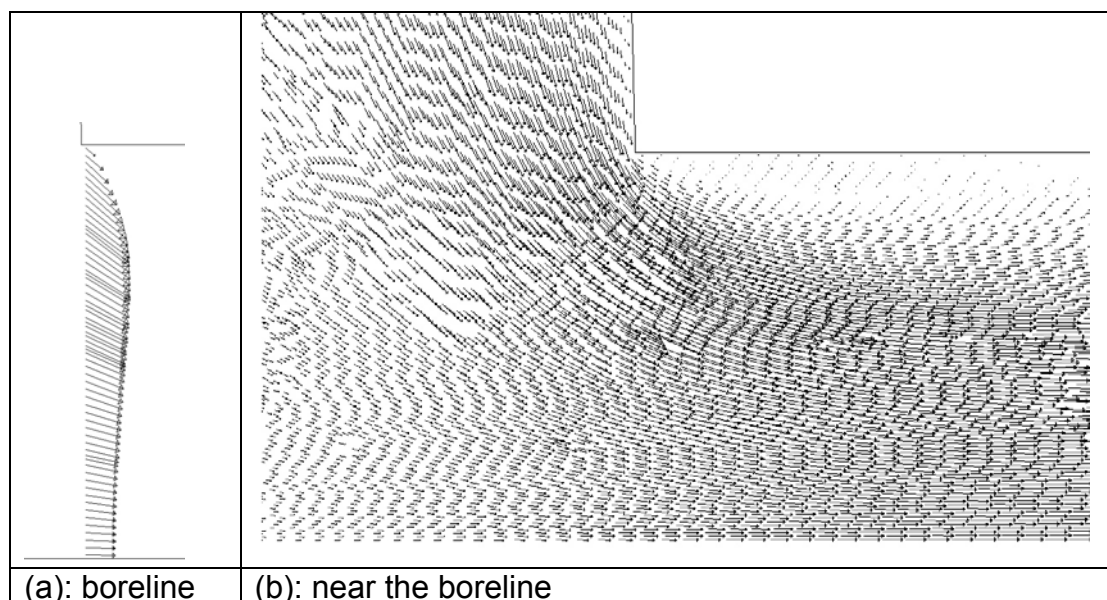


Figure 5 – Velocity vectors in the boreline (5a) and near the boreline (5b).

The droplet size depends mainly on the discharge slit diameter and the number of pairs of channels, as stated in Eq (1):

$$D_{drop} = 6 \frac{F_1}{F} \frac{D_{slit}}{n} \quad (1)$$

where: D_{drop} : droplet diameter (μm);
 F_1 : volumetric flow rate of polymeric solution (ml/h);
 F_2 : volumetric flow rate of continuous phase (ml/h);
 $F = F_1 + F_2$ (ml/h);
 n : pairs of channels;
 D_{slit} : slit characteristic dimension (μm).

Such equation is based on the assumption that the droplet is formed at the outlet of the discharge slit. By considering that, once the droplet is formed, the polymer is not removed during the immersion precipitation, we can obtain the minimal diameter of the microcapsule, as follows:

$$m_{PSf} = \rho_{drop}^{PSf} \frac{\pi}{6} D_{drop}^3 = \rho_{mc}^{PSf} \frac{\pi}{6} D_{mc}^3 \quad (2)$$

If both sides of the equation (2) are multiplied by the molar volume of the polysulfone (PSf), we got a correlation between volumetric fractions and diameters:

$$\rho_{drop}^{PSf} V_{PSf} D_{drop}^3 = \rho_{mc}^{PSf} V_{PSf} D_{mc}^3 \rightarrow \phi_{drop} D_{drop}^3 = \phi_{mc} D_{mc}^3 \quad (3)$$

The volumetric fraction is a direct function of the mass fraction:

$$\phi_{PSf} = \frac{wV_{PSf}}{wV_{PSf} + (1-w)V_{DMF}} \quad (4)$$

By using Eq (3), the minimal diameter is obtained when the microcapsule is totally dense, or $\phi_{mc} = 1$. Besides, we adjusted the predictions to the experimental diameters of the microcapsules, by introducing a K_r correction factor. Therefore:

$$D_{NO} = K_r \sqrt[3]{\phi_{drop}} \cdot D_{drop} \quad (5)$$

If we assume that the capsules without perfume are dense and that the VNL ones are a dense shell covering a product core, a relationship between the diameters of those capsules may be derived:

$$m_{PSf} = \rho_{PSf} \frac{\pi}{6} D_{NO}^3 = \rho_{PSf} \frac{\pi}{6} (D_{VNL}^3 - D_{core}^3) \quad (6)$$

Eq.(6) is based on the mass balance of the polysulfone. We may introduce a parameter K, which is the ratio between the diameter of the product core to the diameter of the VNL microcapsule, as in Eq.(6):

$$K = \frac{D_{core}}{D_{VNL}} \quad (7)$$

K may be related to an average 'porosity', if we define it as the empty volume divided by the total volume of the microcapsule:

$$\varepsilon = \frac{D_{core}^3}{D_{VNL}^3} = K^3 \quad (8)$$

Therefore, the relationship between the diameters of VNL microcapsules and the ones without perfume may be rewritten in terms of K or porosity ε :

$$\frac{D_{VNL}}{D_{NO}} = (1 - K^3)^{-1/3} = (1 - \varepsilon)^{-1/3} \quad (9)$$

Thermodynamics of the polymeric solutions

For a ternary system, the Gibbs free energy of mixing for a polymeric solution may be expressed by the following equation [12]:

$$\frac{\Delta G}{RT} = n_1 \ln \phi_1 + n_2 \ln \phi_2 + n_3 \ln \phi_3 + \chi_{12} n_1 \phi_2 + \chi_{13} n_1 \phi_3 + \chi_{23} n_2 \phi_3 \quad (10)$$

By using Eq. (10) it is possible to determine the spinodal curve, which is the line where all concentrations fluctuations lead to instability, leading to phase separation. The spinodal may be obtained by the following matrix:

$$|G| = \begin{vmatrix} G_{22} & G_{23} \\ G_{32} & G_{33} \end{vmatrix} = 0 \rightarrow G_{22}G_{33} = G_{23}G_{32} \quad (11)$$

$$\text{where } G_{ij} = \frac{\partial^2 G_M}{\partial \phi_i \partial \phi_j} \quad (12)$$

$$\text{and } G_M = \frac{V_1}{\sum n_i V_i} \frac{\Delta G}{RT} \quad (13)$$

By considering the ternary system Cyclohexane(1) – DMF (2) – PSf (3) and using Eq. (11) it is possible to determine theoretically when the system separates into two phases, i.e. the limits where an emulsion may be obtained. The DMF-PSf (χ_{23}) and the cyclohexane-PSf (χ_{13}) interaction parameters were calculated by using a classic Flory-Huggins equation and a three-dimensional approach, respectively [13]. On the other hand, the DMF-Cyclohexane

interaction parameter was calculated as a function of the volumetric fraction of cyclohexane, by using the VLE data at 101.33 kPa [14] and a correlation discussed in the literature [12].

Results

Molar volumes and cohesion parameters of the chemicals used are listed on Table 1.

Table 1 – Microcapsules production: cohesion and Hansen parameters (n: PSf).

Component i	V, cm ³ /gmol	δ_i , MPa ^{1/2}	δ_d , MPa ^{1/2}	δ_p , MPa ^{1/2}	δ_{hb} , MPa ^{1/2}	χ_{in}
Cyclohexane	87.6	15.8	16.5	3.1	0.0	1.04
DMF	67.7	24.8	17.4	13.7	11.3	0.90
Vanillin	87.8	36.6	28.1	15.3	17.7	3.98
Water	19.3	46.0	12.2	22.8	40.4	3.65
PSf	329.4	20.3	21.5	2.8	6.8	

In Table 1, the cohesion and Hansen parameters for cyclohexane, DMF and water were obtained from the literature [15], and for vanillin and PSf they were calculated by using contribution rules [16]. The same applies for the molar volumes. The Flory-Huggins interaction parameter was calculated by using a three-dimensional model [13], except in the case of the pair PSf-DMF, where the classic Flory-Huggins equation proved to be more accurate. Although the Flory-Huggins parameter for PSf-cyclohexane is relatively low, the polymer is not dissolved by just cyclohexane, at 3 wt% and 6 wt%, as checked experimentally. By using the cyclohexane-DMF VLE data [14], we correlated the cyclohexane-DMF Flory-Huggins interaction parameter as a logarithmic function of the DMF volumetric fraction:

$$\chi_{12} = 1.88 - 0.28 \ln \phi_2 \quad (14)$$

By using Eq. (11), Eq. (14) and the interaction parameters listed in Table 1, we were able to draw the spinodal curve for the system cyclohexane-DMF-PSf, shown in Figure 6.

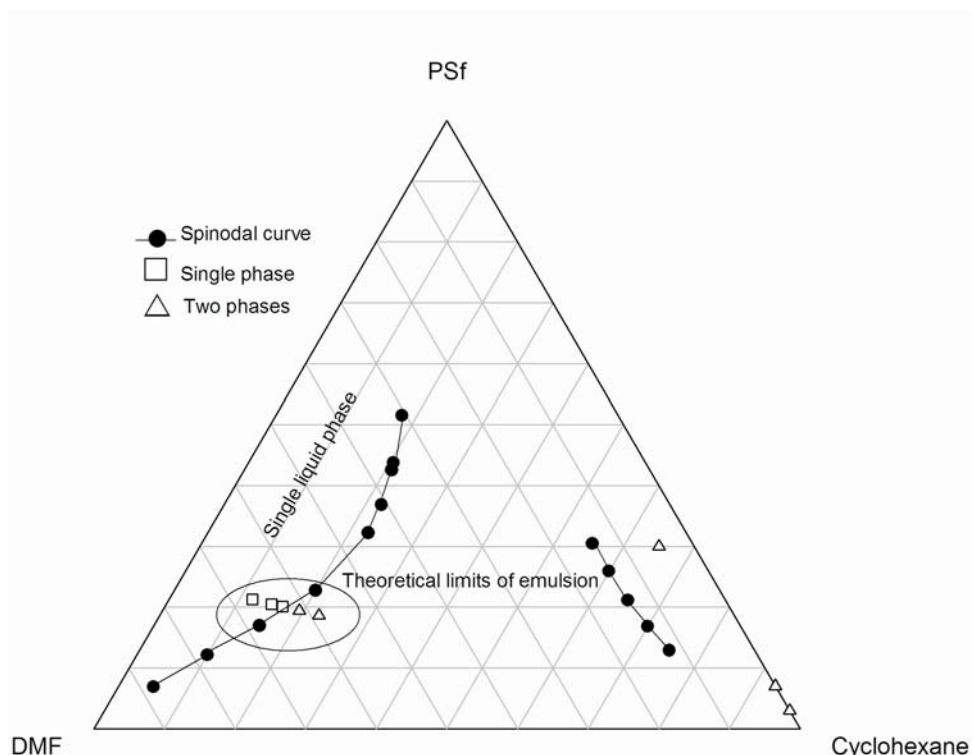


Figure 6 – Cyclohexane-DMF-PSf spinodal curve.

Figure 6 shows the spinodal curve for the system cyclohexane-DMF-PSf, that is composed by two lines, each one closer either to the cyclohexane vertex or to the DMF one. Emulsions can be obtained in any region between the two spinodal curve segments. In the case of low concentrations of cyclohexane, it was possible to verify experimentally that there was a good agreement with the predicted data. On the other hand, when there was no DMF or in low concentrations, it was not possible to dissolve the PSf, what was not expected considering the predictions. The data collected in Table 1 will be useful for the further modeling of the microcapsules formation. However, some interaction parameters are missing, as seen in Figure 7.

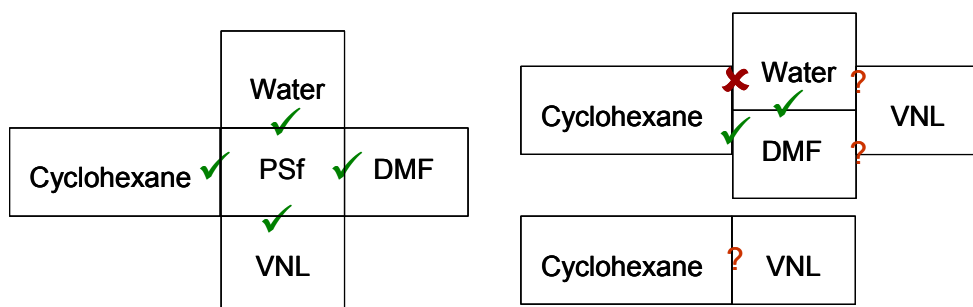


Figure 7 – Flory-Huggins interaction parameters. The ones marked with ✓ were already determined, whereas the ones marked with '?' are missing. The cyclohexane-water parameter is marked with ✗, since both components are immiscible [17].

The interaction parameter for the binary system water-DMF is already published [18]. The other pairs still need to be calculated, by using either vapor-liquid equilibrium data [19] or by UNIFAC. Once all the parameters are obtained, it is possible to perform a more rigorous treatment of the microencapsulation process.

Figure 8 shows SEM micrographs of microcapsules produced in some experiments, where the flow rate of cyclohexane was set to 30 ml/h, and the flow rate of water equal to 120 ml/h.

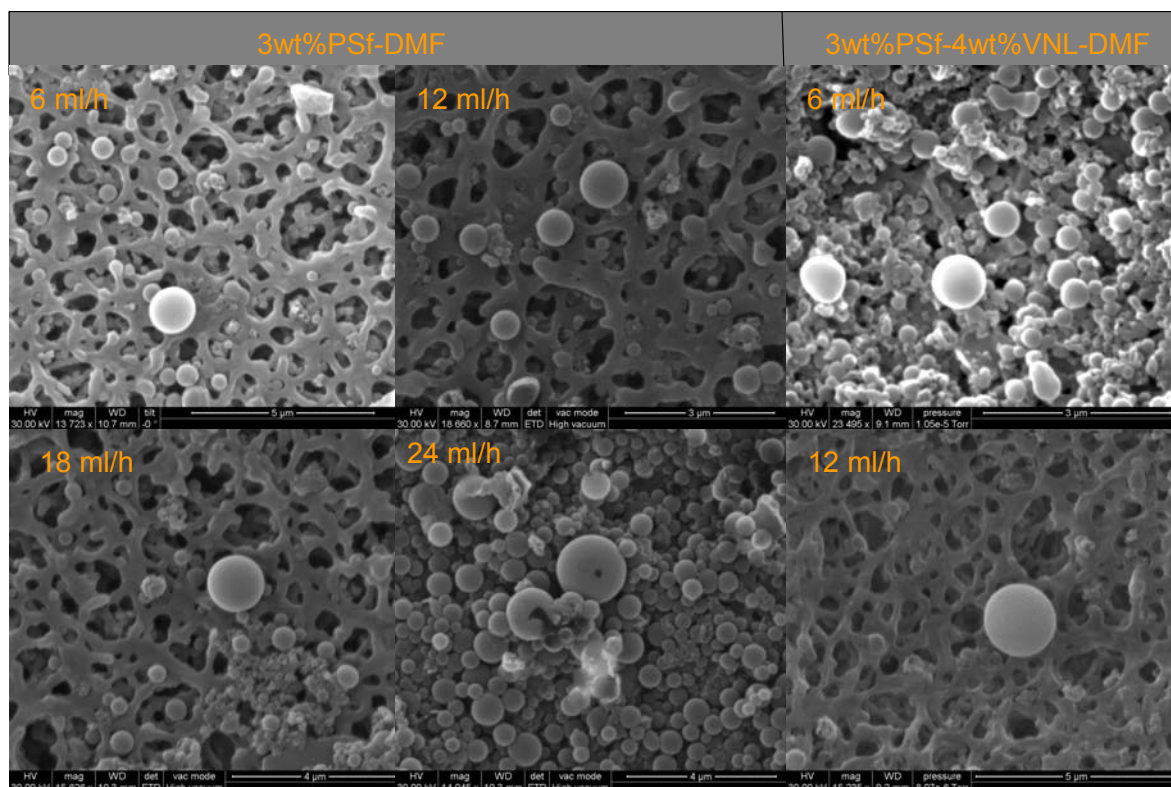


Figure 8 – SEM micrographs of microcapsules. The flow rate of the polymeric solution is indicated at the top of each one.

The average diameters of the pure PSf microcapsules, as well as the ones containing VNL are plotted as a function of the volumetric flow rate of polymeric solution in Figure 9.

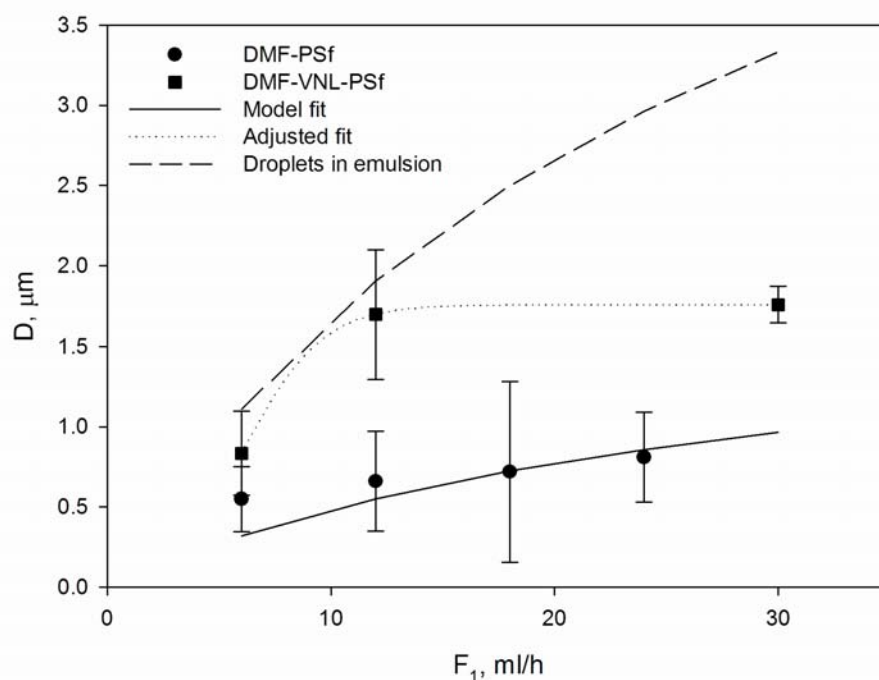


Figure 9 – Average microcapsule diameter for each experimental condition.

In Figure 9 we present the average diameters of the microcapsules, obtained after analyzing several SEM images for each condition. We observe that the addition of VNL to the initial polymeric solution leads to the obtention of bigger microcapsules, and the diameters describe an asymptotic curve. However, there exists for some cases, wide standard deviations of the average values. The model fit was obtained by fitting Eq. (5) to the experimental data by adjusting the parameter K_r , that finally was set to $1/3$. The predictions, therefore, are in the same magnitude order as the experimental results, what validates this first approach. With this value of K_r , we calculated the size of the droplets varying with the flowrate of polymeric solution, obtaining the curve called *droplets in emulsion*, also shown in Figure 9. By comparing it with the diameters of the VNL microcapsules, we conclude that, at least for low flow rates of polymeric solution, there is not a significant variation in size during the precipitation, from the initial state of droplet to the eventual one of microcapsule. However, that is not valid for the experiment lead at 30 ml/h, where the size of the microcapsule is much smaller.

The water management is an important issue in the process. There should be enough water to precipitate properly the microcapsules. However, it should be optimized in order to avoid the obtention of a very dilute suspension. What we mean by proper precipitation is shown in Figure 10.

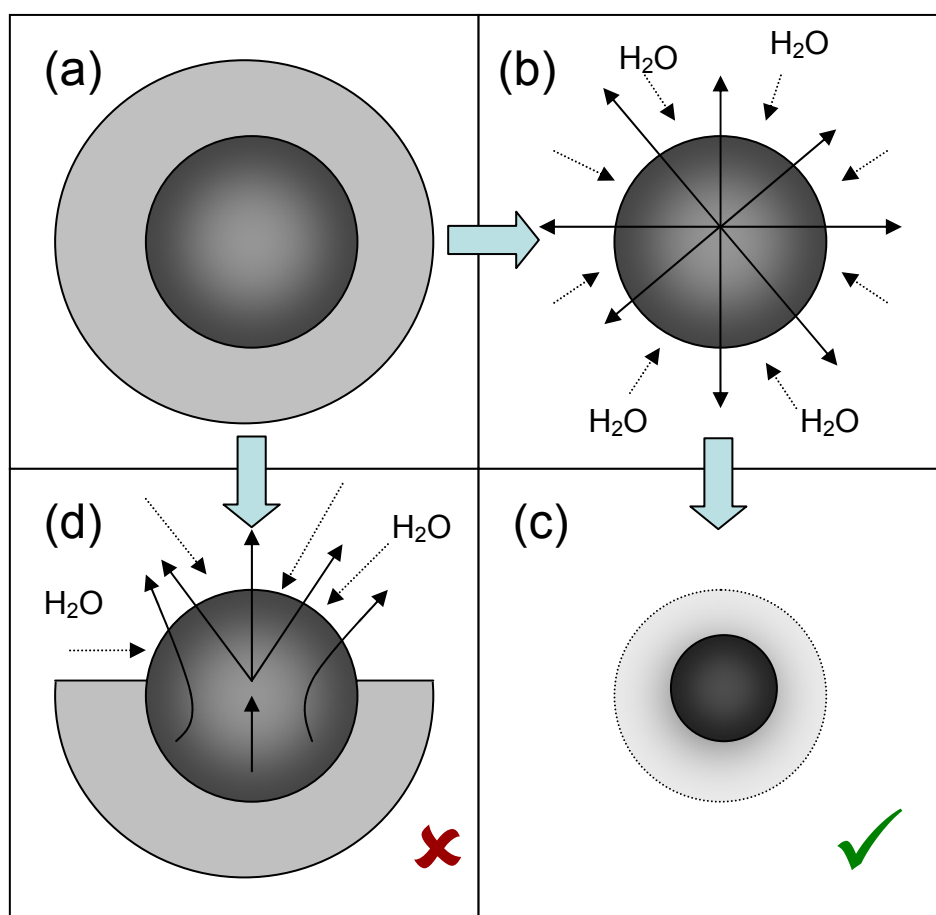


Figure 10 – Schematic representation of the precipitation of microcapsules. Steps:(a) droplet of polymeric solution surrounded by cyclohexane; (b) DMF leaves the droplet in the radial direction; (c) final capsule formed, hatched part is the final diameter and the grey part, the loss of mass during precipitation; (d) still remains cyclohexane in the surface of the droplet.

The precipitation of the polymer to form the microcapsules should be similar to the formation of flat-sheet membranes [3]. However, here an extra component (cyclohexane) exists to form the emulsion. Therefore, we think that water plays an additional role, by washing away the cyclohexane from the droplets surface before the beginning of the precipitation. Figure 10 shows schematically the precipitation of the droplet. The formation path from (a) to (c) summarizes the steps required to the proper precipitation. The flow of water should be enough to complete wash away the layer of the cyclohexane covering the droplet surface. Then, in (b), the mass transfer of DMF and water from the polymeric solution and to the liquid phase can occur symmetrically in the radial direction, generating a perfect microcapsule (c) by the balances of momentum. On the other hand, if the flow rate of water is not enough to clean the surface of the polymeric droplets, the fast inversion phase process generates structures that are not perfectly spherical (d). However, such assumptions should be confirmed by further experiments and modeling.

From the average diameters obtained experimentally at 6 ml/h and 12 ml/h, where we could compare data for both cases, with and without vanillin, and by

using Eq (9), we may deduce the diameter of the product core, shown in Figure 11.

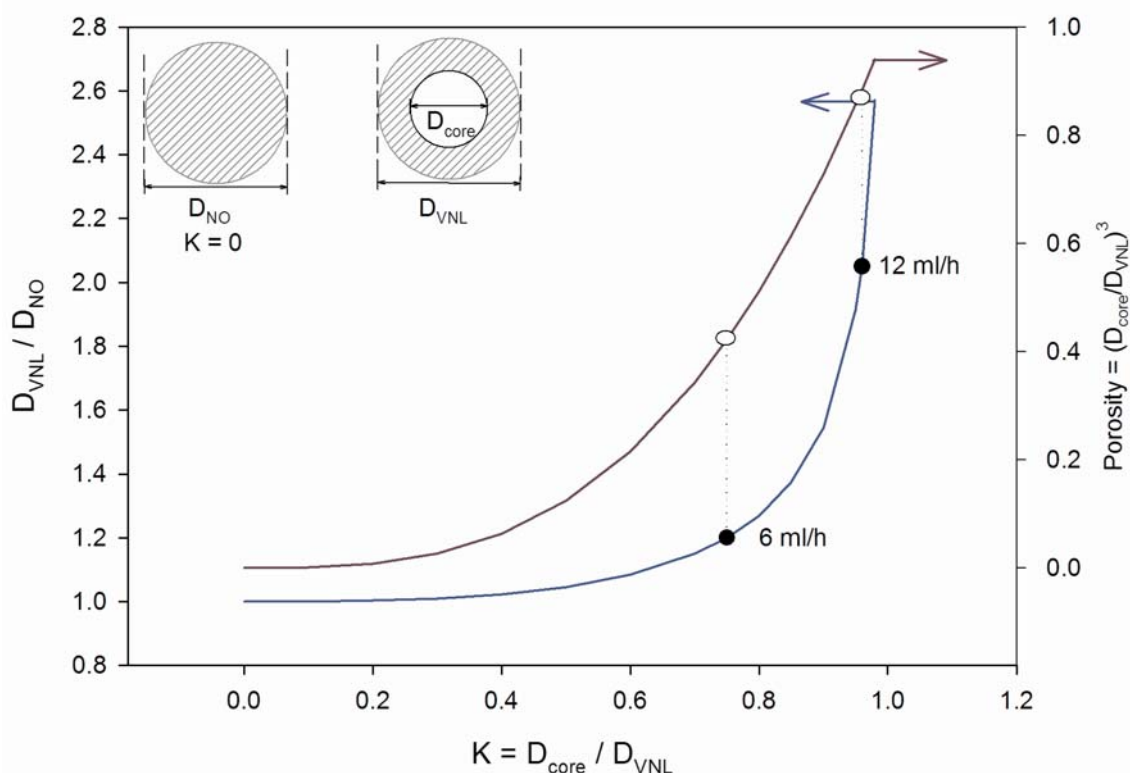


Figure 11 – Ratio between the diameters of the microcapsules with and without VNL. Full circles represent ratios obtained experimentally. Empty circles represent porosity estimated from experimental ratios.

From Figure 11, we can deduce that the presence of vanillin affects so much the system that microcapsules up to 2 times bigger are produced. Considering our hypotheses, the volume of the product core may reach 0.88 of the total volume of the microcapsule. However, further characterization is needed, including microcapsules morphology. We will focus such procedures in future work.

Conclusions

In the present work, by analyzing results of microcapsules production by using micromixers, we were able to identify key parameters for a further robust modeling strategy. According to the flow rate and chemistry of system, we were able to obtain spherical particles of different diameters. By the addition of vanillin, we obtain capsules up to 2 times bigger than the ones produced by just precipitating polymer. By a mass balance based on the amount of polymer, we deduced that the volume fraction available for the storage of products inside the capsules may reach a value up to 0.88. The fluidodynamic model based on Rayleigh mechanism allowed us to predict a microcapsule diameter which is closer to the experimental one, for pure polysulfone capsules. At low flow rates of polymeric solution, the resultant diameter of the microcapsule containing vanillin was closer to the predicted value of the droplet, what evidences that

was no significant change in volume during precipitation. However, this does not apply for the experiment with the maximal flow rate.

Further modeling, including the composition of thermodynamic equilibrium diagrams, should be taken into account to understand the complete formation of the microcapsules. Besides, it should include the study of the surface tensions, to assess the water management of the system, among other issues.

Acknowledgments

Authors would like to thank undergraduate students Agnieszka Stec and Santiago Gascón for their help with the experimental part, and to the Scientific Research Services of URV (especially to Mercè Moncusí and Dr. Mariana Stefanova). This work is supported by the IMPULSE European Project FP6-2003-NMP-IN-3.

Nomenclature

Acronyms

CPMM	Caterpillar Micromixer
DMF	N-N-dimethylformamide
NO	microcapsules of pure polysulfone
PSf	polysulfone
SEM	Scanning Electron Microscopy
SIMM	Slit Interdigital Micromixer
VNL	vanillin

Variables and parameters

D	diameter (μm) of droplets / microcapsules or the characteristic dimension of slit, according to the subscript
F	flow rate ($\text{ml}\cdot\text{h}^{-1}$)
G	Gibbs free energy of mixing
K_r	fitting parameter of the Rayleigh-based equation
K	ratio of the diameter of the product core to the total diameter
m	microcapsule mass (g)
n	number of microchannels
n_i	number of moles of component i
R	ideal gas constant
T	temperature, K
V_i	molar volume of component i ($\text{cm}^3\cdot\text{gmol}^{-1}$)
W	mass fraction

Greek symbols

δ_i	Hansen parameter of component i ($\text{MPa}^{1/2}$)
ε	porosity
ρ	concentration ($\text{g}\cdot\text{cm}^{-3}$)
χ_{ij}	i-j Flory-Huggins interaction coefficient

ϕ volume fraction

Subscripts

core core of product
d dispersive
hb hydrogen-bonding
p polar
1 cyclohexane
2 DMF
n polymer

References

- [1] Y. Matsunami, K. Ichikawa. *International J of Pharmaceutics* 242 (2002) 147-153.
- [2] S.-J. Park, Y.-S. Shin, J.-Rock Lee. *J. Colloid and Interface Science* 241 (2001) 502-508.
- [3] C. Torras. *Obtenció de membranes polimèriques selectives*, PhD Thesis, Chemical Engineering Department, Universitat Rovira i Virgili (2005). ISBN:84-689-3628-6.
- [4] C.Torras, D. Gezahegn, L. Pitol-Filho, R. Garcia-Valls. *Desalination* 200 (2006) 12-14.
- [5] V. Hessel, H. Löwe, F. Schönfeld. *Chemical Engineering Science* 60 (2005) 2479-2501.
- [6] S. Hardt, F. Schönfeld. *AIChE J* 49 (2003) 578-584.
- [7] B. Werner. *Operating manual: Slit Interdigital Micromixer. Version 2.* Institut für Mikrotechnik Mainz.
- [8] W. Ehrfeld, K. Golbig, V. Hessel, H. Löwe, T. Richter. *Ind. Eng. Chem. Res.* 38 (1999) 1075-1082.
- [9] B. Werner. *Manual for the caterpillar micro mixer. Version 1.2.* Institut für Mikrotechnik Mainz.
- [10] P. Löb, H. Pennemann, V. Hessel. *Chemical Engineering J* 101 (2004) 75-85.
- [11] H. Kim. *Physica B* 389 (2007) 377-379.
- [12] J.H. Kim, B.R. Min, J. Won, H.C. Park, Y.S. Kang. *J. Membrane Science* 187 (2001) 47-55.
- [13] T. Lindvig, M.L. Michelsen, G.M. Kontogeorgis. *Fluid Phase Equilibria* 203 (2002) 247-260.
- [14] B. Blanco, S. Beltrán, J.L. Cabezas, J. Coca. *J. Chemical and Engineering Data* 42 (1997) 938-942.
- [15] J.R. Fried. *Polymer science and technology* (1995), Prentice Hall.
- [16] A.F.M. Barton. *CRC Handbook of solubility parameters and other cohesion parameters.* CRC Press, 2nd edition (1991).
- [17] A. Mączyński, B. Wiśniewska-Gocłowska, M. Góral. *J. Phys. Chem. Ref. Data* 33 (2004) 549-577.
- [18] F.W. Altena, C.A. Smolders, *Macromolecules* 15 (1982) 1491-1497.
- [19] L. Pitol-Filho, R. Garcia-Valls. *Polymer Engineering and Science* (2007). In Press.

X. Zhang, L. Pitol-Filho, C. Torras, R. Garcia-Valls

Experimental and computational study of proton and and methanol permeability
through composite membranes

J. Power Sources 145 (2005) 223-230.



Experimental and computational study of proton and methanol permeabilities through composite membranes

Xiao Zhang, Luizildo Pitol Filho, Carles Torras, Ricard Garcia-Valls*

Departament d'Enginyeria Química, Escola Tècnica Superior d'Enginyeria Química, Universitat Rovira i Virgili, Av. Països Catalans 26, 43007 Tarragona, Spain

Accepted 28 January 2005
Available online 23 May 2005

Abstract

To design direct methanol fuel cells, proton permeability and methanol crossover have to be evaluated. A study of the transport of methanol and protons through composite membranes of poly(ethylene glycol) (PEG) and polysulfone (PSf) was performed and permeabilities of these components were determined. PSf was treated with dilute sulfuric acid to enhance hydrophilicity. PEG was found to be a good material for the active layer, because it contains —OH hydrophilic groups which combine with hydrated protons. A composite membrane made of 15 wt.% PSf and 40–50 wt.% PEG showed a lower methanol crossover ($1.0\text{E}-06\text{ cm}^2\text{ s}^{-1}$) than the commercial reference NAFION® 117. Maximal proton conductivity is also lower than NAFION® 117. A mathematical deterministic model, considering transport by diffusion through the composite membrane and equilibrium at the membrane–reservoir interfaces, was derived. However, the PEG layer did not present any pores and diffusion in the dense membrane was estimated using a transport probability. On the other hand, the porous PSf layer required an effective diffusivity that is a function of physical properties such as porosity and tortuosity. The contribution made by each mass transfer phenomenon to the total permeation was calculated by an association of mass transfer resistances.

© 2005 Elsevier B.V. All rights reserved.

Keywords: Composite membranes; Permeability; Mathematical model

1. Introduction

Fuel cells, composed of an anode, a membrane and a cathode, can be used to generate energy by oxidation of either hydrogen or methanol. To take maximum advantage of the fuel, a membrane is needed to conduct protons and avoid methanol crossover.

The most representative kinds of fuel cells are the proton-exchange membrane fuel cell (PEMFC) and the direct methanol fuel cell (DMFC), which use proton-conducting membranes [1]. DMFC is more interesting than PEMFC, because its theoretical potential is higher [2], and because it allows simple liquid handling. Also, as PEMFC operation is based on the supply of hydrogen, the management of water generated is very important. This is not an issue with

DMFC, which already has a liquid phase. On the porous anode, electrochemical oxidation of the methanol occurs to produce carbon dioxide, protons and electrons. The protons diffuse through the membrane to the cathode side, where they react with the oxygen to produce water.

The most used membranes for DMFC are the perfluorinated sulfonated NAFION® membranes of DuPont, due to their chemical stability, high conductivity and high permeability to protons. However, these membranes also allow methanol to permeate, which reduces the efficiency of the electrochemical process, increases fuel consumption and damages the own cells. This phenomenon is known as *methanol crossover*. Several authors have reported the factors behind it, including cell temperature, cathode pressure, methanol concentration and catalyst morphology [3,4].

Many alternative membranes for DMFC are under investigation in the following four aspects: the primary structure of the polymer, the morphology of the polymer, the nature of the

* Corresponding author. Tel.: +34 977 55 96 11; fax: +34 977 55 85 44.
E-mail address: ricard.garcia@urv.net (R. Garcia-Valls).

Nomenclature

A	membrane area (cm^2)
C	concentration (gmol cm^{-3})
d	pore diameter (cm)
D	diffusivity ($\text{cm}^2 \text{s}^{-1}$)
e	elementary charge
k_B	Boltzmann's constant
k_j	mass transfer coefficient on the membrane–reservoir j interface (cm s^{-1})
L	membrane thickness (cm)
p	number of pores of different diameters
P	permeability (cm min^{-1})
Q	volumetric permeate flow ($\text{cm}^3 \text{min}^{-1}$)
S	selectivity for proton transport
t	time (s)
T	temperature (K)
V_j	volume of reservoir j (cm^3)
x	axial position (cm)
z	non-dimensional axial position (cm cm^{-1})
Z	total ionic strength (ion m^{-3})

Greek symbols

α_j	mass transfer at reservoir j –membrane interface
ε	porosity
θ	non-dimensional time
μ	time factor
π_j	mass transfer number at reservoir j –membrane interface
τ^2	tortuosity
φ	non-dimensional concentration
Ψ	transport probability on dense layer

Subscripts

0	initial, for concentrations, or infinite dilution diffusion coefficient
c	calculated through simulations
D	diffusive
e	experimental
f	feed
H^+	proton
L	liquid
MeOH	methanol
PEG	poly(ethylene glycol) layer
PSf	polysulfone layer
s	stripping

acid group, and the nature of the medium within the polymer matrix [5]. Other membranes have been tested and results of these tests have been compared to those with NAFION® [6–8]. A better ratio between conductivity and methanol permeability has been reported. Much attention is given to polysulfone (PSf), poly(ether ketones) and poly(benzimidazole).

PSf is the simplest of these polymers and the morphologies of its membranes have been well characterized. Sulfonation is an efficient way to activate polysulfone in proton permeability. There are two methods for obtaining proton-selective PSf membranes: one is to introduce anionic moieties into a performed solid membrane [9]. The other is to introduce anionic moieties into a polymer as a kind of modification, then to dissolve of the polymer and cast it into a film [10]. The second method is more complicated from an industrial point of view, and the sulfonated polysulfone itself cannot perform as a membrane with enough physical strength. The first method is industrially easier. The treatment is with sulfuric acid, and this does not change the physical strength of a performed polysulfone membrane.

To reduce the methanol crossover, the dense layer may serve as a barrier for methanol, and at the same time may facilitate the proton transport. PEG is a kind of polymer that is widely used in many fields. For example, it is used as a lubricant and as a preservative for conserving archaeological materials, because it is reasonably inexpensive and compatible with many organic materials. In biosensors, PEG is presented as “hydrogel” [11] to immobilize enzyme or protein on the carbon electrode surface and transport electrons. PEG is therefore used as a proton-selective layer.

For the reasons outlined above, the asymmetric PSf membrane was chosen as support and treated by thermal sulfonation to improve its proton conductivity. A PEG dense layer was then produced on top of PSf support.

Despite the interest in DMFCs, only a little effort is being made to propose mathematical modelling comprising the mass transfer mechanism through the membrane [6,12]. Most studies apply an empirical adjustment to the membrane and predict the electrochemical potential generated. Traditionally, diffusivities through membranes are determined without taking into account mass transfer coefficients at the membrane–reservoir interfaces. In the case of composite membranes, a global coefficient is calculated, and the different layers are not mathematically treated separately.

We have measured the permeability of protons and methanol in membranes comprising a dense layer of poly(ethylene glycol) (PEG) and a porous layer of polysulfone (PSf). The equilibrium cell comprised a feed reservoir, the composite membrane, and a stripping reservoir. Our results are expressed in terms of diffusivity. We fed our data to a mathematical model that considered transport by diffusion through the membrane and equilibrium at the feed–membrane and membrane–stripping interfaces. We then determined diffusivity for each layer was then determined using mass transfer resistances.

2. Methods

The system used in this study comprised a feed reservoir, a composite membrane and a stripping reservoir. The PEG layer of the composite membrane faced the feed reser-

voir, and the PSf layer faced the stripping reservoir. A solution of known pH or methanol concentration is fed into the feed reservoir and the protons or methanol molecules permeate through the membrane, reaching the stripping reservoir, where the concentration is measured. It is possible then to calculate permeability for the components studied. To study permeability with this equilibrium-diffusion model, we need to:

- prepare the membrane and collect the experimental data,
- determine the experimental diffusivity,
- determine the proton, methanol and membrane properties, such as the molar volume of each component, and the porosity and tortuosity of the membrane,
- determine the proton and methanol diffusivities by correlations with the literature,
- develop an equilibrium model, to obtain transient data on concentration for each reservoir,
- associate mass transfer resistances, to evaluate the effect of each transport coefficient on experimental diffusivity, and
- calculate the selectivity of proton transport at the membrane-reservoirs interfaces and through the membrane.

2.1. Preparation of the membranes and experimental data

A polysulfone casting solution was prepared by dissolving 15 wt.% PSf (MW: 16,000, Aldrich) in *N,N*-dimethylformamide (DMF) with vigorous agitation for 12 h at room temperature. The solutions were cast onto a glass plate using a 200 μm thick casting knife, then precipitated in 15 wt.% DMF solution and/or water. The PSf membranes were then taken from the bath and rinsed with distilled water. The PSf membranes obtained were kept at 80 °C in 0.25 M H₂SO₄ aqueous solution for 3, 24 and 72 h. Excess acid on the surface was removed by a short rinse of water. The membranes were then placed in an oven at 80 °C for 1 h. These thermally treated membranes were then soaked in distilled water and rinsed daily until the pH of the rinsed water was neutral.

Usually sulfonation process requires using strong acids. However, in the present work the degree of sulfonation is not under investigation. The treatment of the PSf with dilute sulfuric acid aims enhancing proton permeability by increasing hydrophilicity of the membrane. Indeed, preliminary experiments using blank PSf membranes (not treated with H₂SO₄) provided a proton diffusivity of 10⁻¹² cm² s⁻¹. On the other hand, after sulfonation, proton diffusivity increased to 10⁻¹¹ cm² s⁻¹.

Wax-like PEG (MW 1000, from Aldrich) was dissolved in methanol at several concentrations (5, 10, 20, 30, 40, 50, 60, 70 and 80 wt.%). The solution was deposited onto the top surface of support PSf membranes. The PEG-covered PSf membranes were placed in an oven to cross-link at 80 °C

for 30 and 60 min, and the composite membranes were then stored in water before use. For biosensors, often PEG film is dried overnight at room temperature to cross-link [13]. In the case studied here the PEG film was dried at 80 °C to avoid the membrane to peel off in DMF solutions.

Experiments to evaluate proton and methanol permeability were carried out by using a testing cell, consisting of two reservoirs separated by a composite membrane with a dense layer of poly(ethylene glycol) and a porous layer of polysulfone. The transversal area of tested membranes was 8.51 cm² and both reservoirs (that of the feed solution and that of the stripping solution) had a volume of 200 cm³. To measure proton permeability the feed reservoir was filled with a solution of HCl 1.0 M. Also, to evaluate methanol crossover a 1.0 M solution of methanol was used. Experimental data were the initial feed concentration *C_f* (methanol concentration, in M, or pH) and the initial stripping concentration *C₀*. The stripping concentration was also plotted against time.

The permeability coefficient *P* (cm min⁻¹) was calculated according to Eq. (1):

$$-\ln \frac{C_f}{C_0} = \frac{QP}{V_f} t \quad (1)$$

Permeability was then multiplied to membrane thickness (95 μm) to obtain diffusivity (cm² s⁻¹). Proton conductivity was obtained by using the Nernst-Einstein equation [14] as follows:

$$\sigma = \frac{DZe^2}{k_B T} \quad (2)$$

2.2. Determination of porosity and tortuosity

Important properties in mass transfer through porous media are porosity and tortuosity. In the case of tortuosity, diffusion is more difficult when the pore geometry is irregular. The diffusion mechanisms for transient and steady states are different. In the transient state, the component tends to distribute itself homogeneously for the whole solid matrix, even reaching pores that are blocked at any of the extremities. Once the system reaches steady state, there is preferential diffusion through the sections with a concentration gradient, which is the driving force for diffusion. Therefore, transport does not occur in blocked pores. To make calculations easier, we decided to determine tortuosity for the steady state, by a model that considers a porous medium as an association of pores of different diameters [15]. If we consider pores to be spheres, steady-state tortuosity may be written as in Eq. (3):

$$\tau^2 = \sum_{i=1}^p \frac{1}{d_i} \frac{\sum_{i=1}^p d_i^3}{(\sum_{i=1}^p d_i)^2} \quad (3)$$

After comparing effective diffusivity and binary diffusivity coefficients for various compounds, some authors [16] have reported that expression for tortuosity should be a function of the transported molecule structure, since cyclic and acyclic compounds have different preferential paths within

Membrane:

$$\mu = \frac{L^2}{D}$$

$$\frac{\partial C}{\partial t} = \frac{\partial}{\partial x} \left(D \frac{\partial C}{\partial x} \right) \Rightarrow \frac{\partial \varphi}{\partial \theta} = \pi_D \frac{\partial^2 \varphi}{\partial z^2}$$

$$\pi_D = \mu \frac{D}{L^2} = 1$$

$$\left. \begin{aligned} \varphi(\theta=0) &= 0 \\ \frac{\partial \varphi}{\partial z} \Big|_{z=0} &= -\pi_f (\varphi_f - \varphi_{z=0}) \\ \frac{\partial \varphi}{\partial z} \Big|_{z=1} &= -\pi_s (\varphi_{z=1} - \varphi_s) \end{aligned} \right\}$$

Change of variables:

$$\varphi = \frac{C - C_0}{C_f - C_0} \quad \theta = \frac{t}{\mu} \quad z = \frac{x}{L}$$

Feed – membrane interface:

$$\frac{d\varphi_f}{d\theta} = -\alpha_f (\varphi_f - \varphi_{z=0})$$

$$\varphi_f(\theta=0) = 1$$

$$\pi_f = k_f \frac{L}{D} \quad \alpha_f = \mu \frac{Ak_f}{V_f}$$

Membrane - stripping interface:

$$\frac{d\varphi_s}{d\theta} = \alpha_s (\varphi_{z=1} - \varphi_s)$$

$$\varphi_s(\theta=0) = 0$$

$$\pi_s = k_s \frac{L}{D} \quad \alpha_s = \mu \frac{Ak_s}{V_s}$$

Fig. 1. Equations for the feed–membrane–stripping equilibrium model.

the porous media. In our study, however, the size of transported molecules is small enough to assume there are no significant differences in transport.

By digitally treating data from scanning electron microscopy, the pore size distribution of the polysulfone (PSf) layer [17] can be evaluated. Then, tortuosity can be calculated by applying Eq. (3). Porosity, on the other hand, is the ratio of the total volume of pores to the volume of the membrane.

2.3. Feed–membrane–stripping equilibrium model

As a first approach, the system can be modelled just by considering the diffusive transport through the membrane, which is made up of a single polymeric layer. Fig. 1 shows the model equations, which consist of a partial differential equation, describing the change in concentration through the membrane, and an ordinary differential equation of each reservoir.

Our experimental data are the initial feed concentration and the stripping concentration varying on time. Data are collected and converted into stripping non-dimensional concentrations according to time. By comparing both stripping concentrations (simulated and experimental), it is possible to find the μ parameter, which relates the thickness of the membrane to the diffusivity.

We can reduce the complexity of the numeric system, which is made up of one partial differential equation (PDE) and two ordinary differential equations (ODEs), by applying finite differences. The decision on how many elements are necessary to do the simulations is based on calculated errors and required calculation time. For a hypothetic situation in which the volumes of the membrane and both reservoirs are equal, the equilibrium concentration should be one third of the initial concentration at the feed reservoir. Choosing 25 ODEs may be then justified, since a very accurate solution can then be provided (less than 1.5% error) in a short simulation time (less than 6 min), when the simulations are

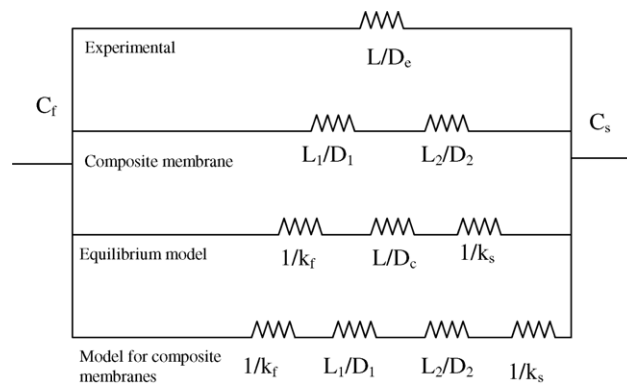


Fig. 2. Association of mass transfer resistances.

performed in a Pentium IV of 2.66 GHz with 256 MB RAM for 10,000 time iterations.

2.4. Association of mass transfer resistances

Mass transfer may be seen as a series of resistances, as in Fig. 2. Experimental diffusivity can be evaluated using a single parameter model. According to this approach, a composite membrane should have two diffusivities – one for each layer, as expressed by Eq. (4):

$$\frac{L}{D_e} = \frac{L_1}{D_1} + \frac{L_2}{D_2} \quad (4)$$

The literature reports several correlations for diffusivities and describes their relative advantages and disadvantages. To calculate diffusivities in liquids, the Wilke–Chang equation [18,19] provides acceptable data, while proton diffusivity can be determined from the Nernst–Haskell [19] equation, which is more suitable to transport of ions. To apply the Wilke–Chang equation we needed to calculate the molar volumes, which were determined according to the Le Bas rule. However, liquid diffusivity must be corrected, depending on the medium considered. For a composite membrane, one proposal is

$$D = \begin{cases} D_L \Psi \rightarrow 0 < z \leq L_{PEG}, \\ D_L \frac{\varepsilon}{\tau^2} \rightarrow L_{PEG} < z \leq L \end{cases} \quad (5)$$

When transport occurs through the poly(ethylene glycol) (PEG) layer, liquid diffusivity is multiplied to the probability of the molecule passing through the molecules. In the porous polysulfone (PSf) layer, effective diffusivity is the product of liquid diffusivity and the ratio of porosity to tortuosity. Both porosity and tortuosity, on the other hand, can be estimated by analysing the membrane with electron microscopy.

One way to find transport probability may be to assume an association of resistances for the composite membrane, as shown in Fig. 2. Using Eq. (5), experimental diffusivity can

Table 1
 Equations used to determine proton selectivity

Membrane or layer	Proton selectivity
Membrane, experimental	(8) $S_e = \frac{D_{e,H^+}}{D_{e,MeOH}}$
Membrane, calculated	(9) $S_c = \frac{D_{c,H^+}}{D_{c,MeOH}}$
PEG layer	(10) $S_{PEG} = \frac{D_{L,H^+} \psi_{H^+}}{D_{L,MeOH} \psi_{MeOH}}$

be rewritten as in Eq. (6):

$$\frac{L}{D_c} = \frac{1}{D_L} \left[\frac{L_{PEG}}{\psi} + \frac{L - L_{PEG}}{\varepsilon} \tau^2 \right] \quad (6)$$

Therefore, if we accept that the solutions are dilute, we can establish a relationship between the experimental data and the simulation parameters, i.e. the transport probability and coefficients (Eq. (7)):

$$\frac{L}{D_e} = \frac{1}{k_s} + \frac{1}{k_f} + \frac{1}{D_L} \left[\frac{L_{PEG}}{\psi} + \frac{L - L_{PEG}}{\varepsilon} \tau^2 \right] \quad (7)$$

The mass transfer coefficients should be properly correlated to the chemical structure of the membrane, since they are interpreted as interaction parameters. However, for the first approach, we will assume the film mass transfer theory. According to this theory, the interfacial mass transfer coefficients are directly proportional to diffusivity and inversely proportional to boundary layer thickness [20].

2.5. Selectivity for proton transport

Once the experimental and calculated diffusivities and the mass transfer coefficients are obtained, the selectivity can be calculated for proton transport at the membrane–reservoirs interfaces and through the membrane. Table 1 lists the procedures for determining selectivities. Eqs. (8)–(10) in this table can be used to analyse each transport process separately and evaluate selectivity for different membrane compositions.

3. Results and discussion

In this section we present our experimental results and the data obtained from simulations.

3.1. Physico-chemical properties

By analysing the membrane using electron microscopy and the equations in Section 2, we determined porosity and tortuosity for the polysulfone layer. Table 2 lists the average data for the membranes, the thickness of both layers, expressed in micrometers and the diffusivities calculated from Wilke–Chang (for methanol) or from Nernst–Haskell (for protons, in this case considered as HCl molecules) theories. Although thickness of PEG layer may vary according to the PEG content in the casting solution, we assumed an average value of 1 μm for all membranes. Tortuosity shows that the

Table 2
 Physico-chemical and geometric data

Property	Value
L (μm)	95.00
L_{PEG} (μm)	1.00
A (cm^2)	8.51
ε	0.13
τ^2	1.04
D_{MeOH} ($\text{cm}^2 \text{s}^{-1}$)	1.70E–05
D_{H^+} ($\text{cm}^2 \text{s}^{-1}$)	3.33E–05

membrane structure was well represented by a sequence of straight channels, because the value was not far from 1.0.

3.2. Experimental data

The membranes were placed in the equilibrium cell between the feed and the stripping reservoirs, and the concentration (for methanol crossover experiments) or pH (for proton permeability experiments) was measured. Initial feed pH in all experiments was 0.12.

We made preliminary experiments using NAFION[®] 117. Methanol crossover of $2.54\text{E}–06 \text{ cm}^2 \text{ s}^{-1}$ was obtained, in perfect agreement with values available in the literature [21]. Proton diffusivity was $9.54\text{E}–06 \text{ cm}^2 \text{ s}^{-1}$. Therefore, by using Nernst–Einstein equation, diffusivity was converted to proton conductivity (71.80 mS cm^{-1}).

Composite membranes used had a polysulfone (PSf) (15% PSf–water) porous layer covered by a PEG layer. Diffusivities are presented in the Fig. 3. Proton permeation presents a maximum for a membrane with 50 wt.% of PEG in the casting solution. On the other hand, maximal methanol crossover for composite membranes is less than a half of the value obtained using NAFION[®] 117. Data of proton conductivity (Fig. 4) of composite membranes may help assessing if they are appropriated for fuel cells. Proton conductivity for the composite membranes is still too low if compared to NAFION[®] 117.

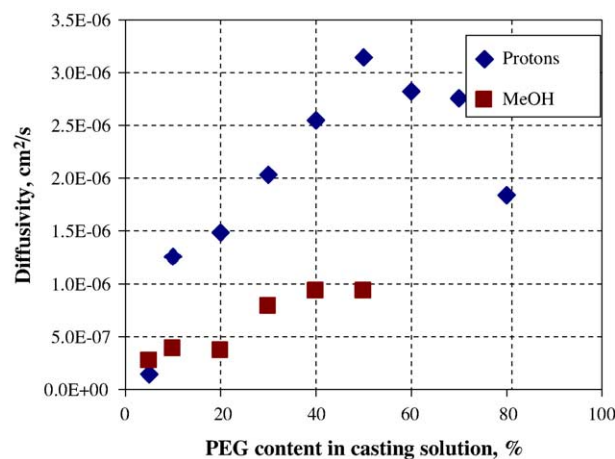


Fig. 3. Experimental diffusivities for proton and methanol.

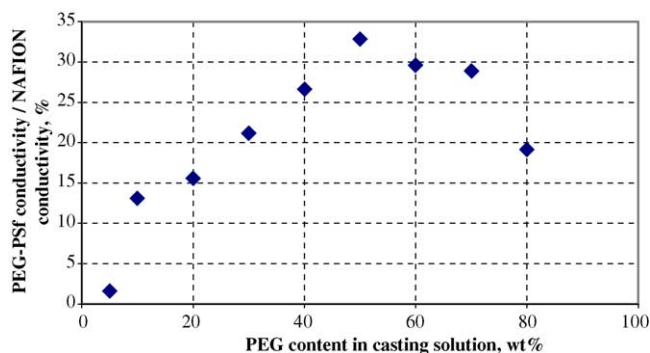


Fig. 4. Correlated proton conductivity, compared to value obtained using NAFION® 117 (71.8 mS cm^{-1}).

3.3. Determination of transport probability

From the association of mass transfer resistances we divided our experimental results for diffusivity into the several factors that contribute to its value. In this section, we analyse transport probability (see Fig. 5), which shows the change in the transport probability of protons and methanol through the dense layer, depending on the content of PEG in the casting solution.

We used the equilibrium model to calculate the transport probability from our experimental data. Simulations were performed in FORTRAN as follows:

1. Experimental concentrations were converted into non-dimensional concentrations varying (in terms of dimensional time), according to the equations presented in Section 2.
2. Interfacial mass transfer coefficients were set to 1 (case of low external mass transfer resistance).
3. Simulation was performed until the calculated non-dimensional concentrations (in terms of non-dimensional time) reached the maximum values of the experimental non-dimensional concentrations of the stripping solution.
4. Experimental and simulated non-dimensional concentrations were compared and the values of the calculated diffusivities were found.

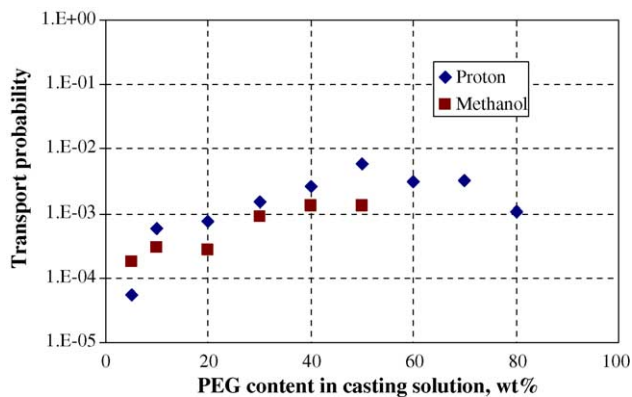


Fig. 5. Transport probabilities for protons and methanol obtained through the equilibrium model.

Table 3
Proton selectivity

w_{PEG} (wt.%)	S_e	S_c	S_{PEG}
5	0.570	0.663	0.608
10	3.210	3.289	3.877
20	4.094	4.132	5.372
30	2.542	2.554	3.227
40	2.714	2.606	3.872
50	3.349	3.232	8.807

5. The transport probabilities were calculated from the correlation between experimental and calculated diffusivities.

Fig. 5 compares the transport probabilities for protons and for methanol, determined by the equilibrium model. The PEG content in the casting solution determines the number of active sites that are responsible for the mass transfer. The transport probability for protons increased significantly when the PEG content increased from 10 to 50 wt.% and reached a maximum at this composition. Thereafter, the probability decreases, because the amount of PEG in the casting solution also helped to block any transport paths. This was because, in the dense layer, transported molecules had to pass in the free spaces between molecules. The more concentrated was the casting solution, the fewer the free spaces there were when the solvent was evaporated and the PEG layer was formed. This effect of maximum can also be seen by analysing the fit of the transport of methanol. In this case, probabilities were much lower, because:

- the molecules of methanol are much bigger than protons, so there is less space between PEG molecules is reduced for such component,
- fewer molecules of methanol are transferred by electronic effects than protons.

Transport probabilities could be estimated in a first attempt as the ratio of the molecule size to free volume in the polymer cell size. If there was a correlation between the PEG content in the casting solution and the polymer conformation, the transport probabilities of any molecule, once its molar volume had been calculated, could at least be estimated in order to design a membrane to separate one of two components or, as in the present case, to allow protons to flow and avoid methanol crossover.

As mentioned in Section 2, we can also use these results to calculate proton selectivity (see Table 3). Whether calculated directly from experimental data or indirectly by applying the equilibrium model, selectivity was maximum for a membrane with 20 wt.% of PEG in the casting solution. This property could also be calculated for the PEG layer. This was maximum for 50 wt.%, which shows that selectivity may increase if another support layer is used.

From these results, we calculated the relative resistance of each mass transfer phenomenon to the experimental diffusivity. See Fig. 6 for data on protons and Fig. 7 for data on methanol. The resistance to the permeation of pro-

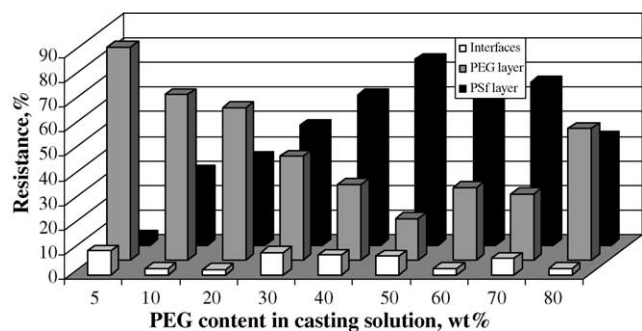


Fig. 6. Relative contribution of each mass transfer phenomenon to total resistance to permeation of protons.

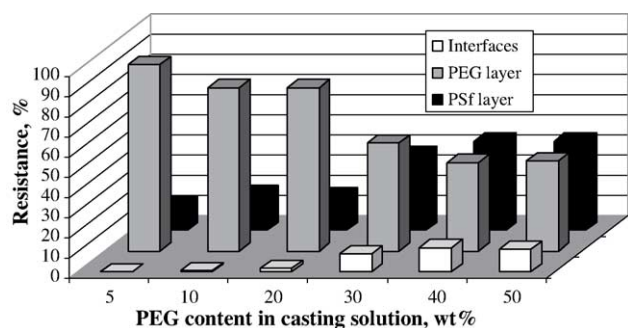


Fig. 7. Relative contribution of each mass transfer phenomenon to total resistance to permeation of methanol.

tons of the PSf layer was maximum when the PEG content in the casting solution was 50 wt.%. When we evaluated the methanol crossover, we found that the resistances of the two layers were almost equal at this composition. When membrane–reservoirs equilibrium was instantaneous, the mass transfer resistance at both interfaces could be as much as 10%, which confirms that this effect must be taken into consideration when simulating membrane permeation. It is important to evaluate mass transfer coefficients because they govern equilibrium at membrane–reservoir interfaces and also promote the transport through the membrane by increasing chemical potential. Mass transfer coefficients represent the relative affinity of the membrane for a given component and may be used to recommend optimal materials.

4. Conclusions

In this study we aim to contribute to the phenomenological knowledge of the permeation transport processes occurring in a fuel cell, by identifying the dominant mechanisms and contributions to permeability of mass transfer phenomena. The permeation of protons and methanol through composite membranes provided data for modelling. The main conclusions of this study are:

- The composite membranes tested provided a lower methanol crossover than NAFION® 117. As this happens

also for proton permeation, more materials should be tested in order to manufacture a fuel cell with better performance.

- Transport probabilities for protons and methanol were maximum for the membrane whose casting solution had 50 wt.% of PEG. For higher PEG contents, there may be less free space for transport in the dense layer, so transport probability decreased.
- Overall selectivity is maximum for a membrane with 20 wt.% of PEG in the casting solution. However, this value was higher when only the PEG layer was considered, which indicates that selectivity may be enhanced if another support layer is used.
- When evaluating the resistance of the different mass transfer phenomena, the PEG layer had the lowest resistance when the casting solution had 50 wt.% of PEG. Choosing a suitable porous support may reduce total mass transfer resistance and increase overall selectivity.
- Even if we consider instantaneous membrane–reservoirs equilibrium, the interfacial mass transfer resistance may represent 12% of the total mass transfer resistance.

At the moment, this model only takes into account the diffusive processes. However, in the values of diffusivity obtained through simulations other effects, like complexation reactions or hopping, may appear. Physico-chemical interactions of the membrane with the transported species should also be considered, for example by the Enskog–Thorne theory.

Once the transport phenomena have been evaluated, we can derive a phenomenological model for the whole fuel cell, including the kinetics of methanol oxidation. Unlike those already published, this model will not treat the membrane as a black box and will not depend exclusively on experimental data. It can therefore also recommend materials for a better fuel cell performance.

References

- [1] H.Y. Chang, C.W. Lin, *J. Membr. Sci.* 218 (2003) 295–306.
- [2] C.K. Dyer, *J. Power Sources* 106 (2002) 31–34.
- [3] A. Heinzl, V.M. Barragán, *J. Power Sources* 84 (1999) 70–74.
- [4] K. Scott, W.M. Taama, P. Argyropoulos, K. Sundmacher, *J. Power Sources* 83 (1999) 204–216.
- [5] T. Schulz, S. Zhou, K. Sundmacher, *Chem. Eng. Technol.* 24 (2001) 12, 1223.
- [6] H. Dohle, J. Divisek, R. Jung, *J. Power Sources* 86 (2000) 469–477.
- [7] B.S. Pivovar, Y. Wang, E.L. Cussler, *J. Membr. Sci.* 154 (1999) 155–162.
- [8] K.D. Kreuer, *J. Membr. Sci.* 185 (2000) 29–39.
- [9] M.J. Ariza, D.J. Jones, J. Roziere, *Desalination* 147 (2002) 183–189.
- [10] C. Manea, M. Mulder, *J. Membr. Sci.* 206 (2002) 443–453.
- [11] K. Habermüller, M. Mosbach, W. Schuhmann, *J. Anal. Chem.* 366 (2000) 560–568.
- [12] P. Argyropoulos, K. Scott, A.K. Shukla, C. Jackson, *J. Power Sources* 123 (2003) 190–199.
- [13] Y. Xu, W. Peng, X. Liu, G. Li, *Biosens. Bioelectron.* 20 (2004) 533–537.
- [14] Sh. Obeidi, B. Zazoum, N.A. Stolwijk, *Solid State Ionics* 173 (2004) 77–82.

- [15] L.T. Pinto, Um estudo do transiente da difusão gasosa em meios porosos, Doctorate Thesis in Chemical Engineering, Chemical Engineering Programme, COPPE, Universidade Federal do Rio de Janeiro, Rio de Janeiro, 1994, 197 pp.
- [16] M. Sato, M. Goto, A. Kodama, T. Hirose, *Sep. Sci. Technol.* 33 (1998) 1283–1301.
- [17] C. Torras, R. Garcia-Valls, *J. Membr. Sci.* 233 (2004) 119–127.
- [18] W.Y. Fei, H.-J. Bart, *Chem. Eng. Process.* 40 (2001) 531–535.
- [19] R.C. Reid, J.M. Prausnitz, T.K. Sherwood, *The Properties of Gases and Liquids*, McGraw-Hill, New York, 1987.
- [20] C. Geankoplis, *Transport Processes and Unit Operations*, 3rd ed., Prentice-Hall, 1993, 921 pp.
- [21] P. Mukoma, B.R. Jooste, H.C.M. Vosloo, *J. Membr. Sci.* 243 (2004) 293–299.

L. Pitol-Filho, S. Alsoy Altinkaya, R. Garcia-Valls

Evaluation of poly(ethylene glycol) of different chain length as a potential selective layer for direct methanol fuel cells

Evaluation of poly(ethylene glycol) of different chain length as a potential selective layer for direct methanol fuel cells

Luizildo Pitol-Filho¹, Sacide Alsoy Altinkaya², Ricard Garcia-Valls^{1*}

¹Departament d'Enginyeria Química
Escola Tècnica Superior d'Enginyeria Química
Universitat Rovira i Virgili
Av. Països Catalans, 26, 43007, Tarragona, Spain
Tel.: +34 977 55 85 35; Fax:+34 977 55 85 44; E-mail: ricard.garcia@urv.cat

²Department of Chemical Engineering
Izmir Institut of Technology
Gülbahçe Koyu
35437 Urla-Izmir, Turkey
Email: sacidealsoy@iyte.edu.tr

An important issue in the operation of direct methanol fuel cells is the amount of methanol that crosses the polymeric membrane, i.e. the methanol crossover. In a previous work, we evaluated the permeability of methanol and protons through a composite membrane, where the selective layer was poly(ethylene glycol) (PEG) of 1000 g/gmol. By using literature data of water diffusivity in PEG of different chain length and applying the free-volume theory, we were able to evaluate the diffusive flux of methanol and water through a hypothetical layer of PEG.

Introduction

The direct methanol fuel cells accomplish several requirements for mobile applications: renewable source, fast refuelling, high efficiency and low level of emissions [1]. However, some methanol still permeates through the polymeric membrane, generating what is known as methanol crossover, that not only reduces the available amount of fuel, but also reduces the cell voltage by the mixed potential [2]. In this sense, for example, lignosulfonates were tested as alternative materials and methanol permeability was reported to be lower than NAFION® (DuPont) [3]. In a previous work we also reported experiments with composite membranes having poly(ethylene glycol) (PEG) as selective layer and polysulfone to provide mechanical stability, with similar results [4]. We pointed out, however, the little effort done towards the comprehension of the diffusion processes in the membrane of the fuel cells. We believe the accurate execution of such task is mandatory if we want to improve the efficiency of the fuel cells.

A good starting point to study the diffusive processes in the polymeric systems is the free-volume Vrentas-Duda theory [5,6]. By using such theory with the extensive lists of both solvent and polymer parameters [7,8], the diffusion in several polymeric systems may be predicted, with applications that range from the transport of the molecules itself to the formation of polymeric membranes.

Diffusion data for water-PEG systems were obtained by using the Gouy interferometric technique [9,10]. From those data we regressed the free-volume parameters for PEG from 200 g/gmol to 10,000 g/gmol and, by coupling the Flory-Huggins thermodynamic theory, we estimated the diffusive fluxes of water and methanol through a hypothetic PEG membrane at 298K. We aimed to determine the difference in fluxes between the methanol and water, to recommend a PEG of determined chain length as a potential material for the membrane-electrode assembly.

Theory

To calculate the diffusive fluxes by using the literature data, we have to perform some previous steps:

- Calculation of molar volume of the species, as well as the Flory-Huggins parameters;
- Regression of PEGs free-volume parameters y treating the binary diffusivity data;
- Determination of ternary diffusivity data.

Calculation of molar volumes and Flory-Huggins interaction parameters

Among the methods to calculate the molar volumes, there are the group contribution rules compiled by Sugden and Blitz [7]. The latter is more adequate to polar molecules, such as PEG.

When the components are polar or make hydrogen bonds, a three-dimensional (3D) Flory-Huggins parameter is preferred [11], as stated in Eq (1):

$$\chi_{i3} = \alpha \frac{V_i}{RT} D_{i3}^2 \quad (1)$$

$$D_{i3}^2 = w_d (\delta_{i,d} - \delta_{3,d})^2 + w_p (\delta_{i,p} - \delta_{3,p})^2 + w_{hb} (\delta_{i,hb} - \delta_{3,hb})^2 \quad (1.1)$$

In Eq (1.1), δ_d , δ_p and δ_{hb} represent the Hansen parameters (a.k.a cohesion parameters) that comprehend the dispersive, polar and hydrogen-bonding effects of a given component. There are group contribution methods to calculate each one [12]. A commonly used weight distribution for those effects is a (4:1:1) distribution, where $(w_d:w_p:w_{hb}) = (1:0.25:0.25)$ while α is equal to the unity.

The water-MeOH interaction parameter should be calculated from vapor-liquid equilibrium data, according to Eqs.(2) and (3) [13]:

$$\frac{\Delta G^E}{RT} = \sum x_i \ln \gamma_i \quad (2)$$

$$\chi_{12} = \frac{1}{y_1 \phi_2} \left(y_1 \ln \left(\frac{y_1}{\phi_1} \right) + y_2 \ln \left(\frac{y_2}{\phi_2} \right) + \frac{\Delta G^E}{RT} \right) \quad (3)$$

Literature provides VLE data for the water-MeOH systems [14]. Then, we calculated the activity coefficients by using the Van Laar rule at 760mmHg. The interaction parameter finally becomes a polynomial function varying with the MeOH as in Eq.(4):

$$\chi_{12} = \sum_{i=1}^5 c_i \phi_2^{i-1} \quad (4)$$

Treatment of binary diffusivity data

The diffusivity data obtained by the Gouy interferometric technique [9,10] may be written as the product of a mobility Ω_i to a thermodynamic factor B_i :

$$D_i = \Omega_i \cdot B_i \quad (5)$$

where the thermodynamic factor is:

$$B_i = \left(1 + \frac{\partial \ln \gamma_i}{\partial \ln x_i} \right) \quad (6)$$

Activity coefficients may be calculated through the Van Laar equation and parameters at 298 K are listed for the water-PEG systems of interest [9].

The mobility of the species is equivalent to the self-diffusion coefficient [5], according to Eq (3):

$$\Omega_i = D_0 \exp\left[\frac{-E_1}{RT}\right] \exp\left[-\frac{w_1 V_1 + w_3 \xi_{13} V_3}{w_1 \left(\frac{K_{11}}{\gamma}\right) (K_{21} - T_{g1} + T) + w_3 \left(\frac{K_{13}}{\gamma}\right) (K_{23} - T_{g3} + T)}\right] \quad (7)$$

For some chain lengths (PEG ranging from 200 to 1,000 g/gmol) also the diffusion coefficients at infinite dilution of PEG in water are available [10]. In this case, Eq.(5) is directly reduced to:

$$D_{infinite} = D_0 \exp\left[\frac{-E_1}{RT}\right] \exp\left[-\frac{V_1}{\left(\frac{K_{11}}{\gamma}\right) (K_{21} - T_{g1} + T)}\right] \quad (8)$$

The diffusivity at infinite dilution is reported as to be dependent on molecular weight. Therefore, since the temperature for all the data is constant, we decided to lump the pre-exponential term and the activation energy into a term based on the infinite dilution, as stated in Eq.(9):

$$A_{i3} = D_0 \exp\left[\frac{-E_1}{RT}\right] = D_{infinite} \exp\left[\frac{V_1}{\left(\frac{K_{11}}{\gamma}\right)(K_{21} - T_{g1} + T)}\right] \quad (9)$$

By applying the free-volume parameters of water in Eq.(9), it is therefore possible to calculate the A term. Then, since all the experimental data were obtained at 298K, it is possible to simultaneously eliminate the dependence on temperature and reduce the number of unknowns by introducing a lumped free-volume parameter:

$$K_{lumped} = \left(\frac{K_{13}}{\gamma}\right)(K_{23} - T_{g3} + T) \quad (10)$$

Of course, the drawback of such strategy remains on the reduced capability of extrapolating the prediction to temperatures different than 298K. For our purposes, however, this assumption is still valid. With the introduction of the lumped parameters, Eq.(5) now becomes:

$$D_i = A_{i3} \exp\left[-\frac{w_1 V_1 + w_3 \xi_{13} V_3}{w_1 \left(\frac{K_{11}}{\gamma}\right)(K_{21} - T_{g1} + T) + w_3 K_{lumped}}\right] \quad (11)$$

By using the sets of experimental data for each chain length we regressed the unknown parameters: A_{i3} , K_{lumped} and ξ_{i3} . K_{lumped} just depends on the polymer itself. Therefore, it will be constant for prediction of diffusivities of any species in it. The objective function that we used to regress the free-volume parameters was the following integral:

$$\Psi = \int \left| \ln \frac{D_{experimental}}{D_0} - \ln \frac{D_{prediction}}{D_0} \right| dw_{PEG} \quad (12)$$

Such objective function was chosen since it was able to minimize the area between predicted and experimental logarithmic curves.

Conversion of $\xi_{water,polymer}$ into $\xi_{MeOH,polymer}$.

Since both water and MeOH are very polar, they are expected to behave similarly. Therefore, the ratio of the molar volume of one of these components to the molar volume of the polymer jumping unit can be directly converted into the equivalent property of the other one. First, we should determine the molar mass of the polymer jumping unit, by the following relation [7]:

$$M_{3j} = \frac{M_1 V_1}{V_3} \frac{1}{\xi_{13}} \quad (13)$$

Once the molar mass of the polymer jumping unit is determined, it allows us to obtain the ξ_{23} parameter by just applying the molar mass and volume of methanol:

$$\xi_{23} = \frac{M_2 V_2}{M_{3j} V_3} \quad (14)$$

Ternary diffusivity data

The mutual coefficients are predicted from Vrentas-Duda free-volume theory as follows:

$$D_1 = D_{01} \exp\left[\frac{-E_1}{RT}\right] \exp\left[-\frac{w_1 V_1 + w_2 \frac{\xi_{13}}{\xi_{23}} V_2 + w_3 \xi_{13} V_3}{\hat{V}/\gamma}\right] \quad (15)$$

$$D_2 = D_{02} \exp\left[\frac{-E_2}{RT}\right] \exp\left[-\frac{w_2 V_2 + w_1 \frac{\xi_{23}}{\xi_{13}} V_1 + w_3 \xi_{23} V_3}{\hat{V}/\gamma}\right] \quad (16)$$

where

$$\frac{\hat{V}}{\gamma} = \sum_{i=1}^3 w_i \left(\frac{K_{li}}{\gamma}\right) (K_{2i} - T_{gi} + T) \quad (17)$$

Considering that the literature data neglect the activation energy for MeOH diffusion and introducing the lumped free-volume parameters, we may rewrite Eqs(15-17):

$$D_1 = A_{13} \exp\left[-\frac{\phi_1 V_1 + \phi_2 \frac{\xi_{13}}{\xi_{23}} V_2 + \phi_3 \xi_{13} V_3}{\hat{V}/\gamma}\right] \quad (18)$$

$$D_2 = D_{02} \exp\left[-\frac{\phi_2 V_2 + \phi_1 \frac{\xi_{23}}{\xi_{13}} V_1 + \phi_3 \xi_{23} V_3}{\hat{V}/\gamma}\right] \quad (19)$$

where

$$\frac{\hat{V}}{\gamma} = \phi_3 K_{lumped} + \sum_{i=1}^2 \phi_i \left(\frac{K_{1i}}{\gamma} \right) (K_{2i} - T_{gi} + T) \quad (20)$$

The diffusion also requires the thermodynamic contribution, to compose the free-volume matrix:

$$\begin{aligned} D_{11} &= D_1 \phi_1 (1 - \phi_1) \frac{1}{RT} \frac{\partial \mu_1}{\partial \phi_1} - D_2 \phi_1 \phi_2 \frac{1}{RT} \frac{\partial \mu_2}{\partial \phi_1} \\ D_{12} &= D_1 \phi_1 (1 - \phi_1) \frac{V_2}{V_1} \frac{1}{RT} \frac{\partial \mu_1}{\partial \phi_2} - D_2 \phi_1 \phi_2 \frac{V_2}{V_1} \frac{1}{RT} \frac{\partial \mu_2}{\partial \phi_2} \\ D_{21} &= D_2 \phi_2 (1 - \phi_2) \frac{V_1}{V_2} \frac{1}{RT} \frac{\partial \mu_2}{\partial \phi_1} - D_1 \phi_1 \phi_2 \frac{V_1}{V_2} \frac{1}{RT} \frac{\partial \mu_1}{\partial \phi_1} \\ D_{22} &= D_2 \phi_2 (1 - \phi_2) \frac{1}{RT} \frac{\partial \mu_2}{\partial \phi_2} - D_1 \phi_1 \phi_2 \frac{1}{RT} \frac{\partial \mu_1}{\partial \phi_2} \end{aligned} \quad (21)$$

where the chemical potentials are given by Flory-Huggins model:

$$\frac{\mu_1 - \mu_1^0}{RT} = \ln \phi_1 + \phi_3 + (\chi_{12} \phi_2 + \chi_{13} \phi_3)(1 - \phi_1) - \chi_{23} \phi_2 \phi_3 \quad (22)$$

$$\frac{\mu_2 - \mu_2^0}{RT} = \ln \phi_2 + \phi_3 + (\chi_{12} \phi_1 + \chi_{23} \phi_3)(1 - \phi_2) - \chi_{13} \phi_1 \phi_3 \quad (23)$$

The thermodynamics of the binary systems was described by the Van Laar equation. However, we decided to use the Flory-Huggins approach to the ternary systems just because their coefficients may be predicted from the chemical structures of the components.

Methanol and water fluxes through a hypothetical membrane

The diffusive fluxes for MeOH and water (Figure 1) are calculated by using Eq.(24) [6]:

$$J_i = - \sum_{j=1}^2 \frac{D_{ij}}{V_j} \frac{\partial \phi_j}{\partial z} \quad (24)$$

with the following assumptions:

- Thickness of the PEG selective layer: $\Delta z = 1 \mu\text{m}$;

- Components totally removed at the end of the selective layer, to provide the maximal flow rate (the porous support does not interfere with the mass transfer);
- Volume fractions at $z = 0$ are calculated by using the equations of chemical potential (22) and (23), where the left-hand side is expressed in terms of molar fraction.

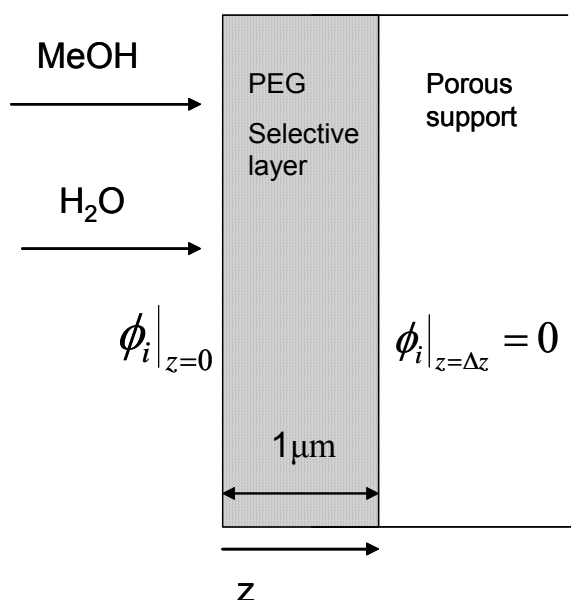


Figure 1 – Scheme for the determination of diffusive fluxes through the PEG selective layer

Since the results of the total fluxes may vary in scale, we decided to derive the selectivity for MeOH, as described by Eq (25):

$$S_{MeOH} = \frac{J_{MeOH}}{J_{MeOH} + J_{H_2O}} \quad (25)$$

Eq (25) will be helpful to evaluate which membrane is less selective for MeOH.

Results

Water and methanol free-volume parameters

Table 1 summarizes the data regressed for the system. Free-volume parameters for water and MeOH were collected from literature [8]. We can observe that, as long as the PEG chain length increases, the molar volume and the Flory-Huggins interaction parameters also increase, due to the preponderance of the aliphatic contribution to the total chain. PEGs with higher χ_{13} and χ_{23} have low affinity for water and MeOH. The variation of the parameter A_{13} with the molecular weight of PEG may be explained by the increasing energy of activation for diffusion when chain length increases. On the other hand, ξ_{13} and ξ_{23} exhibit a minimum for PEG 3400 and, following this tendency, the value obtained for PEG 10000 is unexpected. Maybe there is some reason

for this behavior that was not explained in the reference papers, such as crosslinking degree, that also affects the diffusion process.

Table 1 – Free-volume parameters for water and methanol.

Property	Component		$\chi_{12} = \sum_{i=1}^5 c_i \phi_2^{i-1}$				
	H ₂ O (1)	MeOH (2)	C ₁	C ₂	C ₃	C ₄	C ₅
D ₀ , cm ² /s	-	8.75.10 ⁻⁴					
V, cm ³ /g	1.071	0.957					
K _{1i} /γ, cm ³ /(g.K)	0.00218	0.00117	6.1	-37.3	120.7	-181.3	98.8
K _{2i} – T _{g2} , K	-152.29	-48.41					
PEG(3)	V ₃ , cm ³ /g	K _{lumped}	A ₁₃ , cm ² /s	ξ ₁₃	ξ ₂₃	χ ₁₃	χ ₂₃
200	0.904	0.310	1.83.10 ⁻⁴	1.65	2.62	1.68	0.62
300	0.935	0.317	1.47.10 ⁻⁴	1.61	2.55	2.22	0.92
400	0.941	0.301	1.28.10 ⁻⁴	1.46	2.33	2.37	1.01
600	0.952	0.320	1.02.10 ⁻⁴	1.47	2.33	2.64	1.20
1000	0.961	0.331	0.78.10 ⁻⁴	1.35	2.15	2.88	1.38
1500	0.964	0.309	0.66.10 ⁻⁴	1.20	1.91	3.00	1.47
2000	0.966	0.300	0.54.10 ⁻⁴	0.97	1.54	3.08	1.53
3400	0.969	0.304	0.47.10 ⁻⁴	0.93	1.47	3.19	1.61
10000	0.971	0.297	0.37.10 ⁻⁴	1.77	2.81	3.31	1.71

Ternary equilibrium data according to Flory-Huggins theory

Before calculating the fluxes for water and MeOH, we obtained the equilibrium data for the ternary systems varying the molar fraction of MeOH in the liquid solution for all the studied PEGs. The volume fraction of water almost does not change, as seen in Figure 2.

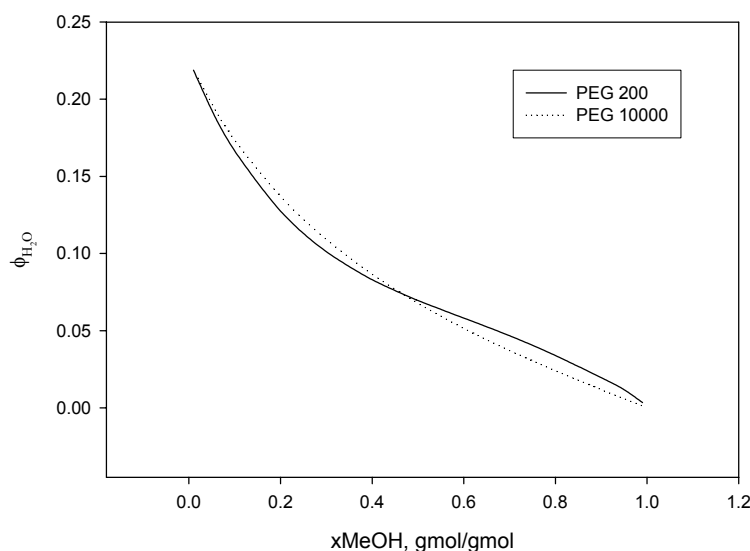


Figure 2 – Volume fraction of water varying with the MeOH molar fraction in the liquid solution (PEG 200 and PEG 10000).

Since its values do not change much, we decided to plot just the data for PEG 200 and PEG 10000. Figure 3 shows the tridimensional behavior of the MeOH volume fraction.

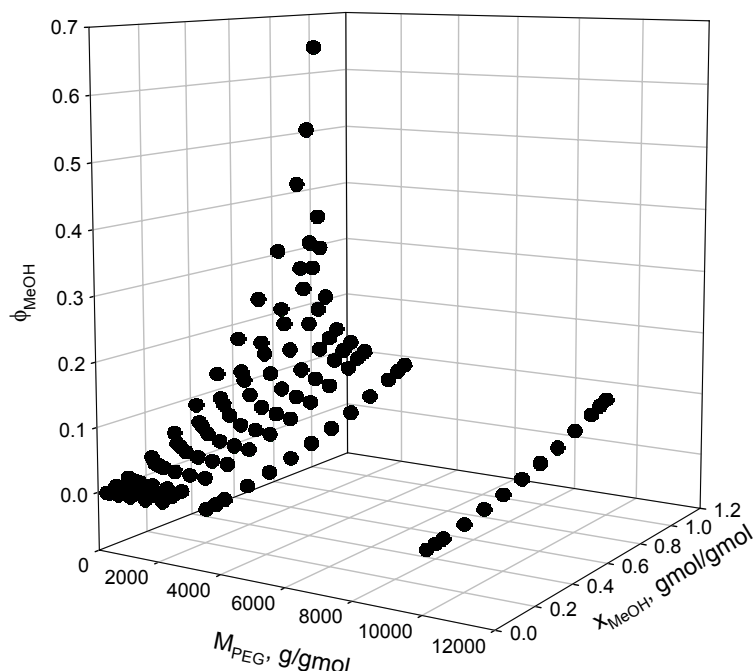


Figure 3 - Volume fraction of MeOH varying with the MeOH molar fraction in the liquid solution and with the molecular weight of PEG.

In Figure 3 we can observe that at low molecular weight of PEG, the volume fraction of MeOH can reach values up to 0.7, what indicates complete dissolution. In fact, in a previous work [4], we obtained membranes by dissolving PEG 1000 in MeOH. However, the maximal volume fraction diminishes as long as the chain length increases, owing to the reduction of affinity between MeOH and PEG, revealed by their correspondent Flory-Huggins interaction parameter, as discussed in the previous section. There is no significant variation, though, for the fits of PEG 3400 and PEG 10000.

Methanol and water fluxes through a hypothetical PEG membrane

Figure 4 shows the diffusive flux of water obtained for the studied PEGs at several MeOH molar fractions in the liquid phase, whose maximal value was set to 0.25, close to high concentrations recently studied [15]. According to our simulations, the flux of water is significantly reduced when any PEG is used instead of PEG 200 and, naturally, the minimal one is obtained with a membrane of highest PEG.

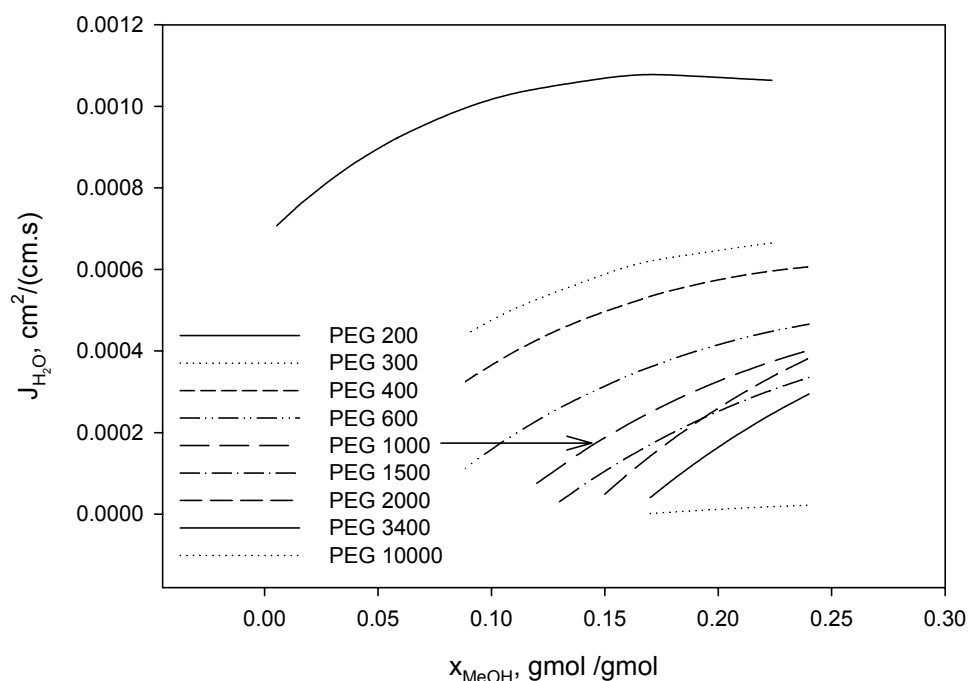


Figure 4 – Water diffusive flux varying the molar fraction of MeOH in the liquid solution and the PEG chain length.

In some cases the numerical procedure did not converge for low concentrations and such difficulty increased with the PEG chain length, maybe owing to the few experimental data. Probably such problem would be overcome if more sets of data were available. Figure 5 shows the same curves, but for MeOH.

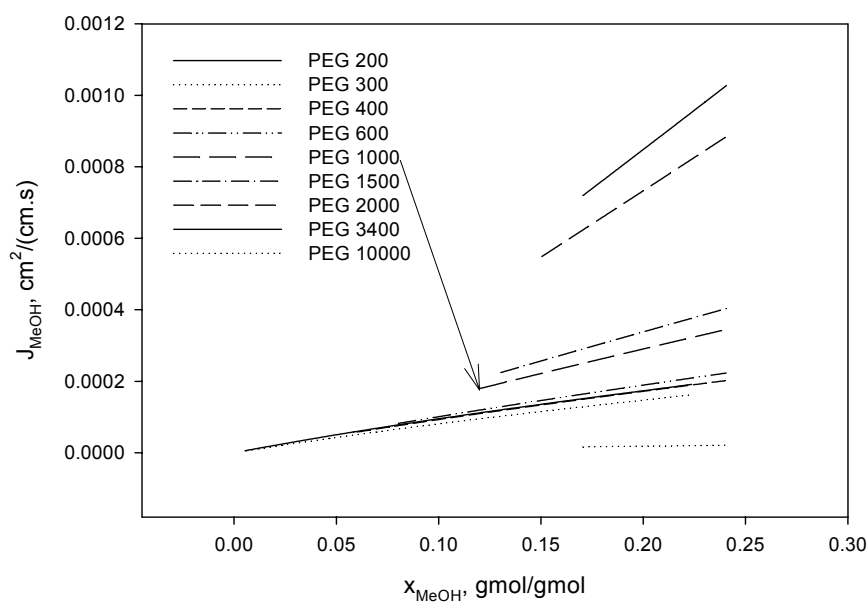


Figure 5 - MeOH diffusive flux varying the molar fraction of MeOH in the liquid solution and the PEG chain length.

In Figure 5 we can observe that the flux of MeOH increases with the chain length until PEG 3400, and then it experiences a significant reduction to minimal values. Such trend may be explained by the ξ_{13} and ξ_{23} parameters, as discussed previously. We can observe the selectivity curves for MeOH in Figure 6.

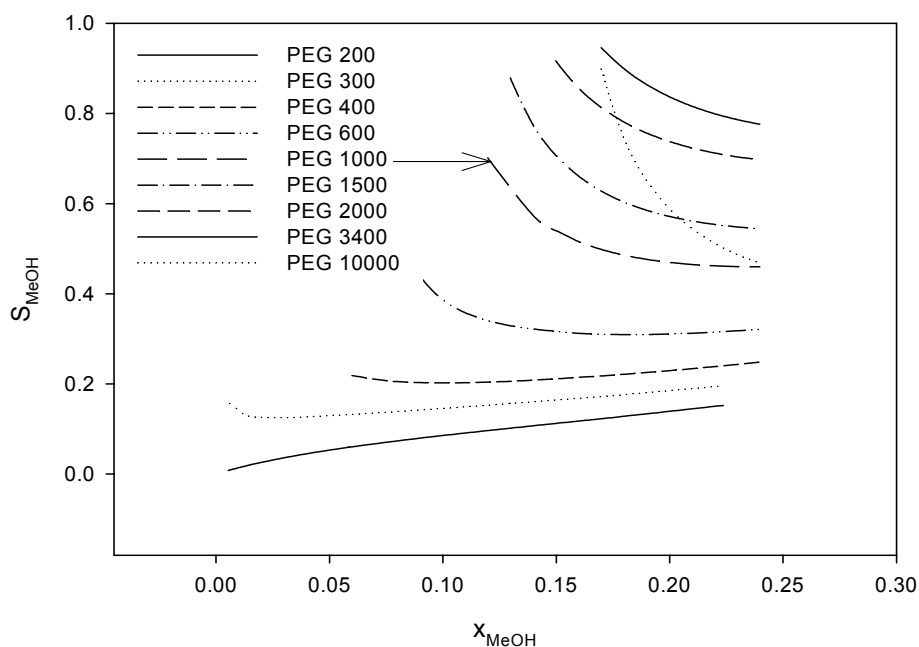


Figure 6 – MeOH selectivity curves varying the molar fraction of MeOH in the liquid solution and the PEG chain length.

Figure 6 shows what Figures 4 and 5 allowed us to conclude: that the selectivity for MeOH increases with chain length and, for lower concentrations, just MeOH would cross the membrane. However, selectivity can be reduced when feed MeOH solutions are more concentrated, as in the case for PEG 10000.

Conclusions

The present study intended to evaluate several PEG chain lengths as potential materials to obtain selective layers for direct methanol fuel cells. We used literature data to regress free-volume parameters for water-PEG systems and converted them into MeOH-PEG data. We could observe the following:

- As long as the PEG chain length increases, the molar volume and the Flory-Huggins interaction parameters also increase, due to the preponderance of the aliphatic contribution to the total chain. PEGs with higher χ_{13} and χ_{23} have low affinity for water and MeOH.
- The variation of the parameter A_{13} with the molecular weight of PEG may be explained by the increasing energy of activation for diffusion when chain length increases.
- ξ_{13} and ξ_{23} exhibit a minimum for PEG 3400 and, following this tendency, the value obtained for PEG 10000 is unexpected. Another factor not

explained in the reference papers, such as crosslinking, may be the reason.

- The flux of water is significantly reduced when any PEG is used instead of PEG 200 and, naturally, the minimal one is obtained with a membrane of highest PEG.
- The flux of MeOH increases with the chain length until PEG 3400, and then it experiences a significant reduction to minimal values. The reason could be the behavior of the ξ_{13} and ξ_{23} parameters.
- Finally selectivity for MeOH increases with chain length and, for lower concentrations, just MeOH would cross the membrane. However, selectivity can be reduced when feed MeOH solutions are more concentrated, as in the case for PEG 10000.

The reasons above allowed us to conclude that PEGs with high molecular weight are promising materials to manufacture selective layers for methanol fuel cells, since it would be possible to work at higher concentrations of MeOH than 1.0M, that is typically used. However, other important aspects, such as proton conductivity and chemical resistance to the feed solution, were out of the scope of the present work and should be taken into account before final decision for a determined material.

Nomenclature

Acronyms

DMFC	direct methanol fuel cell
MeOH	methanol
PEG	poly(ethylene glycol)

Variables and parameters

A_{i3}	pre-exponential term based on the diffusivity at infinite dilution ($\text{cm}^2 \cdot \text{s}^{-1}$)
B_i	thermodynamic factor based on Van Laar equation
c_i	coefficient of the water-MeOH Flory-Huggins expression
D_i	binary diffusivity ($\text{cm}^2 \cdot \text{s}^{-1}$)
D_{ij}	diffusion coefficient matrix for ternary systems ($\text{cm}^2 \cdot \text{s}^{-1}$)
D_{i3}^2	composition factor of Flory-Huggins parameter
D_0	pre-exponential term on diffusivity expression ($\text{cm}^2 \cdot \text{s}^{-1}$)
E_i	activation energy for diffusion
G^E	excess Gibbs free energy
J_i	diffusive flux of component i ($\text{cm}^2 \cdot \text{cm}^{-1} \cdot \text{s}^{-1}$)
K_{1i}/γ	free-volume parameter for component i ($\text{cm}^3 \cdot \text{g}^{-1} \cdot \text{K}^{-1}$)
$K_{2i} - T_{gi}$	free-volume parameter for component i (K)
K_{lumped}	lumped free-volume parameter for polymer ($\text{cm}^3 \cdot \text{g}^{-1}$)
M_i	molecular weight of PEG ($\text{g} \cdot \text{gmol}^{-1}$)
R	ideal gas constant
S_{MeOH}	selectivity for MeOH based on total diffusive flows
T	temperature, K

V_i	molar volume of component i ($\text{cm}^3 \cdot \text{g}^{-1}$)
w_i	mass fraction of component i
x_i	molar fraction of component i
y_i	molar fraction of component i in vapor phase

Greek symbols

α	multiplier factor of Flory-Huggins parameter
γ_i	activity coefficient of component i
δ_i	Hansen parameter of component i ($\text{MPa}^{1/2}$)
μ_i	chemical potential of component i
ξ_{i3}	ratio of the molar volumes for solvent i and polymer jumping unit
Ψ	area between experimental and predicted binary diffusivity curves
χ_{ij}	i-j Flory-Huggins interaction coefficient
Ω_i	mobility of component i

Subscripts

d	dispersive
hb	hydrogen-bonding
p	polar
1	water
2	methanol
3	polymer
3j	jumping unit polymer

References

- [1] K. Scott, W. Taama, J. Cruickshank. *J. Applied Electrochemistry* 28 (1998) 289-297.
- [2] T. Schaffer, V. Hacker, T. Hejze, T. Schinder, J.O. Besenhard, P. Prenninger. *J. Power Sources* 145 (2005) 188-198.
- [3] X. Zhang, A. Glösen, R. Garcia-Valls. *J. Membrane Science* 276 (2006) 301-307.
- [4] X. Zhang, L. Pitol-Filho, C. Torras, R. Garcia-Valls. *J. Power Sources* 145 (2005) 223-230.
- [5] S. Alsoy, J.L. Duda. *AIChEJ* 45 (1999) 896-905.
- [6] S.-S. Wong, S. Alsoy Altinkaya, S.K. Mallapragada. *Polymer* 45 (2004) 5151-5161.
- [7] J.M. Zielinski, J.L.Duda, *AIChEJ* 38 (1992) 405-415.
- [8] S.-U. Hong, A.J. Benesi, J.L. Duda. *Polymer International* 39 (1996) 243-249.
- [9] A. Vergara, L. Paduano, V. Vitagliano, R. Sartorio. *Phys. Chem. Chem. Phys* 1 (1999) 5377-5383.
- [10] A. Vergara, L. Paduano, V. Vitagliano, R. Sartorio. *J. Phys. Chem. B* 105 (2001) 11044-11051.
- [11] T. Lindvig, M.L. Michelsen, G.M. Kontogeorgis. *Fluid Phase Equilibria* 203 (2002) 247-260.
- [12] A.F.M. Barton, *CRC Handbook of Solubility Parameters and Other Cohesion Parameters*, CRC Press, 2nd edition (1991).

- [13] J.H. Kim, B.R. Min, J. Won, H.C. Park, Y.S. Kang, *J. Membrane Science* 47 (2001) 181-
- [14] DECHEMA
- [15] P. Mukoma, B.R. Jooste, H.C.M. Vosloo. *J. Membrane Science* 243 (2004) 293-299.

Curriculum Vitae

Personal information

Surname(s) / First name(s)	Pitol Filho, Luizildo	Nationality	Brazilian
Address(es)	C/ Sant Miquel 9, 2-4 43004 Tarragona (Spain)	Date of birth	18/05/1974 (dd/mm/yyyy)
Mobile:	+34 620452226	Gender	Male
E-mail	luizildo.pitol@urv.net		

Work experience

Dates	October 1999 – September 2002
Occupation or position held	R&D Engineer
Main activities and responsibilities	Analysis of Fluid Catalytic Cracking (FCC) data obtained in a pilot plant Simulation of FCC to obtain reaction rate constants using a lumped deterministic model Development of a mathematical model for evaporation of fuels in pre-combustion chambers
Name and address of employer	PETROBRAS (Brazilian Petroleum Co.) São Mateus do Sul – PR (Brazil)
Type of business or sector	Petroleum Company / R&D Department

Education and training

Dates	October 2002 – June 2007
Title of qualification awarded	PhD in Chemical and Process Engineering
Principal subjects/occupational skills covered	Dense and porous membranes operations Production of dense and porous membranes from polymeric solutions. Thermodynamics of polymeric materials Mathematical modeling
Name and type of organisation providing education and training	Universitat Rovira i Virgili Chemical Engineering Department Tarragona, Spain
Dates	March 1997 – August 1999
Title of qualification awarded	MSc in Chemical Engineering
Principal subjects/occupational skills covered	Supercritical fluid extraction for purification of orange peel oil Coupling of adsorption and extraction with carbon dioxide at high pressures Work developed both experimentally and theoretically
Name and type of organization providing education and training	Universidade Federal de Santa Catarina Chemical Engineering Department Florianópolis, Brazil
Dates	March 1992 – January 1997
Title of qualification awarded	Chemical Engineer
Principal subjects/occupational skills covered	Transport Phenomena Unit Operations Analysis and Simulation of Chemical Processes Homogeneous Reactors and Heterogeneous Catalysis
Name and type of organization providing education and training	Universidade Federal de Santa Catarina Chemical Engineering Department Florianópolis, Brazil

Personal skills and competences

Mother tongue(s)

Other language(s) self-assessment

European level (*)

Catalan

English

French

German

Spanish

Portuguese

Understanding				Speaking				Writing	
Listening		Reading		Spoken interaction		Spoken production			
C2	Proficient user	C2	Proficient user	C2	Proficient user	C2	Proficient user	C2	Proficient user
C1	Proficient user	C1	Proficient user	C1	Proficient user	C1	Proficient user	C1	Proficient user
B2	Independent user	B2	Independent user	B2	Independent user	B1	Independent user	B1	Independent user
A2	Basic user	B1	Independent user	B1	Independent user	A2	Basic user	A2	Basic user
C2	Proficient user	C2	Proficient user	C2	Proficient user	C2	Proficient user	C2	Proficient user

(*) Common European Framework of Reference for Languages

Social skills and competences

- good ability to adapt to different environments, gained through my PhD years (the colleagues were from several countries and I have made a short research stay outside Spain);
- good communication skills gained through the preparation of seminars and presentation of oral works;
- mediation skills, obtained as a representative of graduate students to the department councils and to the graduate committee (during MSc and PhD years).

Organisational skills and competences

- participation in organising committees of scientific meetings in Brazil and Spain.

Technical skills and competences

- good command of deterministic modelling strategies of chemical processes;
- good level of understanding phenomena involving polymeric materials: obtention, kinetics of formation, diffusion and interaction with chemical species

Computer skills and competences

- good command at user level of tools such as internet, Excel, Word and Power Point;
- programming skills in Fortran, including libraries for numerical solutions and parameters regression;
- good command of commercial simulators such as HYSYS®;
- good experience in Pinnacle editor for movie making.

Other skills

Teaching assistant at Universitat Rovira i Virgili during PhD years in the following subjects:

- Control Elements;
- Simulation and Optimization of Chemical Processes;
- Simulation of Unit Operations;
- Practice on Projects Supervision.

All the teaching has been performed in Catalan and Spanish

Artistic skills and competences

- co-producer of a short documentary movie for extracurricular classes, involved in all steps: script, filming, preparation of interviews and final edition.

Driving license

Brazilian and International driving license, category B

Additional information

References

Dr Ricard Garcia-Valls (PhD thesis advisor): ricard.garcia@urv.net
 Dr Xavier Farriol: xavier.farriol@urv.net
 Dr. Waldir Pedro Martignoni: martignoni@petrobras.com.br

Papers

- 1.X. Zhang, L. Pitol Filho, C. Torras, R. Garcia-Valls. Experimental and computational study of proton and methanol permeabilities through composite membranes. J. Power Sources 145 (2005) 223-230.
2. L. Pitol-Filho, C. Torras, J. Bonet-Avalos, R. Garcia-Valls. Modeling of polysulfone membranes formation by immersion precipitation. Desalination 200 (2006) 427-428.
3. C. Torras, D. Gezahegn, L. Pitol-Filho, R. Garcia-Valls. Novel polymeric membrane structures: microcapsules. Desalination 200 (2006) 12-14.
4. L. Pitol-Filho, R. Garcia-Valls. A method to assess the choice of polymers for specific applications. Polymer Engineering & Science (in press).